Simulation of the sulphur iodine thermochemical cycle

Bothwell Nyoni

BEng (Chemical Engineering)

Dissertation submitted in partial fulfilment of the requirements for the degree *Master of Engineering in Chemical Engineering* at the Potchefstroom Campus of the North-West University.

Supervisor:	Dr. Percy van der Gryp
Assistant supervisor:	Dr. Mike Dry
Date:	November 2011

NORTH-WEST UNIVERSITY
YUNIBESITI YA BOKONE-BOPHIRIMA
NOORDWES-UNIVERSITEIT

DECLARATION

I hereby declare that all the material used in this dissertation is my own original unaided work except where specific references are made by name or in the form of a numbered reference. The work herein has not been submitted for a degree at another university.

Signed at _____ on the _____ day of _____

_____

Bothwell Nyoni

ABSTRACT

The demand for energy is increasing throughout the world, and fossil fuel resources are diminishing. At the same time, the use of fossil fuels is slowly being reduced because it pollutes the environment. Research into alternative energy sources becomes necessary and important. An alternative fuel should not only replace fossil fuels but also address the environmental challenges posed by the use of fossil fuels. Hydrogen is an environmentally friendly substance considering that its product of combustion is water. Hydrogen is perceived to be a major contender to replace fossil fuels. Although hydrogen is not an energy source, it is an energy storage medium and a carrier which can be converted into electrical energy by an electrochemical process such as in fuel cell technology.

Current hydrogen production methods, such as steam reforming, derive hydrogen from fossil fuels. As such, these methods still have a negative impact on the environment. Hydrogen can also be produced using thermochemical cycles which avoid the use of fossil fuels. The production of hydrogen through thermochemical cycles is expected to compete with the existing hydrogen production technologies. The sulphur iodine (SI) thermochemical cycle has been identified as a high-efficiency approach to produce hydrogen using either nuclear or solar power.

A sound foundation is required to enable future construction and operation of thermochemical cycles. The foundation should consist of laboratory to pilot scale evaluation of the process. The activities involved are experimental verification of reactions, process modelling, conceptual design and pilot plant runs. Based on experimental and pilot plant data presented from previous research, this study presents the simulation of the sulphur iodine thermochemical cycle as applied to the South African context. A conceptual design is presented for the sulphur iodine thermochemical cycle with the aid of a process simulator.

The low heating value (LHV) energy efficiency is 18% and an exergy efficiency of 24% was achieved. The estimated hydrogen production cost was evaluated at $18/kg.

Keywords: *Simulation; sulphur iodine; thermochemical cycle; low heating value; exergy.*

ACKNOWLEDGEMENTS

Special thanks go to the supervisors of this study: Dr. Percy van der Gryp at the School of Chemical and Minerals Engineering and Dr. Mike Dry from Arithmetek Inc. in Ontario, Canada.

Thank you to Mr. Frikkie van der Merwe and all my colleagues at the North West University's Potchefstroom Campus:

- Liberty Mapamba
- Bongibethu Hlabano Moyo
- Foster Mahlamvana
- Sakumzi Gwicana
- Richard Sutherland
- Sammy Rabie
- Andrew Phiri
- Takalani Enos Marubini

To my beloved parents and above all, the Almighty God, thank you.

TABLE OF CONTENTS

NOMENCLATURE

Symbol	Definition	SI Unit
E_η	Energy efficiency	-
E_ε	Exergy efficiency	-
ΔH_f	Standard enthalpy of formation	J/mol
ΔH_c	Standard enthalpy of combustion	J/kg
ε	Electric heat energy conversion efficiency	-
W	Electrical work	J/mol
Q	Heat energy	J/mol
ρ	Density of material/compound	kg/m^3
$	United States of America Dollar	-
€	European Union Euro	-
(g)	Gas phase	-
(l)	Liquid phase	-
(aq)	Aqueous phase	-
P	Pressure	Pa
R	Universal gas constant	J/K.mol
T	Temperature	K
V	Volume	m^3
C_P	Purchase cost	$
S	Size factor	-
C_V	Cost of empty vessel	$
F_M	Material factor	-
C_{PL}	Cost for platforms and ladders	$
W	Weight of the shell	kg
D_i	Internal diameter of vessel	m
P_d	Internal design gauge pressure	Pa
P_o	Operating pressure	Pa

Nomenclature continued

Symbol	Definition	SI Unit
t_S	Shell thickness	m
t_P	Vessel wall thickness	m
E	Weld efficiency	-
F_T	Motor type factor	-
C_B	Base cost	$
P_C	Power consumption	W
A	Surface area	m^2
F_L	Tube length correction factor	-
F_T	Pump type factor	-
F_{PR}	Production factor	-
F_{PI}	Piping and Instrumentation factor	-
H	Pump head	m
Q	Flow rate	m^3/s
C_{alloc}	Allocated costs for utility plants	$
C_{DPI}	Direct permanent investment	$
C_M	Module cost	$
C_{TDC}	Total depreciable capital	$

ABBREVIATIONS

ANL	Argonne National Laboratory
BIP	Binary Interaction Parameter
CEA	French “Commissariat å l’Energie Atomique”
CE	Chemical Engineering
CuCl	Copper-chlorine
COM	Cost of manufacture
CW	Cooling water
DCFRR	Discounted cash-flow rate of return
DW&B	Direct wages and benefits
ELECNRTL	Electrolyte Non Random Two Liquid
GA	General Atomics
GE	General expenses
HC	Hydrocarbon
HHV	Higher heating value
HTGR	High-temperature gas reactor
HyS	Hybrid sulphur
JAERI	Japan Atomic Energy Research Institute
LHV	Lower heating value
LLE	Liquid-liquid Equilibrium
LNG	Liquefied natural gas
MSE	Mixed solvent electrolyte
MW&B	Maintenance wages and benefits
M&O-SW&B	Maintenance and operations salary, wages and benefits
NIST	National Institute of Standards and Technology
NRTL	Non Random Two Liquid
NRTL-RK	Non Random Two Liquid-Redlich Kwong
PBD	Payback period
PC	Polar compound

Abbreviations continued

PEM	Proton exchange membrane
PID	Proportional integral derivative
PPS	Possible phase splitting
PTFE	Polytetrafluoroethylene
RK	Redlich Kwong
ROI	Rate of return on investment
RPI	Rensselaer Polytechnic Institute
RWTHA	Rheinisch-Westfalische Technische Hochschule Aachen
SDE	Sulphur dioxide depolarised electrolyser
SI	Sulphur iodine
SiC	Silicon carbide
SLE	Solid liquid equilibria
SMC	Special Metals Industries
SNL	Sandia National Laboratory
SRK	Soave Redlich Kwong
SRNL	Savannah River National Laboratory
TM	Trademark
UN	United Nations
UT	University of Tokyo
VHTR	Very high temperature reactor
VLE	Vapour-liquid equilibrium
VLLE	Vapour-liquid-liquid equilibrium

LIST OF FIGURES

List of figures continued

List of figures continued

LIST OF TABLES

List of tables continued

CHAPTER 1: Introduction

"A case is made for an energy regime in which all energy sources would be used to produce hydrogen, which could then be distributed as a non-polluting multipurpose fuel". (Gregory, 1973:1)

1.1 Background and motivation

The demand for energy is increasing every year, as most developing nations get industrialized and industrialized nations increase their productivity. Fossil fuels and oil contribute 86% and 33% of the total world energy respectively (World Energy Outlook, 2010). With an energy supply that is based on fossil fuels, there is so much uncertainty about the future of the world energy. Fossil fuels emit carbon based gases which are known as the green house gases. Green house gases have been proven to be the major cause of global warming. The United Nations (UN) conference held in Copenhagen in 2009 on climate change resulted in the signing of the Copenhagen Accord by major emitting countries (World Energy Outlook, 2010). The Accord sets a non-binding aim of limiting the increase of the global temperature by 2^{o} C. The aim can be achieved by cutting global emissions, meaning that there should be a cut in the use of fossil fuels. The energy demand will still be the same after a reduction in the use of fossil fuels; therefore a replacement fuel will need to be introduced to meet the demand. Alternative fuels have been suggested as one of the solutions to the problems brought about by the use of fossil fuels (Alternative Fuels Data Centre, 2011).

The alternative fuels are biodiesel, bio-ethanol and hydrogen. Biodiesel is produced by the trans-esterification of oils or fats and is a liquid similar in composition to fossil diesel. The main sources of the fuel are soy-bean oil, waste cooking oil and animal fat. Bio-ethanol is produced through the fermentation of sugars, starches and cellulose by the action of micro-organisms and enzymes. Corn grains and agricultural waste are one of the most common sources of bio-ethanol (Alternative Fuels Data Centre, 2011). Biodiesel and bio-ethanol have one major disadvantage, that some of the raw materials come from agricultural produce. The main method of obtaining food is through agriculture; therefore a diversion of some food products like soy bean into the energy sector will create a burden to the agriculture sector.

Hydrogen is not a natural fuel but can be synthesized from coal, oil, water or natural gas. Also it can be produced by splitting molecules of water when an electrical current passes through the water (Gregory, 1973:19). From an environmental perspective, hydrogen produced from water with a non polluting energy source is environmentally friendly because when hydrogen burns, its only combustion product is water. None of the fossil fuel pollutants – carbon based oxides, sulphur based oxides, hydro-flouro-carbons, particulates and photo-chemical oxidants can be produced in the combustion of hydrogen (Gregory, 1973:19). There are major disadvantages associated with the use of hydrogen as a fuel. Kreith & West (2004:249) argued that currently no available hydrogen technology, irrespective of the primary energy source to produce electricity has a comparable efficiency to using the electric power directly from any of the primary sources. Therefore it is implied that using hydrogen as an energy carrier has a disadvantage of energy losses due to inefficiencies of the technologies employed.

Methane gas constitutes 80% as a source of the hydrogen gas produced currently. 10 and 33.5% of produced hydrogen is used in the metallurgy and petroleum industries respectively today (Fraser, 2003:6). In comparison to different hydrogen production methods, electrolysis and thermochemical cycles do not depend on natural gas as the primary raw material. Producing hydrogen via electrolysis and thermo-chemical cycles has an advantage considering that the processes can be run at low temperatures and emissions can be controlled depending on the energy source. However high temperature electrolysis is more favoured than the traditional room temperature electrolysis because the process is cheaper when energy is supplied as heat and the electrolysis reaction is faster at high temperatures.

In thermochemical processes, water, heat and electricity are the inputs; hydrogen and oxygen are produced by a series of reactions (Mullin *et al.* 2006:3). The reactants are compounds which are consumed and regenerated within the process. The reactions occurring within are fired thermally or through electrical energy. Heating, cooling and separation processes are applied to reaction products between reaction vessels. Normally hydrogen and oxygen are produced and separated in different reactions or sections. This eliminates the problem of having a mixture of the two gases, hydrogen and oxygen. Figure 1.1 shows a basic two reaction steps thermochemical cycle.

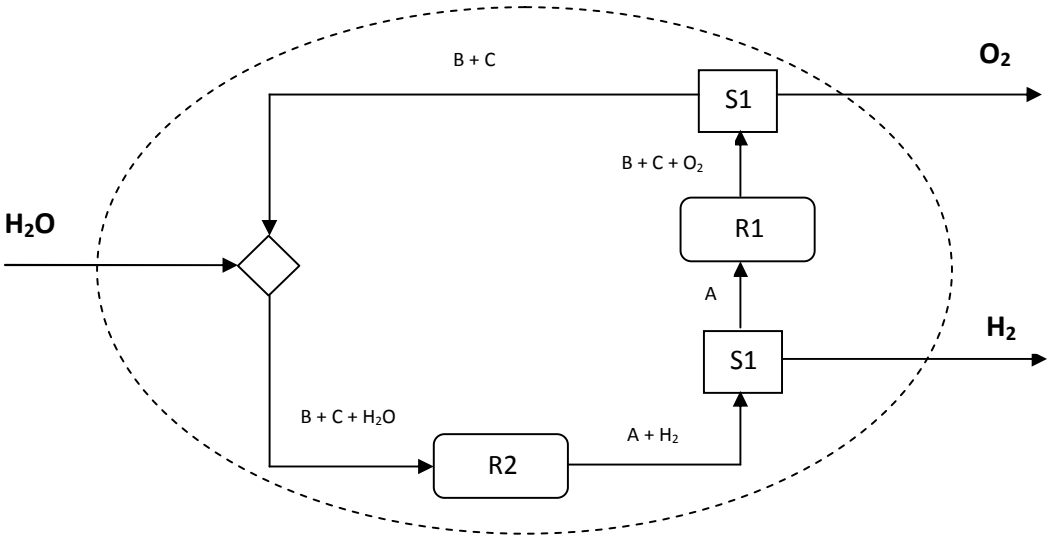

Figure 1.1: Basic two step thermochemical cycle

It is assumed that the two reactions take the form of Equation 1.1 and 1.2 and take place in reactors R1 and R2.

$$A \longrightarrow B + C + O_2 \quad (1.1)$$

$$B + C + H_2O \longrightarrow A + H_2 \quad (1.2)$$

In Figure 1.1 and Equations 1.1 to 1.2, a simple two step thermochemical cycle involves reactant A decomposing into B, C and oxygen in reactor R1. Oxygen is separated from the other products in separator S1, and, B and C are sent to the next reactor R2, where water is added by means of a mixer. B and C are oxidized into A and hydrogen is produced in reactor R2. Hydrogen is separated and A is sent to the first reactor, completing the thermochemical cycle. It is clear from Figure 1.1 and Equations 1.1 to 1.2 that the process only consumes water and the end products are oxygen and hydrogen.

Unlike high temperature electrolysis, thermo-chemical cycles can convert low-level thermal energy directly into chemical energy; the temperature of operation can go as low as 500^{o}C compared to 2000^{o}C in high temperature water electrolysis. Graf *et al.* (2008:4511) performed an economic sensitivity analysis for three different solar powered hydrogen producing technologies, i.e. hybrid sulphur thermo-chemical cycle, metal oxide based thermo-chemical cycle and electrolysis. The hydrogen costs compared well with that for electrolysis. Thermochemical

cycles are set to be the solution for large scale production of hydrogen to meet the consumer market because they are continuous processes with water as the main feedstock. There are over 200 documented thermo-chemical cycles (Funk, 2001:185). Conceptual studies and design of different thermochemical cycles have been presented by different authors. Leybros *et al.* (2009:9060), Gonzales *et al.* (2009:4179), Chukwu (2008:1) and Gorensek & Summers (2009:4097) presented the conceptual designs and simulations of the sulphur iodine, copper sulphate, copper chlorine, and hybrid sulphur cycles respectively. Included in the conceptual designs presented where the unit production costs for the processes. Table 1.1 shows a summary of the thermochemical cycles.

Table 1.1: Summary of thermo-chemical cycles.

Cycle	Operating Temperature (^{o}C)	Production Cost ($/kg)	Year of evaluation	Factored cost
Sulphur Iodine	867	1.95 (1)	2009	1.95
Hybrid Sulphur	867	1.60 (2)	2005	1.78
Copper Chlorine	540	2.02 (1)	2009	2.02
Copper Sulphate	850	>2.50 (3)	2009	>2.50
UT-3	760	5.00 (4)	1996	6.84
Hybrid Chlorine	850	3.00 (5)	2009	3.00

(1) Wang *et al.* (2009:1); (2) Summers & Buckner (2005:324); (3) Gonzales *et al.* (2009:4179); (4) Sakurai *et al.* (1996a:866); (5) Gooding (2009:4177)

To factor for the time value of money, annual chemical (CE) indices given by the Chemical Engineering journal, (Chemical Engineering, 2011) are used. 2009 is chosen as the base year to create the factored cost column on the table. Sakurai *et al.* (1996a:866), evaluated the production cost for the UT-3 cycle as $35/GJ which translates to a cost of $5/kg.

From Table 1.1, the copper chlorine cycle has the lowest temperature of operation which makes it favourable; however the presence of solid reactants within the processes is a major drawback. It is clear that the two sulphur based thermochemical cycles have low hydrogen production costs. Sulphur cycles are considered one of the simplest thermochemical cycles comprising of only fluid reactants and a few reaction steps, two and three for the hybrid sulphur and sulphur iodine cycles respectively (Gorensek & Summers, 2009:4098). Unlike the hybrid sulphur cycle, the sulphur iodine cycle is purely thermochemical. A cycle is considered hybrid when one of the

reactions requires an electrical input, for example, an electrolysis reaction occurring within the cycle of reactions. It is against this background that the sulphur iodine cycle was chosen for study in this dissertation.

Conceptual studies and design of the sulphur iodine thermochemical cycle have been presented by different authors (Leybros *et al.* 2010:1018; Wang *et al.* 2009:1; Norman *et al.* 1977:2; Goldstein *et al.* 2005:619). The studies have been done with support from different institutions such as General Atomic, Savannah River National Laboratory, Sandia National Laboratory and Argonne National Laboratory. Research is being undertaken to evaluate the possibility of using platinum based catalysts for the high temperature decomposition of sulphuric acid (Ginosar *et al.* 2007:482). South Africa has become the focus of the world for the research and development of the production of hydrogen because South Africa has 75% of the world's platinum mineral deposits (Cawthorn, 1999:481). Generally, some of the studies that have been presented concerning the SI cycle have not addressed the following issues:

- The suitable technology and materials of construction used
- The resulting product selling price
- A presentation of a detailed process heat exchanger network
- A detailed exergy analysis
- The possibility of matching of the SI cycle with a high temperature source

In an effort to foster the research and development on the production of hydrogen, The South African Department of Science and Technology, through the National Hydrogen and Fuel Cells Technologies Research, Development and Innovation Strategy established Hydrogen South Africa (HySA) in 2007. HySA is based in three competence centres:

- HySA Systems hosted by the University of Western Cape, is a technology validation and systems integration centre on hydrogen and fuel cell technology (HySA, 2011)
- HySA Catalysis co-hosted by the University of Cape Town and MINTEK, focuses on catalysis associated with the hydrogen production and storage (HySA, 2011)

- HySA Infrastructure co-hosted by the North West University and the Centre for Scientific and Industrial Research (CSIR) which focuses on a number of key technologies in hydrogen production, storage and distribution. Further research on the production of hydrogen from other energy generators such as natural gas, biomass, solar, wind, and nuclear is intended (HySA, 2011)

This study falls under the HySA Infrastructure in the Department of Chemical and Minerals Engineering at the North West University and is intended to be a contribution to research on hydrogen production through the SI cycle in view of the South African context. However not all the shortcomings pointed out can be addressed, but a detailed heat exchanger network, an exergy analysis and an economic analysis to determine the product selling price are performed.

1.2 Objectives

The main objective of this study is to develop an Aspen Plus^{TM} simulation of the sulphur iodine cycle for the production of hydrogen. The sub-objectives of this study are as follows:

- To give a conceptual design of the sulphur iodine cycle for 1 kmol/s hydrogen production.
- Complete an economic and energy analysis of the sulphur iodine thermochemical cycle
- Present a comparison with other studies that have been done.

1.3 Scope of study

The hydrogen produced is assumed to meet the hydrogen demand for the replacement of fossil fuels used in the transport industry. South Africa is the target market, and a design basis is determined via the market survey. Aspen Plus^{TM} is the simulation package that is going to be used for the production of flowsheets. In the design optimisation, emphasis is on the energy efficiency and economic viability of the process. The dissertation is structured as follows, with Figure 1.2 showing a summary of the scope:

- Chapter 1: Introduction – Details of the background and motivation, objectives and scope of the study.
- Chapter 2: Literature survey – Literature study of hydrogen production and special attention on different types of thermochemical cycles.
- Chapter 3: Design Framework – Process design, market survey and design basis.
- Chapter 4: Simulation Framework – Simulation packages, their selection and validation.
- Chapter 5: Aspen Plus™ Process Simulation – Conceptual development of the sulphur iodine cycle.
- Chapter 6: Process Energy Optimisation – Heat integration, exergy and energy analysis.
- Chapter 7: Economic Evaluation – Estimation of investment cost, product selling price and profitability analysis.
- Chapter 8: Conclusion and Recommendations – Conclusions and recommendations for future work.

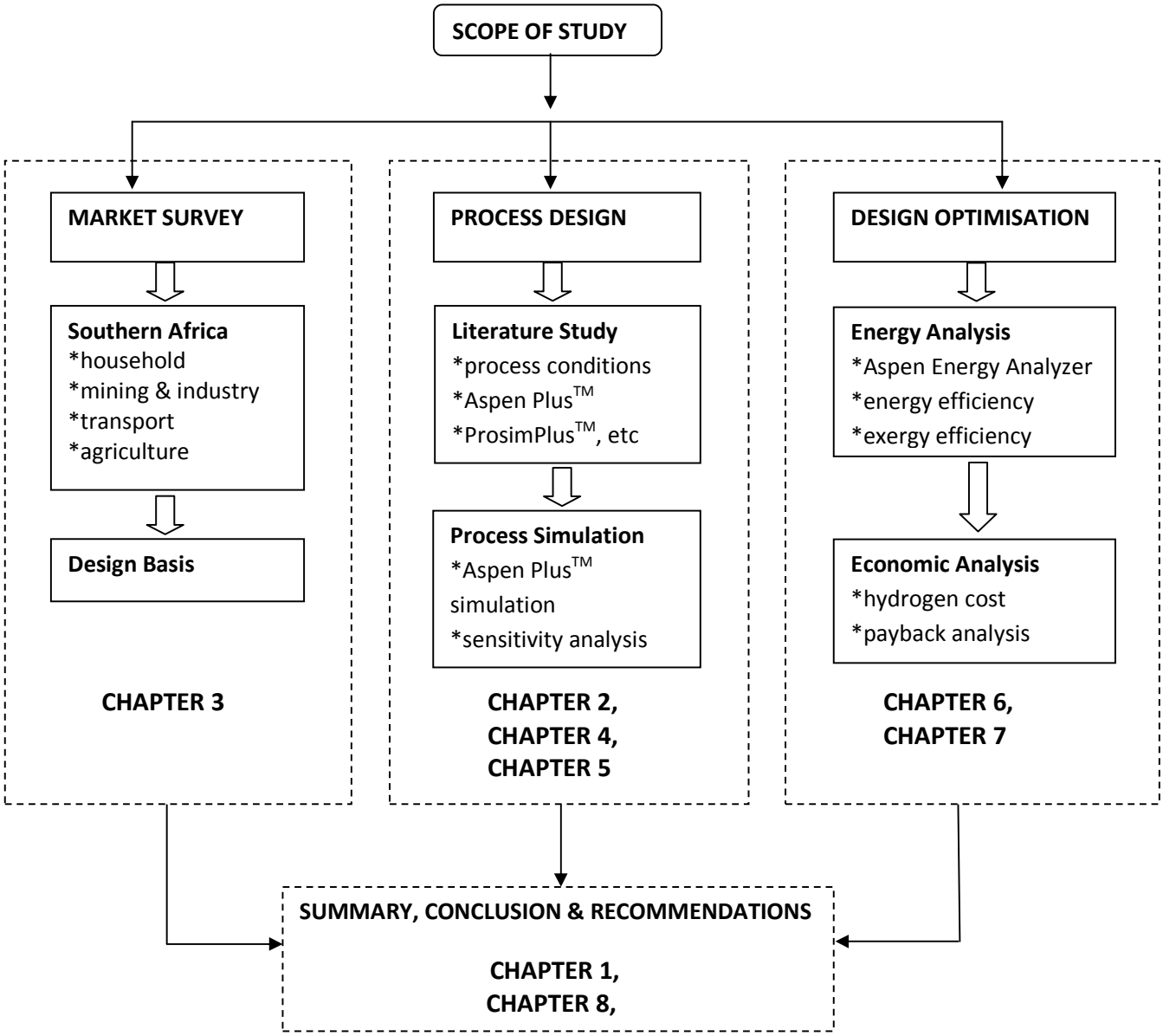

Figure 1.2: Scope of study

1.4 References

ALTERNATIVE FUELS DATA CENTRE. 2011. Alternative Fuels Report. http://www.afdc.doe.gov/afdc. Date of access: 04 Sep 2010

CAWTHORN, R.G. 1999. The platinum and palladium resources of the Bushveld Complex. *South African Journal of Science,* **95**:481-489, Nov.

CHEMICAL ENGINEERING. 2011. Economic Indicators. http://www.che.com. Date of access: 25 Sep 2011

CHUKWU, C. 2008. Process analysis and Aspen Plus simulation of Nuclear-based Hydrogen production with a Copper-Chlorine Cycle. Ontario: UOIT. (Dissertation – M.Sc.) 125p.

FUNK, J.E. 2001. Thermochemical hydrogen production: Past and Present. *International Journal of Hydrogen Energy,* **26**:185-190, Feb.

FRASER, D. 2003. Solutions for Hydrogen Storage and Distribution. (Presentation at The PEI Wind-Hydrogen Symposium on June 22 -24, 2003)

GINOSAR, D.M., GLENN, A.W., PETKOVIC, L.M. & BURCH, K.C., 2007. Stability of supported platinum sulfuric acid decomposition catalysts for use in thermochemical water splitting cycles. *International Journal of Hydrogen Energy,* **32**:482-488, Apr.

GOLDSTEIN, S., BORGARD, J.M. & VITART, X. 2005. Upper bound and best estimate of the efficiency of the iodine sulfur cycle. *International Journal of Hydrogen Energy*, **30**:619-626, Aug.

GONZALES, R.B., LAW, V.J. & PRINDLE, J.C. 2009. Analysis of the hybrid copper oxide–copper sulfate cycle for the thermo-chemical splitting of water for hydrogen production. *International Journal of Hydrogen Energy,* **34**:4179-4188, Dec.

GOODING, C.H. 2009. Analysis of alternative flow sheets for the hybrid chlorine cycle. *International Journal of Hydrogen Energy,* **34**:4168-4178, Jul.

GRAF, D., MONNERIE, N., ROEB, M., SCHMITZ, M. & SATTLER, C. 2008. Economic comparison of solar hydrogen generation by means of thermo-chemical cycles and electrolysis. *International Journal of Hydrogen Energy,* **33**:4511-4519, May.

GREGORY D.P. 1973. The Hydrogen Economy. *Scientific American,* **228**:13-21, Jan.
HYSA. 2010. HySA systems. http://hydrogen.qsens.net/centers-of-competence/hysa-systems. Date of access: 12 Sep 2010

KREITH, F. & WEST, R. 2004. Fallacies of a Hydrogen Economy: A Critical Analysis of Hydrogen Production and Utilization. *Journal of Energy Resources Technology,* **126**: 249-257, Dec.

LEYBROS, J., GILARDI, T., SATURNIN, A., MANSILLA C. & CARLES, P. 2010. Plant sizing and Evaluation of hydrogen production costs from advanced processes coupled to a nuclear heat source. Part I: Sulphur-Iodine cycle. *International Journal of Hydrogen Energy,* **35**:1008-1018, Jan.

LEYBROS, J., GILARDI, T., SATURNIN, A., MANSILLA C. & CARLES, P. 2010. Plant sizing and Evaluation of hydrogen production costs from advanced processes coupled to a nuclear heat source. Part II: Hybrid-Sulphur cycle. *International Journal of Hydrogen Energy,* **35**:1019-1028, Jan.

MULLIN, S., ODI, U. & TARVER, J. 2006. Evaluation and Design of Thermochemical and Hybrid Water Splitting Cycles. (Report delivered to the Department of Chemical Engineering, University of Oklahoma in May 2006.) Norman. 29p.

NORMAN, J.H., RUSSELL, J.L., PORTER, J.T., McCORKLE, K.H., ROEMER T.S. & SHARP, R. 1978. Process for the thermochemical production of hydrogen. Patent: US 4,089,940. 6p.

WANG, Z.F., NATERER, G.F., GABRIEL, K.S., GRAVELSINS, R. & DAGGUPATI, V.N. 2009. Comparison of sulfur–iodine and copper–chlorine thermo-chemical hydrogen production cycles. *International Journal of Hydrogen Energy,* **xxx:** 1-11, Sep.

WORLD ENERGY OUTLOOK. 2010. Executive Summary. http://www.worldenergyoutlook.org. Date of access: 25 Sep 2011

CHAPTER 2: Literature survey

"A man's feet must be planted in his country, but his eyes should survey the world" George Santayana

2.1 Introduction

The demand for more energy and electrification will increase as developing countries get fully industrialised, at the same time, the petroleum fuel reserves will be disappearing. Petroleum is mainly used in the transport industry. The energy consumption share for the transport industry is 20%. Figure 2.1 shows the share of energy consumption for South Africa in 1990 (Winkler, 2006:24)

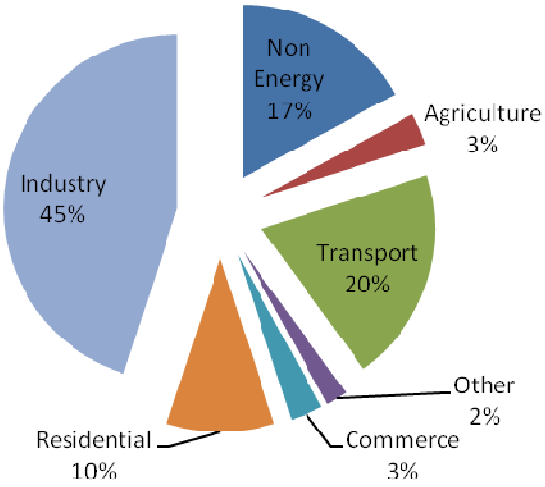

Figure 2.1: Share of energy consumption in South Africa, 1990 (Winkler, 2006:24).

The Non Energy sector consumes 17% of the total energy; this is the energy resource that is converted into another product such as wood being converted to paper.

There are alternative energy sources to petroleum, the most common being biodiesel, light natural gas and ethanol. Hydrogen and natural gas have major sources which do not depend on agriculture, but natural gas may face the same problem as that of petroleum reserves, as the underground natural gas reserves may run out in the future. Compared to natural gas, energy

transferred through hydrogen as a carrier has zero emissions when used in fuel cell applications. Therefore in anticipation of the expected energy crisis there will be a need for supplementation and the eventual substitution of fossil fuels with clean energy supplied in the form of hydrogen as a carrier. The estimated annual world total consumption of electricity in 2002 was 16PWh and when extrapolated to the year 2050 could range between 36 – 82PWh, also the estimated world vehicle fleet of about 900 million vehicles consuming about 360 billion gallons of petrol will increase to about 1.5 billion vehicles in 2050 and could be operated by 260 billion kilograms of hydrogen (Kruger, 2005:1515). To meet the demand, there should be a large scale production of hydrogen.

2.2 Hydrogen production

2.2.1 Introduction

The steam-iron process is one of the oldest methods for producing hydrogen from a wide variety of fossil fuels such as coal (Hacker *et al.* 2000:531). Today, almost half the hydrogen produced in the world is obtained from natural gas via steam reforming process (Padro & Lau, 2002:2). The energy efficiency of the processes for hydrogen production varies around 50 – 60%. Energy efficiency in this dissertation is defined as the ratio of the energy output to the energy input for a process that is converting one form of energy to another. The different methods of producing hydrogen are as follows:

- Steam reforming
- Partial oxidation
- Steam-iron process
- Thermal decomposition
- Electrolysis
- Thermo-chemical processes

2.2.2 Methods of producing hydrogen

In **steam reforming**, natural gas or other fossil fuel such as coal or hydrocarbons reacts with high pressure steam in a catalytic converter. The process strips away the hydrogen atoms, leaving carbon dioxide as the by product. Coal can be reformed through the gasification process to produce hydrogen, but this is more expensive than using natural gas and also releases more CO_2. Steam reforming is energy intensive since it operates at very high temperatures (850 – 950^{o}C) and pressure (35 atm), the energy efficiency is seldom greater than 50% (Padro & Lau, 2002:2). Steam reforming of ethanol has also been reported with ethanol conversion as high as 98% at 380^{o}C and 100% at 500^{o}C (Sun *et al.* 2004:1075). One major disadvantage of steam reforming is the production of carbon dioxide gas.

In **partial oxidation** processes, a hydrocarbon fuel such as ethanol or methanol and oxygen or air are combined in proportions such that the fuel is converted into a mixture of H_2 and CO

(Padro & Lau, 2002:2). There are several modifications of partial oxidation processes, depending on the composition of the feed and type of the fossil fuel used. Partial oxidation processes can be carried out as catalysed reactions. The non-catalytic partial oxidation process operates at high temperatures (1100-1500°C), and can use any possible feedstock, including heavy oils and coal (Padro & Lau, 2002:2). The catalytic process is carried out at lower temperatures (600-900°C) and in general, uses light hydrocarbon fuels as feedstock, e.g. natural gas and naphtha. A conversion efficiency of 50% has been reported by Lyubovsky *et al*. (2004:114).

The **steam-iron process** is one of the oldest methods for producing hydrogen from a wide variety of fossil fuels, such as coal and petrochemical products (Hacker *et al.* 2000:531). The steam iron process produces high-purity hydrogen (CO < 10ppm) by separating the hydrogen production and fuel oxidation steps using an iron oxide reduction-oxidation regenerative system. The steam iron process has been modified for fuel cell applications, where the sponge iron is oxidised in a multiple bed reactor to provide high-purity hydrogen to a fuel cell. Depleted beds are regenerated by a reduction reaction using synthesis gas delivered from a methane-fuelled steam reformer. The process is multi-stage, requires high temperatures for the reduction of the magnetite (Fe_3O_4) to sponge iron and has an additional step of natural gas steam reforming (Padro & Lau, 2002:3). Practically all carbon present in a hydrocarbon fuel used for hydrogen production is converted into carbon dioxide and vented to the atmosphere. Bleeker *et al*. (2009:125) reported energy conversion efficiency of 53% for the pyrolysis of oil using the steam iron process.

Thermal decomposition processes, thermally decompose hydrocarbon fuel, particularly natural gas, into its constituent elements; hydrogen and carbon. Thermal decomposition has been employed for the production of carbon black with hydrogen being a by-product and supplementary fuel for the process (Padro & Lau, 2002:3). Currently, thermal decomposition processes, as a source of carbon black, have very limited applications. Thermal decomposition of water has also been practiced (Baykara, 2004:1452), more specifically solar thermolysis. Reactor operation is at temperatures above 2200^{o}C and at atmospheric or sub-atmospheric pressure levels. A 31% energy conversion efficiency is predicted by Maag *et al.* (2009:7676) for the solar thermal decomposition of methane.

In **electrolysis**, water is decomposed into hydrogen and oxygen in an electrolysis cell upon the passage of an electrical current through a conductive electrolyte. Hydrogen is produced at the cathode whilst at the same time oxygen is produced at the anode of the electrolysis cell. By mid nineteenth century, electrolysis of water was the cheapest method of producing hydrogen (Bockris *et al.* 1984:179). High temperature electrolysis involves a supply of heat energy which results in high temperature, this process is more efficient than room temperature electrolysis as the heat supplied will result in less electrical energy being supplied to the electrolysis cell, bearing in mind that electrical energy is more expensive than heat. Above all, high temperatures increase the rate of electrolysis reaction. Water electrolysis using proton exchange membrane (PEM) based electrolysers is receiving much attention in the field of research and development and increased efficiency has been reported by several research authors. The theoretical voltage to decompose pure water is 1.23 V, but in industrial applications, conventional electrolysers need at least 1.7 to 2.0 V (Gorensek & Summers, 2009:4099).

In **thermo-chemical processes**, water, heat and electricity are the inputs, hydrogen and oxygen are produced by a series of reactions (Mullin *et al.* 2006:3). The reactants are compounds which are consumed and regenerated within the process. Hybrid cycles include both thermo-chemical and electrochemical reactions for water splitting. This technology offers the possibility of lower temperatures in process reactions and the possibility of using electricity as a substitute for one of the chemical reactions (Summers, 2009:5). The use of nuclear energy or solar as the heat source for a large-scale hydrogen production operation could result in substantially lower carbon emissions (Schultz, 2003:13). Nuclear power plants with graphite moderated high temperature reactors are also capable of co-generating electricity and hydrogen which could provide additional commercial flexibility. The energy conversion efficiency was evaluated to be 42% (Gorensek & Summers, 2009:4099).

Table 2.1 gives a comparative summary of some of the different types of hydrogen production methods.

Table 2.1: Hydrogen production methods.

Process	**Possible Inputs**	**Operating temperature (^oC)**	**Environmental Impact**	**Efficiency %**
Steam reforming	Natural gas, fossil fuel, ethanol, catalyst, heat	850 - 950	CO_2, SO_x and NO_x emissions	50[(1)]
Partial oxidation	Natural gas, fossil fuel, light hydrocarbons e.g. naphtha, heat	600 – 1500	CO_2, SO_x and NO_x emissions	50[(2)]
Steam-Iron	Natural gas, fossil fuel, catalyst, heat	>1000	CO_2, SO_x and NO_x emissions	53[(3)]
Thermal decomposition	Natural gas, water, heat	2200	CO_2, SO_x and NO_x emissions	53[(4)]
Electrolysis	Water, electricity, heat	25 – 2000	Clean if electricity is from hydro power plant	68[(5)]
Thermo-chemical cycle	Water, electricity, heat	>500	Clean if heat is from a clean source	42[(6)]

(1) (Padro & Lau, 2002:2); (2) Lyubovsky *et al.* (2004:114); (3) Bleeker *et al.* (2009:125); (4) Maag *et al.* (2009:7676); (5) (Gorensek & Summers, 2009:4099); (6) (Gorensek & Summers, 2009:4099).

2.2.3 Comparison of hydrogen production methods

It is clear from Table 2.1 that the efficiencies of the hydrogen production methods mentioned varies from 50 to 60% and all the methods have negative environmental impact except electrolysis and thermochemical cycles. The amount of carbon dioxide, SO_x and NO_x gases emitted into the atmosphere when hydrogen is produced by methods other than electrolysis and thermochemical cycles is destructive to the atmosphere. Producing hydrogen via electrolysis and thermo-chemical cycles has an advantage considering the following:

- processes can be run at low temperatures and emissions can be controlled depending on the energy source
- the major raw material is water
- the processes can be coupled with solar energy

Unlike electrolysis, thermo-chemical cycles for splitting water can convert low-level thermal energy directly into chemical energy by forming hydrogen and oxygen. Water splitting is achieved by a series of reactions within the cycle. The overall result is a mole of water input producing a mole of hydrogen and half a mole of oxygen. Graf *et al.* (2008:4511) performed a sensitivity analysis for three different solar powered hydrogen producing technologies, i.e. hybrid sulphur thermo-chemical cycle, metal oxide based thermo-chemical cycle and electrolysis. The hydrogen costs were $7.7/kg for the hybrid sulphur cycle, $9.5/kg for the metal oxide based cycle and $8.2/kg for electrolysis based on a Euro to US$ exchange rate of 1.42. The results show that there are some thermo-chemical cycles from the possible over 200 documented cycles that can produce hydrogen at much lower costs than electrolysis. The investment of a hybrid sulphur cycle is almost 17 times than that of an electrolysis plant. The high investment is attributed by the construction of a complex chemical plant composed mostly of acid corrosion resistant and high temperature construction materials. A hybrid thermo-chemical cycle integrates a Brayton Cycle (Graf *et al.* 2008:4516; Gorensek & Summers, 2009:4099; Simpson *et al.* 2005:1243). Therefore, a hybrid cycle can generate its own electricity, hence the electrical energy supplied to the cycle is bound to be lower than that supplied to an electrolysis plant. This becomes more significant when the cost of electricity is high. The operation and maintenance

costs of electrolysis are considerably higher than that of the hybrid sulphur cycle (Graf *et al.* 2008:4518).

The theoretical voltage for the electrolysis of pure water is 1.23V. However, the majority of conventional electrolysers need at least 2.0 V when economically reasonable current densities are maintained (Gorensek & Summers, 2009:4099). This value translates to a water electrolysis electrical efficiency of about 62%. If a thermal-to-electric conversion efficiency of 45% is assumed (HTGR powered electrolysis), the total heat requirement is 895kJ/mol H_2 (Leybros *et al.* 2009:9073).

Although very few thermo-chemical cycle plants have been commissioned, the efficiencies reported by various authors are slightly higher than that of electrolysis and the total heat requirement is lower than 895kJ/mol H_2 (Leybros *et al.* 2009:9073; Gorensek & Summers, 2009:4097; Lewis *et al.* 2005:10; Chukwu, 2008:79).

2.3 Overview: Thermochemical cycles

2.3.1 Introduction

A number of thermo-chemical cycles have been studied since the early 1960's (Funk, 2001:185). Many cycles have been published, i.e. over 200 cycles. Not many cycles have been put through the rigorous chemical engineering process of detailed thermodynamic calculations, laboratory testing to verify the calculations or to develop necessary chemical and physical properties, preparation of process flowsheets including mass and energy balances and showing low, temperature, pressure and composition throughout the process, equipment design, and finally making the cost estimates which yield both capital and operating costs (Funk, 2001:189). A selection has to be made from the wide range of thermo-cycles that have been studied. The selection was made in the International Round Table on Direct Production of Hydrogen from a nuclear heat source that was held at Ispra in Italy in 1969. The Ispra program had 24 cycles selected and documented, the most studied of the 24 Ispra cycles are shown in Table 2.2 together with the institutions concerned with the study and development of the cycles (Funk, 2001:187)

Table 2.2: Some of the Ispra program documented cycles

Name of cycle	**Ispra Name**	**Institution**	**Key Issues**
Hybrid Sulphur	MARK 11	SRNL, SNL	Electrolysis, peak temperature 850^{o}C , two reactions
Sulphur Bromine	MARK 13	ANL	Electrolysis, peak temperature850^{o}C, three reactions
Iron Chloride	MARK 14	ANL, RPI, RWTHA	Purely thermochemical, peak 650^{o}C, five reactions
Iron Chloride	MARK 15	ANL, RPI, RWTHA	Purely thermochemical, peak 650^{o}C, four reactions
Sulphur Iodine	MARK 16	GA, JAERI, SNL, CEA	Purely thermochemical, peak 850^{o}C, three reactions

The thermochemical cycles described in Table 2.2 are the most commonly studied of the 24 Ispra family of cycles. Ispra Mark 11 and Ispra Mark 16 are known as the Hybrid Sulphur and Sulphur Iodine cycles respectively (Leybros *et al.* 2009:9073; Gorensek & Summers, 2009:4097).

The conclusions arrived at, during the Ispra program were as follows:

- Thermochemical production of hydrogen is demonstrated and feasible.
- Construction materials for industrial-scale plants have been identified, improved materials could be developed.
- Overall thermal efficiency of industrial-scale processes can be higher than 35%.
- Industrial pilot plants can already be built with the present knowledge, chemical engineering data and commercial materials are available, no critical break-through is necessary.
- Improvements in technological solutions and chemical engineering design are still possible.
- Detailed cost evaluations are not yet possible, but the hydrogen production cost, with rough estimates is nearly the same as for advanced electrolysis.
- Economic competitiveness is likely, using nuclear heat sources (HTGR) and dedicated plants of very large size.
- Small-size plants are not competitive.
- The availability of the nuclear heat source is critical if the HTGRs are not commercialised, it is difficult to find other suitable heat sources.

After the Ispra research, thermochemical decomposition of water for hydrogen production was transformed from a theoretical ideal to a practical, promising reality; even if there are challenging problems for chemical and nuclear engineers, the prospects are good in the long term. After the Ispra program, more thermochemical cycles have been developed, the cycles include:

- Copper chlorine cycle
- Hybrid chlorine cycle
- UT-3 process

The following sections describe two thermochemical cycles presented during the Ispra program, i.e. Ispra Mark 11 (Hybrid Sulphur cycle) and Ispra Mark 16 (Sulphur Iodine cycle) including three cycles, Copper chlorine, Hybrid chlorine and UT-3 cycles. which were developed outside the Ispra program

2.3.2 The sulphur iodine (Ispra Mark 16)

The Sulphur Iodine cycle (SI) also called Ispra Mark 16, is a three reaction cycle involving, sulphur and iodine based species. The main reaction is the endothermic decomposition of sulphuric acid at very high temperatures.

The SI cycle has been extensively studied at General Atomics (GA), since the 1970's (Funk, 2001:188). A patent was presented by GA in 1978 which detailed another version of the cycle (Norman *et al.* 1977:2).

The SI cycle consists of three steps:

Step 1: Sulphuric acid decomposition into water, oxygen and sulphur dioxide in two successive reactions involving the formation of sulphur trioxide at temperatures below 800^{o}C as the sulphuric acid rapidly vaporizes above 800^{o}C, sulphur trioxide totally decomposes to sulphur dioxide and oxygen as shown in Reactions 2.1 and 2.2 (Leybros *et al.* 2009:9062; Gorensek & Summers, 2009:4098; Jeong *et al.* 2005:3; Goldstein *et al.* 2005:619)

$$H_2SO_{4(aq)} \longrightarrow SO_{3(g)} + H_2O_{(g)} \qquad (397^{o}C) \qquad (2.1)$$

$$SO_{3(g)} \longrightarrow SO_{2(g)} + {}^{1}/_{2}O_{2(g)} \qquad (867^{o}C) \qquad (2.2)$$

Step 2: The Bunsen reaction is a liquid phase exothermic reaction, involving iodine, sulphur dioxide and water, the products are two immiscible aqueous acids, aqueous sulphuric acid (light phase) and a mixture of hydrogen iodide, iodine and water commonly named as HI_x (heavy phase) (Goldstein *et al.* 2005:619). The reaction is summarised as follows:

$$I_{2(l)} + SO_{2(aq)} + 2H_2O_{(l)} \longrightarrow H_2SO_{4(aq)} + 2HI_{(l)} \qquad (120^{o}C) \qquad (2.3)$$

Step 3: This step is the thermal decomposition of hydrogen iodide and has a low endothermic heat of reaction.

$$2HI_{(l)} \longrightarrow I_{2(l)} + H_{2(g)} \qquad (450^{o}C) \qquad (2.4)$$

All the reactions are purely thermo-chemical and this reduces the amount of electrical power input, on the other hand the thermal energy input is expected to rise. The SI cycle schematic is shown in Figure 2.2.

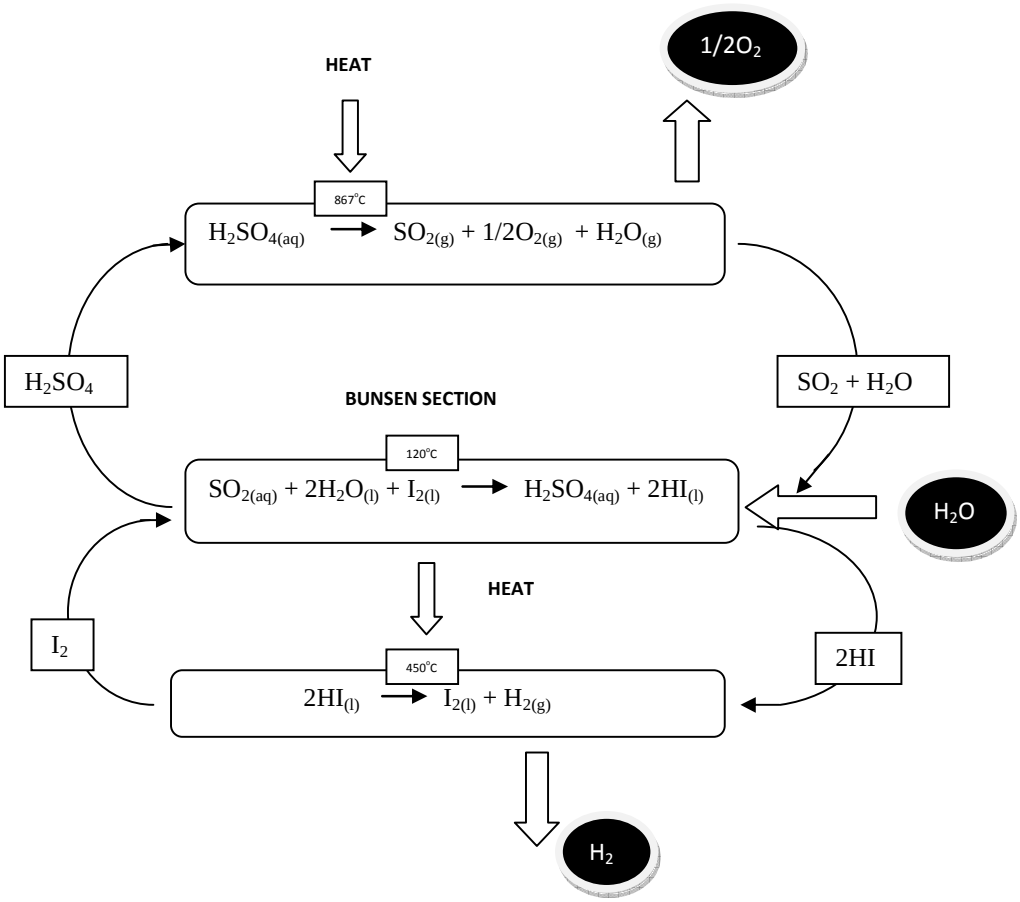

Figure 2.2: The SI cycle schematic

The SI cycle has been regarded as a large scale, cost effective and environmentally friendly cycle to the extent that GA has invested approximately 8 million dollars on the project itself (Funk, 2001:188). More research work on the SI cycle is still done at the Japan Atomic Energy Research Institute (JAERI), Korea Institute of Energy Research, the Technical University at Aachen in Germany and the French "Commissariat å l'Energie Atomique" (Leybros *et al.* 2009:9060; Kubo *et al.* 2004:347; Cho *et al.* 2009:501). However, the very high temperatures involved in the sulphur family of cycles pose a major drawback to the coupling of these cycles with first and second generation reactors, whereas third and the perceived fourth generation reactors can be couple with them and cost factors will definitely come into play. On the other

hand, high temperature solar sources have been reported to reach 2000^{o}C (Schultz, 2003:16), solar is an attractive alternative source, especially in Africa, although much research is needed to ascertain its use to drive large scale processes. The cost of producing hydrogen from the SI cycle was estimated to be $15/kg (€12/kg) for a hydrogen production capacity of 1 kmol/s (≈150 t/day), (Leybros *et al.* 2010a:1008) which is a high cost compared to other cycles. Many uncertainties were attached to this evaluation, as the author mentioned that the accuracy of the method used to calculate investment cost was +/- 30%. This makes it difficult to compare the cost with other competing thermo-chemical cycles. Wang *et al.* (2009:9) estimated a production cost of $1.60 – 1.93/kg for a production capacity of 200 million t/yr.

A number of experimental evaluations for the reactions occurring in the SI cycle have been done (Kubo *et al.* 2004:347; Nakajima *et al.* 1999:1). A continuous and closed cycle operation of the SI process was demonstrated at lab scale and pilot plant scale experiments are underway at the JAERI. Wong *et al.* (2007:497) presented an evaluation of the construction materials that can be used for the SI cycle. Immersion coupon corrosion tests were performed to screen materials selected from four classes of corrosion resistant materials: refractory metals, reactive metals, ceramic, and super alloys. Only Ta and Nb-based refractory metals and ceramic mullite were reported to stand up to the extreme environment in the SI cycle.

2.3.3 The hybrid sulphur cycle (Ispra Mark 11)

The Hybrid Sulphur cycle has other names such as Ispra Mark 11 and The Westinghouse cycle. It is a two step reaction cycle. The main reaction in the sulphur family of cycles is the decomposition of sulphuric acid at very high temperatures, which is endothermic.

The cycle was developed at Westinghouse Electric Corporation in the early 70's. A patent for "Electrolytic decomposition of water", US Patent number 3888750, was issued in 1975 (Brecher & Wu, 1975:1).

The HyS cycle consists of two main steps:

Step 1: Sulphuric acid is decomposed into water, oxygen and sulphur dioxide in two successive reactions involving the formation of sulphur trioxide at temperatures below 800^{o}C as the sulphuric acid rapidly vaporizes, at above 800^{o}C, sulphur trioxide totally decomposes to sulphur dioxide and oxygen as shown in Reactions 2.5 and 2.6 (Leybros *et al.* 2009:9062; Gorensek & Summers, 2009:4098; Jeong *et al.* 2005:3; Goldstein *et al.* 2005:619);

$$H_2SO_{4(aq)} \longrightarrow SO_{3(g)} + H_2O_{(g)} \qquad (397^{o}C) \qquad (2.5)$$

$$SO_{3(g)} \longrightarrow SO_{2(g)} + 1/2O_{2(g)} \qquad (867^{o}C) \qquad (2.6)$$

Overall reaction is;

$$H_2SO_{4(aq)} \longrightarrow SO_{2(g)} + 1/2O_{2(g)} + H_2O_{(g)} \qquad (2.7)$$

The temperatures are approximate and depend on the pressures ranging from 10 to 100 bars.

Step 2: Sulphur dioxide is oxidised, in a process called the sulphur dioxide depolarised electrolysis, to form sulphuric acid, protons and electrons. The protons are attracted to the cathode across the electrolyte separator, where they recombine with electrons to form hydrogen gas:

$$SO_{2(aq)} + 2H_2O_{(aq)} \longrightarrow H_2SO_{4(aq)} + 2H^{+} + 2\grave{e} \qquad (2.8)$$

$$2H^{+} + 2\grave{e} \longrightarrow H_{2(g)} \qquad (2.9)$$

Overall reaction is;

$$SO_{2(aq)} + 2H_2O_{(aq)} \longrightarrow H_2SO_{4(aq)} + H_{2(g)} \quad (2.10)$$

As a result, sulphuric acid is produced at the anode and hydrogen at the cathode. The standard cell potential of the sulphur dioxide depolarised electrolysis is approximately 0.158V at 25^{o}C in water. In 50% aqueous sulphuric acid solution, this value has been determined to be 0.243V.

Figure 2.3 shows the HyS cycle process scheme.

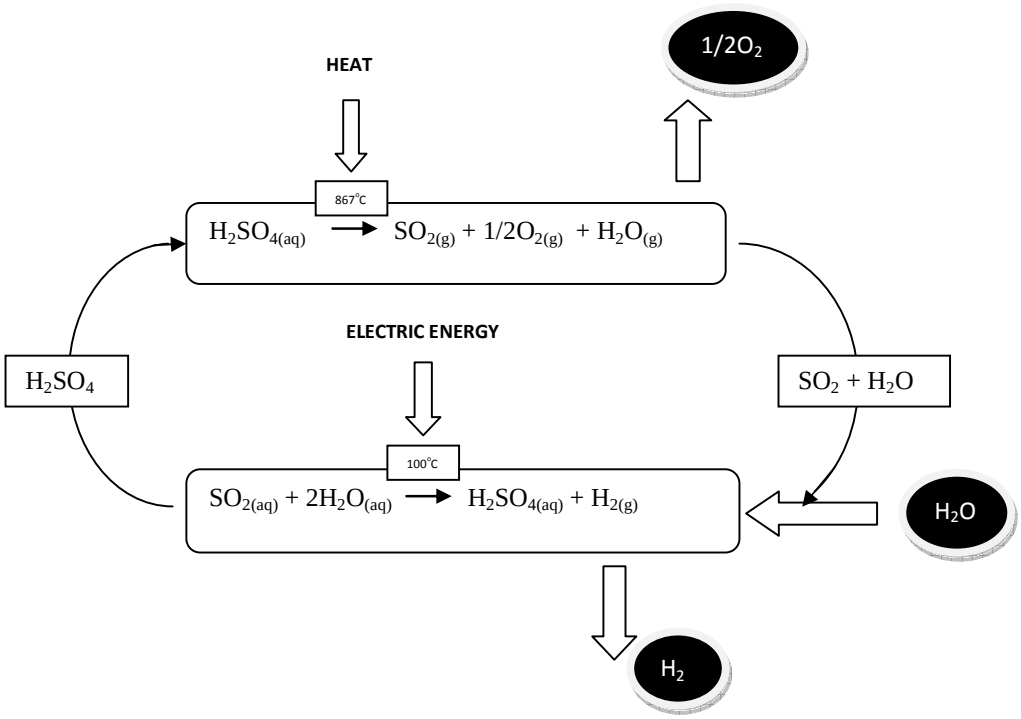

Figure 2.3: HyS cycle schematic

Westinghouse pursued the development of this cycle on the other hand GA developed the SI cycle (Funk, 2001:188). Much research has been done and is still ongoing on the HyS cycle, of note is the research done at the Savannah River National Laboratory (SRNL) (Summers, 2009:9). Solar matching of the process has also been discussed and demonstrations have been carried out at the Sandia National Laboratory (SNL) (Summers, 2009:15). Current research and

development on the HyS cycle is concentrated on the hydrogen producing step, the step is electrochemical which makes the HyS cycle a hybrid thermo-chemical cycle. The use of platinum based catalysts on the hydrogen producing step has been evaluated (Steimke & Steeper, 2006:11) and improved results have been reported, also it has been concluded that sulphur does not poison the catalyst. Staser *et al.* (2007:E17), evaluated the possibility of using gaseous reactants in the hydrogen producing step and showed an improved process over the liquid phase process which has been the subject of matter in the previous years. A cost benefit analysis of the HyS cycle has been presented (Leybros *et al.* 2010b:1019). The hydrogen production cost was assessed to be at $9.4/kg of hydrogen produced for a capacity of 150 t/day. However, Leybros *et al.* (2010b:1019) stress that this estimate is based on quite optimistic assumptions. Many uncertainties were attached to this evaluation, considering that the technology to be used for the hydrogen producing step is still under scrutiny. Leybros *et al.* (2010b:1019) uncertainties are made apparent by Summers & Buckner (2005:324) who reported a hydrogen cost of $1.6/kg.

2.3.4 The hybrid chlorine cycle

The hybrid chlorine cycle is also known as the Hallett Air Products cycle. The Hallett Air Products cycle is described by the following reaction schemes:

Step 1: The reverse Deacon reaction, it is endothermic and Aspen Plus^{TM} simulations show that the equilibrium constant is 6.8 at 850^{o}C but only 0.0001 at 130^{o}C (Gooding, 2009:4168)

$$Cl_{2(g)} + H_2O_{(g)} \longleftrightarrow 2HCl_{(g)} + {}^{1}/_{2}O_{2(g)} \quad (2.11)$$

Step 2: The second reaction is the electrochemical decomposition of hydrochloric acid, with an operating potential of between 0.4 – 0.6V;

$$2HCl_{(aq)} \longrightarrow Cl_{2(g)} + H_{2(g)} \quad (2.12)$$

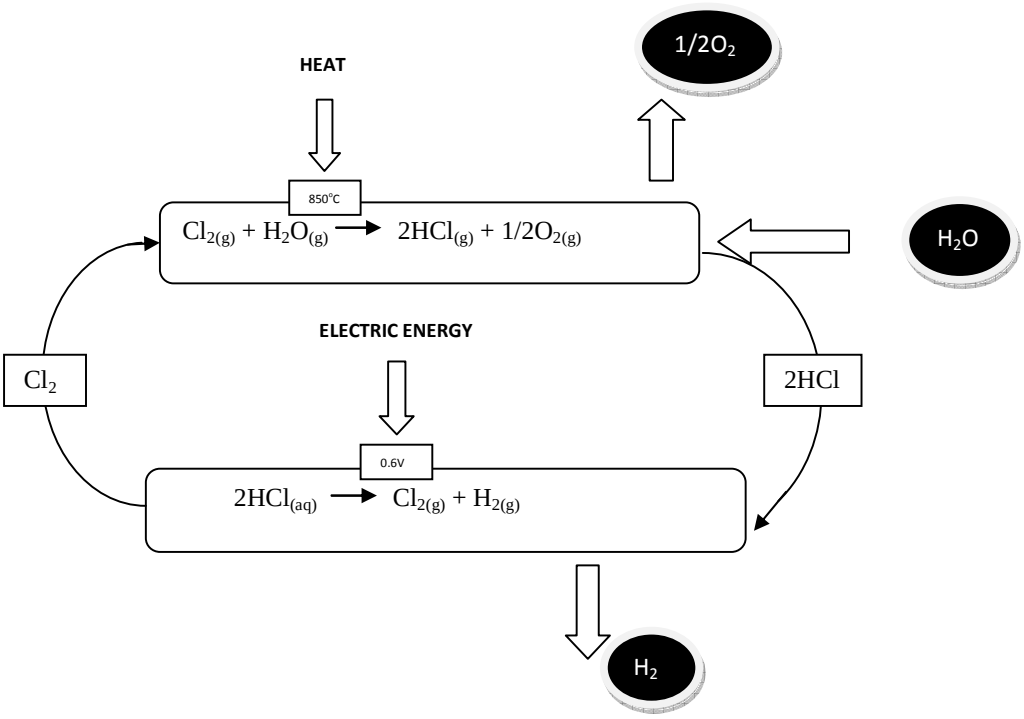

Figure 2.4: Hybrid chlorine cycle schematic

Gooding (2009:4168) presented an analysis of the hybrid chlorine cycle. A conceptual study of the hybrid chlorine process known as the Hallett Air Products cycle was presented. The three process routes for the cycle were evaluated and an efficiency ranging from 30 to 36% was obtained using Aspen Plus^{TM} simulation software, based on the lower heating value of hydrogen produced. The cycle appears to be one of the simplest of all the thermo-chemical cycles, given that no solids are involved in the chemical processes and all the reactions and unit operations have been demonstrated experimentally at laboratory scale. Simpson *et al.* (2005:1241) presented an experimental analysis of the reactions involved in the Hallett Air Products cycle, the voltage requirement for the HCl decomposition reaction (Reverse Deacon Reaction) is equivalent to that of water electrolysis. However, the cycle can be improved if the reactions are conducted differently, for example, the straightforward single step reverse deacon reaction. A two step reverse deacon reaction involving magnesium chloride hydrolysis followed by magnesium oxide chlorination was investigated. From preliminary efficiency estimates and proof of principle experiments, this route seems to be a promising route compared to low temperature hydrogen production. Gooding (2009:4168) recommended that the efficiency analysis of the process should be improved by using a commercial software package such as Aspen Plus^{TM}.

The cost of hydrogen production evaluated by Charles H. Gooding's analysis is $3/kg (Gooding, 2009:4177) compared to $2.25/kg produced by the direct electrolysis of water (Wang *et al.* 2009:9) for 200 and 70 million t/yr capacities respectively. A conclusion that direct water electrolysis will be more attractive compared to the Hallett Air Products cycle was reached. Therefore more research work still needs to be done on this cycle. However, regardless of the energy consumed per unit hydrogen product, the use of this cycle can reduce some of the atmospheric emissions from the currently employed conventional fuel methods. The low maximum temperatures in the process can enable the cycle to be coupled with a solar high temperature source making the production of hydrogen almost environmentally friendly, also the low temperatures presence a great opportunity of savings on the equipment materials cost.

2.3.5 The UT-3 cycle

The UT-3 is known also as the Calcium-Bromide-Iron cycle, and was developed at the University of Tokyo (Sakurai *et al.* 1996a:865), hence the name UT-3. Experimental study of the reactions taking place in the cycle has been studied and verified (Sakurai *et al.* 1996b:875). All reactions in the UT-3 cycle are gas-solid reactions, the reactions were studied to elucidate the reaction mechanism which was proposed and checked against experimental results.

The UT-3 process is described by a set of reactions which entail the hydrolysis and bromination of calcium and iron compounds. Therefore the cycle being described by two pairs of reactions, one pair ensures the formation of hydro-bromic acid, releasing oxygen and the other ensures the oxidation of a bromide to yield hydrogen. The two hydrolysis reactions are endothermic. Heat must be supplied from an external source. The choice of temperature and pressure conditions depends on the physical and chemical properties of the reactants and the thermodynamics of the reactions (Lemort *et al.* 2006:908).

$$CaO_{(s)} + Br_{2(g)} \longrightarrow CaBr_{2(s)} + {}^{1}/_{2}O_{2(g)} \quad (845K) \quad (2.13)$$

$$CaBr_{2(s)} + H_2O_{(g)} \longrightarrow CaO_{(s)} + 2HBr_{(g)} \quad (1033K) \quad (2.14)$$

$$Fe_3O_{4(s)} + 8HBr_{(g)} \longrightarrow 3FeBr_{2(s)} + 4H_2O_{(g)} + Br_{2(g)} \quad (493K) \quad (2.15)$$

$$3FeBr_{2(s)} + 4H_2O_{(g)} \longrightarrow Fe_3O_{4(s)} + 6HBr_{(g)} + H_{2(g)} \quad (833K) \quad (2.16)$$

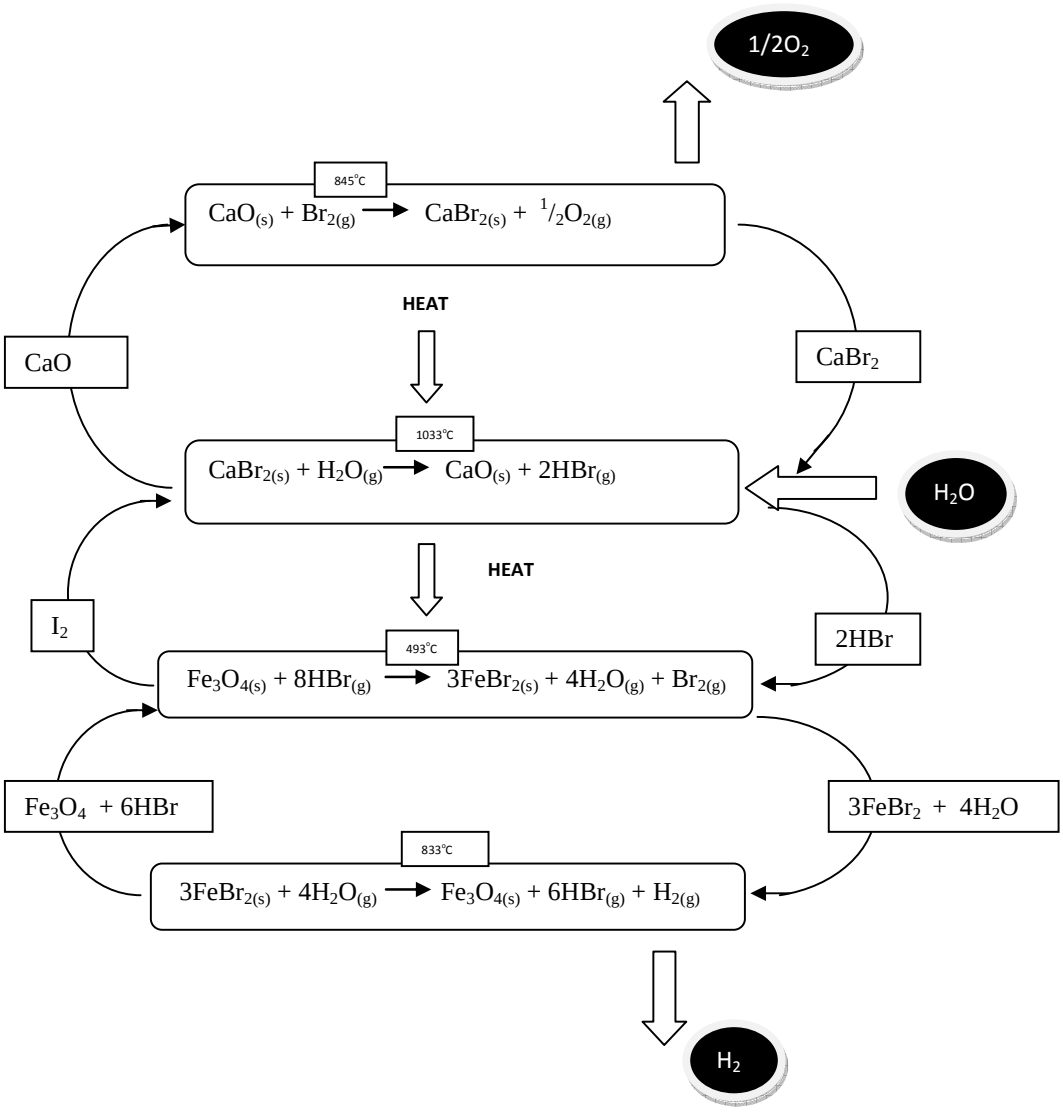

Figure 2.5: The UT-3 cycle schematic

Oxygen and hydrogen are released as products while other gases are circulated. The solid reactants are fixed in reactors.

An adiabatic UT-3 process has been reported as highly efficient and with inherent lower costs than a non adiabatic one. Bench scale plants have been successfully conducted and it has led to a conceptual design for a commercial size plant so as to assess the thermal efficiency (Tadokoro *et al.* 1996:49). On the contrary, Lemort *et al.* (2006:906), in their study on physicochemical and

thermodynamic investigation of the UT-3 process, reported that, based on the current trends in the literature, there are a number of challenges. Lemort *et al.* (2006:906) highlighted that their assessment showed high necessity to make significant technological advances in the field of process technology. The possibility of a modified UT-3 cycle has been presented (Doctor *et al.* 2002:755), whereby the two stage hydrogen bromide dissociation step is reduced to one stage, the modification will be done by hydrogen bromide electrolysis or the use of plasma chemistry. The justification for using this strategy is presented by considering the Gibbs free energies of the cycle which are lowered from 56.7 to 27.3 kcal.gmol^{-1}. This process has become known as the Calcium Bromide cycle. For a plant producing 30000Nm^3/h the cost of producing hydrogen was reported to be \$35/GJ H_2 (Sakurai *et al.* 1996a:866), which should be equivalent to approximately \$5.00/kg H_2.

2.3.6 The copper chlorine cycle

The copper chlorine (CuCl) cycle is a hybrid thermochemical cycle with a solid-fluid system. The CuCl cycle consists of variations of different numbers of steps ranging from three to five, of which some are beyond the scope of this presentation; of interest here is the three step cycle.

Step 1: The electrochemical reaction between aqueous acid and copper to produce cuprous chloride at the anode and hydrogen at the cathode, this reaction has been demonstrated at the Atomic Energy of Canada, Ltd with the following parameters, 500mA/cm^2 at 0.5V (Lewis *et al.* 2005:7; Wang *et al.* 2009:3273).

$$Cu_{(s)} + 2HCl_{(g)} \longrightarrow 2CuCl_{(s)} + H_{2(g)} \qquad (450^oC) \qquad (2.17)$$

Step 2: Cuprous chloride dis-proportionation to form cupric oxide according to the following reaction

$$4CuCl_{(s)} \longrightarrow Cu_{(s)} + 2CuCl_{2(aq)} \qquad (80^oC) \qquad (2.18)$$

Step 3: The cupric chloride is oxy-chlorinated at 530^{o}C to form molten cuprous chloride;

$$2CuCl_{2(aq)} + 5H_2O_{(l)} \longrightarrow {}^1/_2O_{2(g)} + 2CuCl_{(s)} + 4H_2O_{(g)} + 2HCl_{(g)} \qquad (2.19)$$

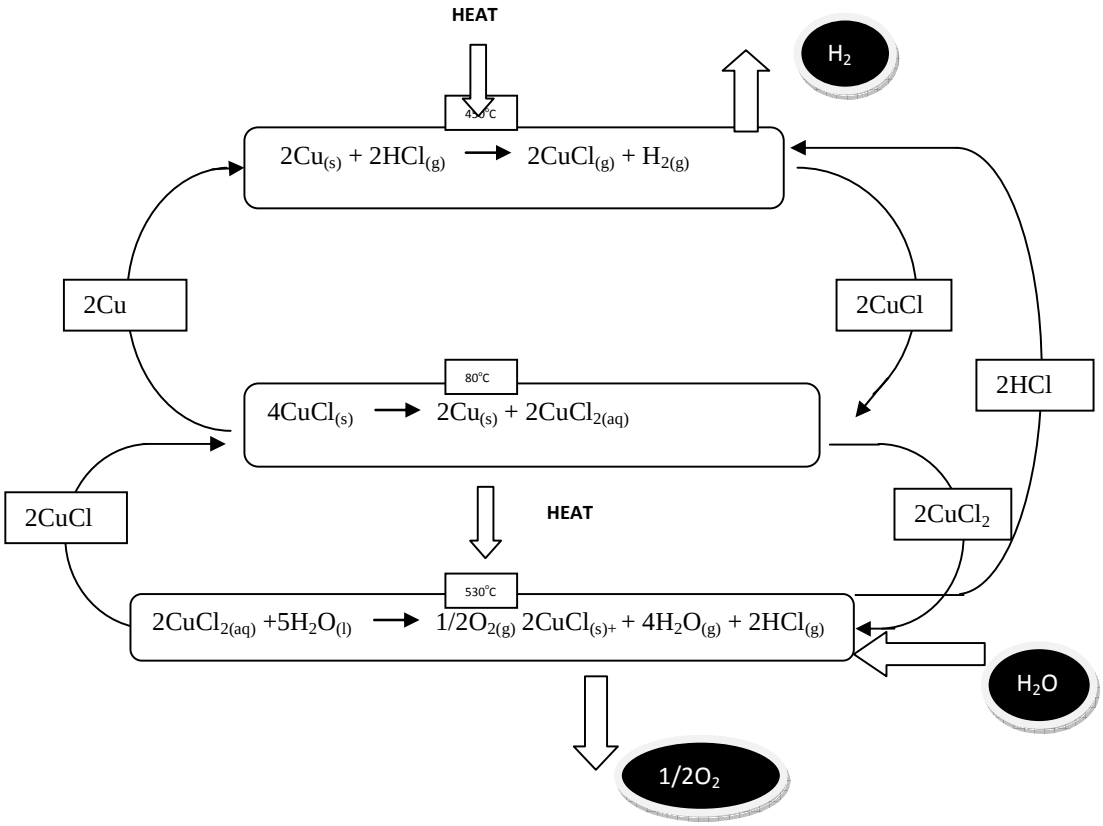

Figure 2.6: The three step CuCl cycle schematic

Much research is ongoing at the Argonne National Laboratory (ANL) for the Copper Chloride cycle (Lewis *et al.* 2005:1). The ANL's research is currently focused on developing low temperature thermo-chemical cycles. The rationale for the ANL's research and development effort is to identify new technologies that can produce hydrogen cost effectively and without greenhouse gas emissions using Generation IV reactor concepts. The CuCl cycle has been identified as one of the most promising lower temperature cycles. A conceptual design together with the H2A cost analysis was done (Ferrandon *et al.* 2009:10); the estimated cost of producing hydrogen was $3.30/kg for a 125 million t/day production, the result from the economic analysis were for the purpose of guiding the further development of the process. On the other hand Wang *et al.* (2009:10) reports a production cost of $2.31/kg for a 10 t/day capacity.

2.3.7 Comparison of thermochemical cycles

Table 2.3, shows a summary of the comparison of different cycles as studied by different researchers. The cost figures are factored to 2009 as the base year.

Table 2.3: Comparison of thermo-chemical cycles.

Cycle	**Variant Name**	**Heat Input (kJ/mol H_2)**	**Efficiency (%)**	**Peak Temperature (^oC)**	**Production Cost ($/kg)**
Sulphur Iodine	Ispra Mark 16	744.4	38	867	1.95 (1)
Hybrid Sulphur	Westinghouse, Ispra Mark 11	685.8	35.3	867	1.78 (2)
Copper Chlorine	-	543.7	45	540	2.02 (1)
Copper Sulphate	-	776.9	25	850	>2.50 (3)
UT-3	Calcium Bromide	494	48.9	760	6.84 (4)
Hybrid Chlorine	Hallett Air Products Cycle	677	36	850	3.00 (5)

(1) Wang *et al.* (2009:1); (2) Summers & Buckner (2005:324); (3) Gonzales *et al.* (2009:4179); (4) Sakurai *et al.* (1996a:866); (5) Gooding (2009:4177)

Wang *et al.* (2009:1) made a detailed comparison of the SI and CuCl cycles based on the following aspects of the cycles; heat quantity, heat grade, thermal efficiency, related engineering challenges, and the cost of producing hydrogen. It was found that the heat requirements and the overall efficiencies were similar and thermal efficiencies ranged from 37 to 54%. The CuCl cycle has a lower maximum temperature of 530^{o}C compared to 850^{o}C for the SI cycle, this presents the CuCl cycle with opportunities to couple it with different heat sources ranging from fossil fuel power stations through nuclear reactors up to solar concentrators. The CuCl cycle development and construction is perceived to present fewer equipment materials selection challenges as compared to the SI cycle. The cost analysis done showed that the two cycles in question have almost similar hydrogen production costs although the SI is slightly lower,

$2.02/kg and $1.95/kg for CuCl and SI respectively, if both cycles use Very High Temperature Reactor (VHTR) as heat and electricity source. Wang *et al.* (2009:1) analysis showed that the major difference between the two cycles is the maximum temperatures of operation which obviously leads to a difference in the materials of construction approach and that the CuCl cycle will use lower heat grade to achieve the same efficiency as the SI cycle. Another difference which was not touched in the analysis is the hybrid nature of the CuCl cycle (Lewis *et al.* 2005:7), brought about by the step which involves the electrochemical reaction between aqueous acid and cuprous chloride, whereas the SI cycle is purely thermochemical. There is a big deal of research to be done to ascertain which of the two cycles, SI and CuCl; is better. This might turn to be a sensitive issue as most researchers will tend to be more biased towards the other. Take for example, it is not expected of a researcher from the GA or JAERI to discredit the SI cycle and the same for a researcher under the SNRL or Westinghouse for the HyS cycle or one from the ANL or University of Ontario Institute of Technology to publicly discredit the CuCl cycle. Above all, the SI and the HyS cycle have been under study for a several number of years.

Mullin *et al.* (2006:1) developed a methodology of evaluating and screening water splitting cycles without the need for process flow diagrams. The thermodynamic efficiency of each cycle was calculated using pure component enthalpy and entropy correlations to determine the heating and separation requirements. The author's methodology is reported to result in a quick dismissal of impractical cycles and a detailed consideration of most promising cycles (Mullin *et al.* 2006:1; Miguel *et al.* 2009:8986). A strategy for future cycle synthesis was presented where, 1) exothermic reactions should be positioned at sufficiently high temperatures to fully cascade released heat to colder zones rather than reject it to cold utility and 2) reactions temperatures should be investigated to exploit phase differences between equilibrium species. This methodology suggested that the Hybrid Sulphur cycle is capable of attaining the highest efficiency of the twelve cycles assessed which included the cycles such as the SI cycle and the Ispra Mark 13.

Miguel *et al.* (2009:8985) in a continuation of the method presented by their work with Mullin *et al.* (2006:1), evaluated the thermochemical cycles by considering equilibrium conversions of the reactions taking place, degrees of freedom of each cycle (temperatures, pressures and excess reactants). The hot utility, electrical work and separation work relating to the cycles was

determined by using the classical pinch point analysis that is the Gibbs energy of mixing of ideal mixtures and the Nernst equation. It was noted that if a cycle has a highly exothermic reaction at low temperature, it will have a low thermal efficiency such as the UT-3 process. The heat source of exothermic reaction at low temperature is unrecoverable through heat exchange which leads to high cold and hot utilities. Miguel *et al.* (2009:8985) noted that processes with endothermic reactions have a good efficiency and suggested that cycles with a highly exothermic reaction at low temperature should not be studied further. The methodology was implemented to ten popular thermochemical and hybrid cycles, the top five cycles based on cycle efficiency included the Hybrid Sulphur (82.7%), Sulphur Iodine (81.3%) and Ispra Mark 13 (53.8%). These efficiencies are upper bounds of the real efficiencies, since there were no flowsheets prepared for the analysis.

2.4 State of the art review of process simulations

2.4.1 Introduction

The evaluation of a thermochemical cycle is a complex and tedious task. Among every aspect of evaluation, the materials of construction, the corrosion science, the equilibrium and kinetic data of the reactions involved will need to be determined and verified before conclusion is reached. Conceptual design of the process is an important step so as to determine the mass and energy balances of the process. From a conceptual design, simulations of the real process are done, the thermal efficiency of the cycle will be determined and a more accurate and representative cost benefit analysis of the cycle is achieved. Simulation can be done using engineering simulation software such as Prosim Plus ™, Aspen Plus ™, Spence ™ and, or Design-II ™ (Kivisari *et al.* 2001:113). The evaluations have been proven to show little or no overall differences regardless of the simulation software used (Kivisari *et al.* 2001:120). However, Aspen Plus™ has proved to be the most popular software employed in industry and research, evidenced by the number of researchers who have used it for their analyses (Gorensek & Summers, 2009:4101; Lewis *et al.* 2005:1; Chukwu, 2008:31; Gooding, 2009:4169).

The following is a brief account of the results of the simulation papers presented so far for some of the thermochemical cycles. The efficiency expression used by most of the authors is as follows (Lewis *et al.* 2005:8; Miguel *et al.* 2009:8986)

$$E_\eta = \Delta H_f/[Q + (W_E/\varepsilon)] \quad (2.20)$$

- where ΔH_f is the standard enthalpy of formation of water (242 kJ/mol H_2), Q is the sum of the heat inputs, W_E is the work input and ε is the heat-to-work conversion efficiency.

2.4.2 The sulphur iodine cycle

Leybros *et al.* (2009:9060) presented a conceptual design of an SI cycle, the process includes a counter-current reactor being developed by the French “Commissariat å l’Energie Atomique” (CEA) within the framework of an international collaboration with the US Department of Energy at General Atomics. The SI flowsheet was developed using ProsimPlus™. The simulations were

done using various thermodynamic models; Leybros *et al.* (2009:9060) point out that the ENGELS model has been shown to represent the $H_2SO_4 – H_2O$ system very well over the entire composition range and temperatures of about 750^oC. The SOUR WATER model has been used to describe the $SO_2 – H_2O$ system in the absorption column. The HI_x system is described using a modified model derived from the NRTL equation and it has been noted that the predicted enthalpies of mixing are not consistent with experimental data. The assumptions made were as follows:

- Passive safety constraints limit the HTGR to be no larger than 600 MW_{th}.
- Minimum temperature difference between hot helium fluid and heat exchangers implementing heat transfer should be at least 50^oC.
- Temperature difference for heat exchangers implementing a phase change should not be less than 5K and should not be more than 10^oC for all other cases.
- Cooling water assumed to be available at 303^oC all year round.

The resultant flowsheet gave a net thermal efficiency of 38%, and it requires 600 kJ/mol H_2 high-temperature heat and 65 kJ/mol H_2 electric power. Combining the heat and electric requirements using a 45% heat-to-electric conversion efficiency, a total of 744.4 kJ/mol H_2 is consumed. This compares favourably to HTGR powered water electrolysis which requires 895 kJ/mol H_2 (with an assumed pressure of 120 bars for the H_2 product).

2.4.3 The hybrid sulphur (HyS) cycle

Gorensek & Summers (2009:4097) presented a conceptual design of a HyS process which employs a proton exchange membrane (PEM) based sulphur dioxide depolarised electrolyser (SDE) technology being developed at SRNL and a silicon carbide bayonet reactor being developed at SNL. The HyS process is simulated using Aspen Plus™. An accurate representation of the H_2SO_4/SO_2 properties and phase equilibria over the entire concentration range is provided by the Oleum Data Package for use with Aspen Plus™, the temperature range for this package extends to not more than 423^oC, Mathias H_2SO_4 properties model is used to counter this limitation. A modification of Mathias' H_2SO_4 properties model was used to track the fluid

physical and chemical changes for the bayonet reactor. The overall flowsheet was prepared using OLI Systems, Inc.'s Mixed Solvent Electrolyte (MSE) model. The assumptions taken on the preparation of the flowsheet were as follows:

- The properties model used for the simulation accurately represent the H_2SO_4-H_2O-SO_3-SO_2-O_2 system.
- Heat transfer can be achieved as needed in the high temperature decomposition reactor in order to achieve the specified approach temperatures.
- High temperature sulphuric acid decomposition proceeds to thermodynamic equilibrium.
- SDE is assumed to operate at a fixed cell potential of -0.6V, an SO_2 conversion of 40% and a fixed 50% H_2SO_4 product composition.
- No piping and vessel pressure drops.
- Cooling water is available year round at 30^oC.

The calculated cycle efficiency is 35.3% LHV (41.7% HHV) provided the electric power heat-to-electricity conversion is 45%.

The flowsheet requires 340.3 kJ/mol H_2 high-temperature heat, 75.5 kJ/mol H_2 low-temperature heat, 1.31kJ/mol H_2 low-pressure steam, and 120.9 kJ/mol H_2 electric power. If a 45% heat-to-power conversion efficiency is assumed, the electric power corresponds to a primary energy input of 268.7 kJ/mol H_2. This gives a total of 685.8kJ.mol^{-1} H_2, which compares favourably with HTGR-powered electrolysis at 791kJ/mol H_2. Gorensek & Summers (2009:4097) also noted that when conventional nuclear reactors are assumed to be the source of electric power, the HyS process has an even larger advantage over water electrolysis (783 versus 1080 kJ/mol H_2, respectively).

2.4.4 The copper chlorine cycle

Chukwu (2008:1) studied two variations of the CuCl cycle, the four step and three step cycles. Aspen Plus™ simulations are done for the two different flowsheets to determine the efficiencies of each. The author chooses to use the Electrolyte Non Random Two Liquid (ELECNRTL) model for modelling processes in stoichiometry reactors. The Soave-Redlich-Kwong (SRK) cubic equation of state is used to evaluate component properties and phase equilibria where there is vapour liquid phase change. A sensitivity analysis was also performed to determine the effects of various operating parameters on the efficiency, yield and thermodynamic properties. The assumptions presented in this work were as follows:

- All reactions go to completion
- 70% heat exchanger effectiveness
- Electrolysis cell potential of 0.5V
- 50% heat to electricity conversion efficiency

The results of the simulations showed that the efficiency of the four step CuCl process is 45% and for the three step process is 42%. The total heat requirements were 543.7 and 584.7 kJ/mol H_2 for the four and three step cycles respectively. A sensitivity analysis showed that temperature increase has no effect on the performance of the electrolyser. The efficiency of the hydrolysis unit decreases with an increase in temperature within the range of 0 – 100^{o}C.

2.4.5 The $CuSO_4$/CuO cycle

The hybrid $CuSO_4$/CuO cycle was presented by Gonzales *et al.* (2009:4179), as a four reaction version of the cycle (known as Cycle H-5). A sensitivity analysis on the effect of the minimum temperature difference approach on heat losses was performed. A cost analysis on a plant designed to produce 100 million kmol/yr of hydrogen was done. A process flowsheet was prepared using Aspen Plus™ simulation engine, employing the Peng-Robinson equation of state

for separations involving oxygen and sulphur oxides, the author noted that this represents a significant departure from ideality.
The assumptions considered on the flowsheet simulation were as follows:

- Process water is supplied at 15 – 25^{o}C at atmospheric pressure.
- Any by-product streams are safe to discharge
- 50% heat-to-electricity conversion efficiency is accounted for

The conclusions drawn from this analysis were as follows:

- Heat input of 795.4 and, 776.9 kJ/mol H_2 must be supplied for the 20 and 10^{o}C approaches respectively.
- Electrical energy input of 86 kJ/mol H_2 must be supplied for both approaches and a pinch heat of 34.3 and 15.7 kJ/mol H_2 for 20 and 10^{o}C temperature approaches respectively.
- Efficiency calculation gave a value of 24.1% for the 20^{o}C temperature approach and 25.0% for the 10^{o}C approach and if the recovery and use of the low quality heat rejected by the cycle is allowed, the efficiency could reach 50.7% and 52.7% for the 20^{o}C and 10^{o}C temperature approaches respectively.
- A turnkey plant cost of $360 million
- Based on a selling price of $2.50/kg hydrogen, the expected revenue could be $500 million per year.
- The results of the analysis do not rule out this cycle as a viable one.

2.5 Critical evaluation of literature survey

2.5.1 Introduction

A number of studies have been conducted on different types of thermochemical cycles and their aspects such as energy, exergy and economic analysis (Leybros *et al.* 2009:9062; Gorensek & Summers, 2009:4098; Jeong *et al.* 2005:3; Goldstein *et al.* 2005:619; Chukwu, 2008:1; Rosen, 2008:6933). Although the studies have been presented and published successfully, there are some aspects which have not yet been addressed by the studies.

2.5.2 Summary

Most of the studies on thermochemical cycles have managed to address the issue of energy efficiency. Detailed energy requirements per section within the cycle have also been presented. The results show that the thermochemical cycles can be competitive compared to electrolysis. The viability of the reactions has been verified experimentally in various institutions and laboratories. Gorensek *et al.* (2009:4097) reported a HyS cycle efficiency of 35.3% and LHV (41.7% HHV) provided the electric power heat-to-electricity conversion of 45%. The flowsheet requires 340.3 kJ/mol H_2 high-temperature heat, 75.5 kJ/mol H_2 low-temperature heat, 1.31 kJ/mol H_2 low-pressure steam, and 120.9 kJ/mol H_2 electric power. If a 45% heat-to-power conversion efficiency is assumed, the electric power corresponds to a primary energy input of 268.7 kJ/mol H_2. This gives a total of 685.8 kJ/mol H_2. Leybros *et al.* (2009:9060) presented a conceptual design of an SI cycle. The flowsheet gave a net thermal efficiency of 38%, and it required 600 kJ/mol H_2 high-temperature heat and 65 kJ/mol H_2 electric power. Combining the heat and electric requirements using a 45% heat-to-electric conversion efficiency, a total of 744.4 kJ/mol H_2 is consumed. The efficiency figures compare favourably to HTGR powered water electrolysis which requires 895 kJ/mol H_2 (with an assumed pressure of 120 bars for the H_2 product).

Proof of concept experiments have been conducted by various institutions and laboratories (Summers, 2009:1; Lewis *et al.* 2005:1) GA has invested approximately 8 million dollars on the SI cycle project (Funk, 2001:188). More research work on the SI cycle is still being done at the Japan Atomic Energy Research Institute (JAERI), Korea Institute of Energy Research, the

Technical University at Aachen in Germany and the French "Commissariat å l'Energie Atomique" (Leybros *et al.* 2009:9060; Kubo *et al.* 2004:347; Cho *et al.* 2009:501). Much research has been done and is still ongoing on the HyS cycle, of note is the research done at the Savannah River National Laboratory (SRNL) (Summers, 2009:9). Solar matching of the process has also been discussed and demonstrations have been carried out at the Sandia National Laboratory (SNL) (Summers, 2009:15). Much research is ongoing at the Argonne National Laboratory (ANL) for the Copper Chloride cycle (Lewis *et al.* 2005:1). The ANL's research is currently focused on developing low temperature thermo-chemical cycles. The rationale for the ANL's research and development effort is to identify new technologies that can produce hydrogen cost effectively and without greenhouse gas emissions using Generation IV reactor concepts.

2.5.3 Limitations of studies

The studies on thermochemical cycles have failed to address the following issues:

- An African based study has not been presented so far, most of the literature for example, (Leybros *et al.* 2009:9062; Gorensek & Summers 2009:4098; Jeong *et al.* 2005:3; Goldstein *et al.* 2005:619; Chukwu, 2008:1) have assumed that prevailing conditions are 15 to 25^{o}C temperature. Most African countries have temperatures as high as 38^{o}C.

- The economic evaluations made in conceptual studies are based on a number of uncertainties. Leybros *et al.* (2010:1027) states that many uncertainties are attached to their evaluation of the production costs of hydrogen from Hybrid Sulphur thermochemical cycle coupled to a nuclear source.

- Most conceptual studies do not address questions like; what will be the final technology to be implemented? What will be the resulting price? How often will the equipment have to be replaced? (Leybros *et al.* 2010:1027). There has been no detailed presentation of the heat integration flowsheets for the processes presented so far. Gorensek & Summers (2009:4098) presented a pinch analysis for the Bayonet reactor, which is a section in the Hybrid Sulphur cycle. There is need to present a heat integration flowsheet for the whole process concerned.

- Many studies have not performed an exergy analysis of the processes being studied; (Leybros *et al.* 2009:9062; Gorensek & Summers, 2009:4098; Jeong *et al.* 2005:3; Goldstein *et al.* 2005:619; Chukwu, 2008:1). Exergy analysis should be used since energy analysis on its own does not point out true process inefficiencies, and often does not provide rational efficiencies. Rosen (2008:6933) has performed an exergy analysis of Ispra Mark-10 cycle and has reported that there exists a substantial potential for improved thermodynamic efficiency in thermochemical water decomposition using the Ispra Mark-10 cycle.

2.5.4 Conclusion and recommendation

The studies on thermochemical cycles presented so far have addressed the issues of process energy, economic viability and reactions feasibility. The research has brought a clearer understanding of the aspects concerning thermochemical cycles operation. Although a great deal of thermochemical processes research has been done, it is clear that some of the aspects pointed out in Section 2.5.3 have not yet been addressed.

The Aspen Tech package offers a capability of performing heat integration, pinch analysis and exergy analysis using the tools, Aspen Energy Analyzer^{TM} or Aspen HX-Net^{TM} for older versions. The tools will enable researchers to construct detailed heat integration flowsheets, determine the enthalpy and availability of the process streams thereby acquiring more knowledge of the performance of the thermochemical cycle.

Considering that the SI cycle, is being regarded as a large scale, cost effective and environmentally friendly cycle. There is need to have a study of the SI cycle that is aimed at addressing all the shortcomings that have been pointed out in Section 2.5.3. GA has invested approximately 8 million dollars on the SI project (Funk, 2001:188), therefore African institutions should do likewise.

2.6 References

BAYKARA, S.J. 2004. Hydrogen production by direct solar thermal decomposition of water, possibilities for improvement of process efficiency. *International Journal of Hydrogen Energy,* **29**:1451-1458, Feb.

BLEEKER, M.F. 2009. Pure hydrogen from pyrolysis oil by the steam-iron process. Ipskamp Drukkers. 232p

BOCKRIS, J.O'M., DANDAPANI, B., COCKE, B. & GHOROGHCHIANI, J. 1984. On the electrolysis of water. *International Journal of Hydrogen Energy,* **10**:179-201, Sep

BRECHER, L.E. & WU, C.K. 1975. Electrolytic decomposition of water. Patent: US 3,888,750. 13p.

CHO, W.C., PARK, C.S., KANG, K.S., KIM, C.H., & BAE, K.K. 2009. Conceptual design of sulfur-iodine hydrogen production cycle of Korea Institute of Energy Research. *Nuclear Engineering & Design,* **239**:501-507, Nov.

CHUKWU, C. 2008. Process analysis and Aspen Plus simulation of Nuclear-based Hydrogen production with a Copper-Chlorine Cycle. Ontario: UOIT. (Dissertation – M.Sc.) 125p.

DOCTOR, R.D., MARSHALL, C.L. & WADE, D.C. 2002. Hydrogen cycle employing calcium bromine and electrolysis. *Fuel Chemistry Div. Preprints,* **47**:755-756, Jan.

FERRANDON, M.S., LEWIS, M.A., TATTERSON, D.F., NANKANI, R.V., KUMAR, M., WEDGEWOOD, L.E. & NISCTHE, L.C. The Hybrid CuCl thermo-chemical cycle. I. Conceptual process design and H2A cost analysis. II. Limiting the formation of CuCl during hydrolysis. 20p. (Unpublished)

FUNK, J.E. 2001. Thermochemical hydrogen production: Past and Present. *International Journal of Hydrogen Energy,* **26**:185-190, Jan.

GOLDSTEIN, S., BORGARD, J.M. & VITART, X. 2005. Upper bound and best estimate of the efficiency of the iodine sulfur cycle. *International Journal of Hydrogen Energy,* **30**:619-626, Aug.

GONZALES, R.B., LAW, V.J. & PRINDLE, J.C. 2009. Analysis of the hybrid copper oxide–copper sulfate cycle for the thermo-chemical splitting of water for hydrogen production. *International Journal of Hydrogen Energy,* **34**:4179-4188, Dec.

GOODING, C.H. 2009. Analysis of alternative flow sheets for the hybrid chlorine cycle. *International Journal of Hydrogen Energy,* **34**:4168-4178, Jul.

GORENSEK, M.B. & SUMMERS, W.A. 2009. Hybrid sulfur flowsheets using PEM electrolysis and a bayonet decomposition reactor. *International Journal of Hydrogen Energy*, **34**:4097-4114, Jun.

GRAF, D., MONNERIE, N., ROEB, M., SCHMITZ, M. & SATTLER, C. 2008. Economic comparison of solar hydrogen generation by means of thermo-chemical cycles and electrolysis. *International Journal of Hydrogen Energy*, **33**:4511-4519, May.

HACKER, V., FRANKHAUSER, R., FALESCHINI, G., FUCHS, H., FRIEDRICH, K., MUHR, M. & KORDESCH, K. 2000. Hydrogen production by steam-iron process. *Journal of Power Sources*, **86**:531-535, Oct.

JEONG, Y.H., KAZIMI, M.S., HOHNHOLT, K.J. & YILDIZ, B. 2005. Optimization of the hybrid sulfur cycle for Hydrogen production. Korea: KOSEF. (Dissertation – Post-Doc Fellowship.) 60p.

KIVISARI, T., LAAG, P.C. & RAMSKOLD, A. 2001. Benchmarking of chemical flow-sheeting software in fuel cell applications. *Journal of Power Sources* **94**:112-121, Oct.

KRUGER, P. 2005. Electric power required in the world by 2050 with Hydrogen fuel production – Revised. *International Journal of Hydrogen Energy*, **30**:1515-1522, Jun.

KUBO, S., NAKAJIMA, H., KASAHARA, S., HIGASHI, S., MASAKI, T., ABE, H. & ONUKI, K. 2004. A demonstration study on a closed-cycle hydrogen production by the thermo-chemical water-splitting iodine–sulfur process. *Nuclear Engineering & Design*, **233**:347-354, Aug.

LEMORT, F., LAFON, C., DEDRYVERE, R. & GONBEAU, D. 2006. Physicochemical and thermodynamic investigation of the UT-3 hydrogen production cycle: A new technological assessment. *International Journal of Hydrogen Energy*, **31**:906-918, Sep.

LEWIS, M.A., MASIN, J.G. & VILIM, R.B. 2005. Development of the Low Temperature Cu-Cl Thermochemical Cycle. (Paper presented at the International Congress on Advances in Nuclear Power Plants on 15 to 19 May 2005. Seoul.)

LEYBROS, J., CARLES, P. & BORGARD, J.M. 2009. Countercurrent reactor design and flowsheet for iodine-sulfur thermo-chemical water splitting process. *International Journal of Hydrogen Energy*, **34**:9060-9075, Sep.

LEYBROS, J., GILARDI, T., SATURNIN, A., MANSILLA C. & CARLES, P. 2010. Plant sizing and Evaluation of hydrogen production costs from advanced processes coupled to a nuclear heat source. Part I: Sulphur-Iodine cycle. *International Journal of Hydrogen Energy*, **35**:1008-1018, Jan.

LEYBROS, J., GILARDI, T., SATURNIN, A., MANSILLA C. & CARLES, P. 2010. Plant sizing and Evaluation of hydrogen production costs from advanced processes coupled to a

nuclear heat source. Part II: Hybrid-Sulphur cycle. *International Journal of Hydrogen Energy,* **35**:1019-1028, Jan.

LYUBOVSKY , M., ROYCHOUDHURY, S., LAPIERRE, R. 2004. Catalytic partial ‘‘oxidation of methane to syngas’’ at elevated pressures. *Catalysis Letters*, **99:**113-117, Feb.

MAAG, G., ZANGANEH, G., & STEINFELD, A. 2009. Solar thermal cracking of methane in a particle-flow reactor for the co-production of hydrogen and carbon. *International Journal of Hydrogen Energy,* **34**:7676-7685, Aug.

MIGUEL, B., CAO, T., CROSIER, R., MULLIN, S., TARVER, J. & NGUYEN, D.Q. 2009. Method of evaluating Thermochemical and Hybrid Water-splitting cycles. *Ind. Eng. Chem,* **48**:8985-8998, Jul.

MULLIN, S., ODI, U. & TARVER, J. 2006. Evaluation and Design of Thermochemical and Hybrid Water Splitting Cycles. (Report delivered to the Department of Chemical Engineering, University of Oklahoma in May 2006.) Norman. 29p.

NAKAJIMA, H., SAKURAI, M., IKENOYA, K., HWANG, J.G., ONUKI, K. & SHIMIZU, S. 1999. A study on a closed cycle hydrogen production by thermo-chemical water splitting IS process. (Paper presented at the 7th International conference on Nuclear Engineering on 19 to 23 April 1999. Tokyo)

NORMAN, J.H., RUSSELL, J.L., PORTER, J.T., McCORKLE, K.H., ROEMER T.S. & SHARP, R. 1978. Process for the thermochemical production of hydrogen. Patent: US 4,089,940. 6p.

PAAL, R.P. 2007. High temperature solar concentrators. (In Encyclopedia of life support systems)

PADRO, C.E.G., & LAU, F. 2002. Advances in Hydrogen Energy. New York: Kluwer. 192p.

ROSEN, M.A. 2008. Exergy analysis of hydrogen production by thermochemical water decomposition using the Ispra Mark-10 Cycle. *International Journal of Hydrogen Energy,* **33**:6921-6933, Oct.

SAKURAI, M., BILGEN, E., TSUTSUMI, A. & YOSHIDA, K. 1996a. Adiabatic UT-3 process for hydrogen production. *International Journal of Hydrogen Energy,* **21**:865-870, Feb.

SAKURAI, M., MIYAKE, N., TSUTSUMI, A. & YOSHIDA, K. 1996b. Analysis of a reaction mechanism in the UT-3 Thermochemical Hydrogen production cycle. *International Journal of Hydrogen Energy,* **21**:871-875, Mar.

SCHULTZ, K. 2003. Thermochemical Production of Hydrogen from Solar and Nuclear Energy. (Presentation to the Stanford Global Climate and Energy Project on 14 April 2003. San Diego.)

SIMPSON, M.F., HERMANN, S.D. & BOYLE, B.D. 2005. A hybrid thermo-chemical electrolytic process for hydrogen production based on the reverse Deacon reaction. *International Journal of Hydrogen Energy,* **3**:1241-1246, Oct.

STASER, J., RAMASAMY, R.P., SIVASUBRAMANIAN, P. & WEDNER, J.W. 2007. Effect of Water on the Electrochemical Oxidation of Gas-Phase SO_2 in a PEM Electrolyser for H_2 Production. *Electrochemical and solid state letters,* **11**:E17-E19, Aug.

STEIMKE, J. & STEEPER, T. 2006. Generation of Hydrogen using Electrolyser with Sulfur Dioxide depolarized anode. (Presentation at the Southeastern Regional Meeting of the American Chemical Society on 2 November 2006.)

SUMMERS, W.A. 2009. Hybrid Sulfur Process Overview. (Paper presented at the SDE Info Exchange and Workshop on 20 April 2009. Aiken.)

SUMMERS, W.A., BUCKNER, M.R. 2005. Hybrid Sulfur thermo-chemical process development. (Progress report delivered to the US Department of Energy, Hydrogen Program, in 23 May 2005. Aiken)

SUN, J., QIU, X., WU, F., ZHU, W., WANG, W. & HAO, S. 2004. Hydrogen from steam reforming of ethanol in low and middle temperature range for fuel cell application. *International Journal of Hydrogen Energy,* **29**:1075-1081, Feb.

TADOKORO, Y., KAJIYAMA, T., YAMAGUCHI, T., SAKAI, N., KAMEYAMA, H. & YOSHIDA, K. 1996. Technical evaluation of UT-3 Thermochemical Hydrogen production process for an Industrial scale plant. *International Journal of Hydrogen Energy,* **22**:49-56, Apr.

WANG, Z.F., NATERER, G.F., GABRIEL, K.S., GRAVELSINS, R. & DAGGUPATI, V.N. 2009. Comparison of sulfur–iodine and copper–chlorine thermo-chemical hydrogen production cycles. *International Journal of Hydrogen Energy,* **xxx:** 1-11, Sep.

WINKLER, H. 2006. Energy policies for sustainable development in South Africa. Options for the future. *Energy Research Centre, University of Cape Town,* **1:** 1-225, Apr.

WONG, B., BUCKINGHAM, R.T., BROWN, L.C., RUSS, B.E., BESENBRUCH, G.E., KAIPARAMBIL, A., SANTHANAKRISHNAN, R. & ROY, A. 2007. Construction materials development in sulfur–iodine thermochemical water-splitting process for hydrogen production. *International Journal of Hydrogen Energy,* **32**:497-504, Sep.

CHAPTER 3: Design framework

"Design can be art. Design can be aesthetics. Design is so simple, that's why it is so complicated" Paul Rand

3.1 Introduction

Different designers manage the process of design in different ways. A study done by the design council of the UK, (The Design Council, 2010) on the design process in eleven leading companies showed similarities among designers. The design process was found to be divided into four distinct phases, i) discover, ii) define, iii) develop and iv) deliver. Chapter 2 of this thesis focused on the 'discover' aspect of the design process. This section concentrates on process design and development using Aspen Plus^{TM} simulation software.

3.2 Design approach

Process synthesis is the overall development of the process flowsheet by combining individual steps into an optimal arrangement (Foo *et al.* 2005). There are two methods for process development, the hierarchical approach and the onion model. The hierarchical approach was developed by Kusiak & Finke (1987:175) and it consists of three sub-problems 1) tool path selection, 2) the tool path sequencing, and 3) the process selection. The onion model splits the candidate set into a number of subsets ("shells" or "layers"). The model makes it possible to select representative sets of structures throughout any process with reasonable design sizes (Eriksson *et al.* 2000:188). Most researchers have done process design and development using simulation software (Kane & Revankar, 2008:5996; Gorensek *et al.* 2009:4098). The design and development process by Kane & Revankar (2008:5996) and Gorensek *et al.* (2009:4098) is as follows:

- selection of the simulation package
- selection of the thermodynamic model
- validation of the model
- flow sheet simulation, and

- process analysis

The method used by Kane & Revankar (2008:5996) and Gorensek & Summers (2009:4098) was adopted for this study. Figure 3.1 shows a schematic representation of the design and development process that was used.

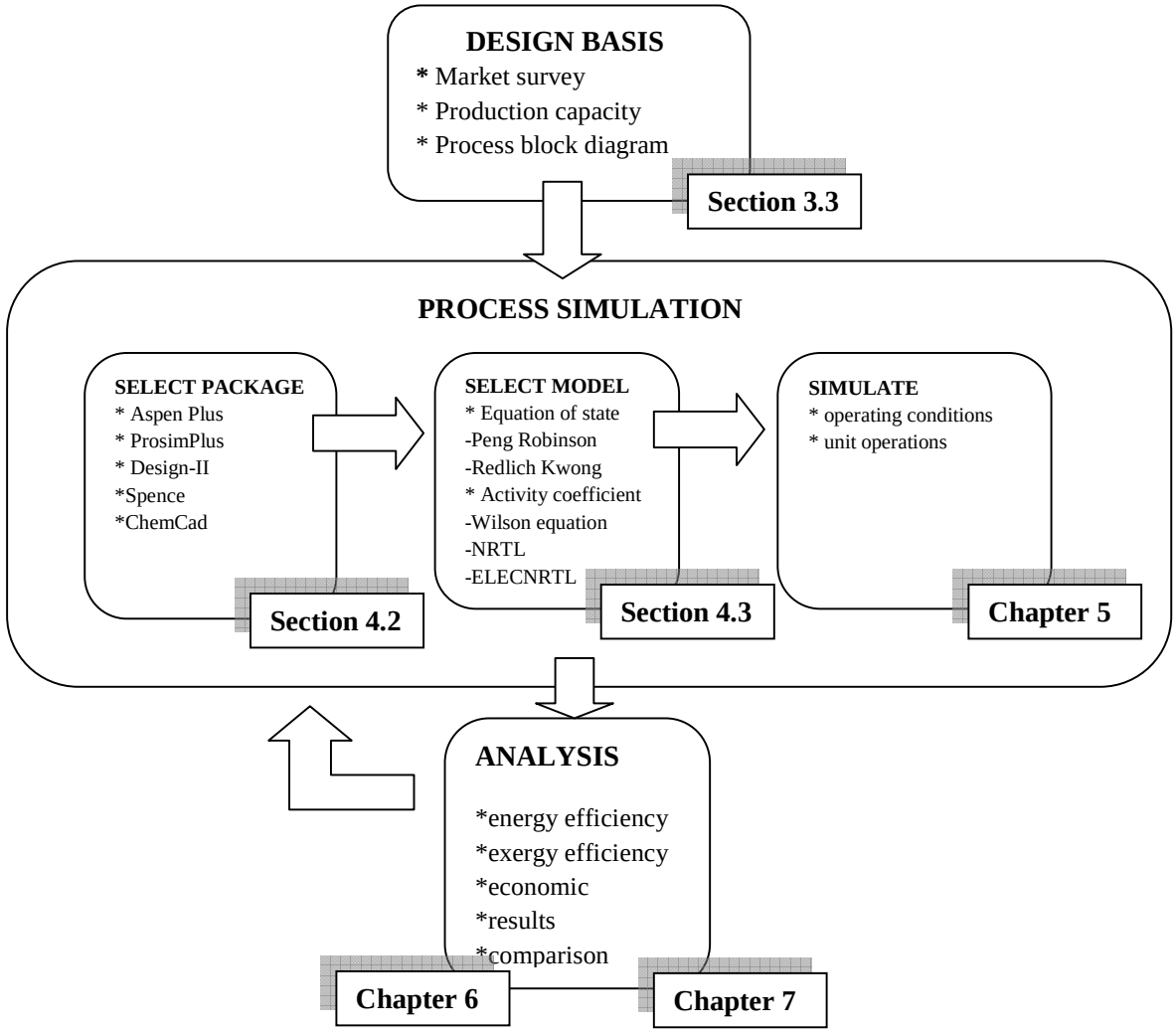

Figure 3.1: Design and development flowsheet

The South African market survey was used in the design to determine the amount of product that would needs to be produced to satisfy demand. Process simulation included selection of a simulation package and thermodynamic properties that are suitable for simulating the sulphur

iodine process. Process conditions were adopted from literature. The analysis included both economic and critical evaluation of the resultant simulation. The feedback loop is included in Figure 3.1, from analysis to process simulation, because not all results of the simulation process will compare well with other results presented in literature. In cases where the results are not satisfactory, the process simulation step is repeated.

3.3 Design basis

3.3.1 Introduction

Production systems design is influenced by product demand, of which is directly proportional production capacity. The SI cycle presented in this thesis is a thermochemical hydrogen production cycle for the South African market. The market is composed of the following sectors (Figure 2.1) (Winkler, 2006:23)

- Industry – 45%
- Transport – 20%
- Non Energy – 17%
- Residential – 10%
- Agriculture – 3%
- Commerce – 3%
- Other – 2%

Kreith & West (2004:249) argued that no currently available hydrogen production method, regardless of whether it uses fossil fuels, nuclear fuels, or renewable technology as the primary energy source to generate electricity or heat is as efficient as using the electric power or heat from any of these primary sources directly. Furthermore, depending on the primary source of the electricity, electric vehicles using batteries to store electricity are shown to be more efficient and less polluting than hydrogen fuel cell powered vehicles. Therefore replacing energy sources with hydrogen will be a difficult and an un-economic exercise, considering that some energy sources such as electricity from hydro power stations are cleaner. In light of Kreith & West (2004:249) arguments, the scope of the study is limited to the transport sector which takes 20% of the South African energy share (Winkler, 2006:23).

3.3.2 Market survey

The petroleum industry is an important source of revenue for the government and contributes to the South African economy by (SAPIA, 2010):

- generating 2% of South Africa's gross domestic product;
- supplying about 18% of South Africa's primary energy, i.e. natural energy that has not been subjected to human made conversion such as crude oil and coal;
- manufacturing more than 90% of South Africa's petroleum products;
- supporting employment for over 100 000 people directly or indirectly;
- investing R30-US billion in refinery technology for the production of unleaded petrol and low sulphur diesel;
- spending more than R115-million on corporate social investment initiatives in 2009; and
- collecting over R35-US billion in fuel taxes on petrol, diesel and paraffin

Table 3.1 shows the South African refinery ownership and crude oil throughput (SAPIA, 2010).

Table 3.1: South African refinery ownership and crude throughput (SAPIA, 2010).

NAME	**THROUGHPUT (barrels/day)**	**OWNERSHIP**
ChevRef	100 000	Chevron South Africa
EnRef	125 000	Engen Petroleum
NatRef	92 000	Sasol/Total South Africa
SapRef	180 000	Shell South Africa/BP Southern Africa

From Table 3.1, the total crude oil throughput is approximately 500 000 barrels per day, and it is refined into various petroleum products including petrol and diesel. The annual consumption of petrol and diesel is 10.8 and 9.5 US billion litres respectively. Figures 3.3 and 3.4 show the petrol and diesel usage by region.

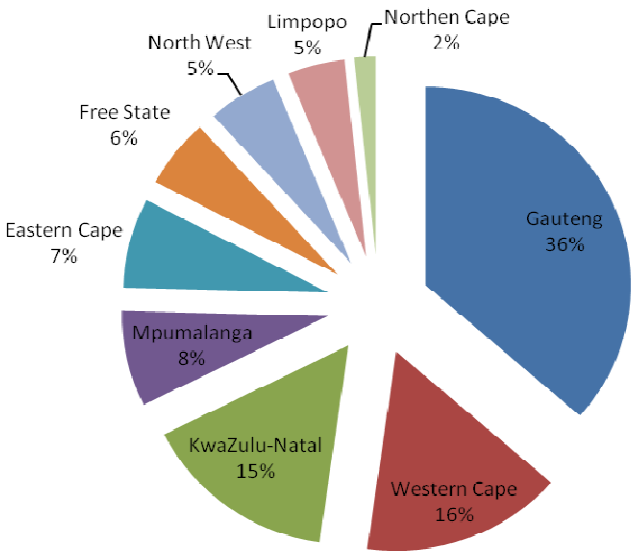

Figure 3.2: Petrol usage in South Africa by region (SAPIA, 2010)

Gauteng consumes 36% of the 10.8 million litres of petrol, and 23% of the 9.5 million litres of diesel consumed in South Africa. The trend is as a result of two major cities, Johannesburg and Pretoria, being situated within the province. The Western Cape and KwaZulu-Natal consume 16% and 15%, respectively, of the country's petrol. This order is reversed in the diesel consumption, with KwaZulu-Natal consuming 18% of diesel in comparison with the Western Cape's 15% consumption (SAPIA, 2010).

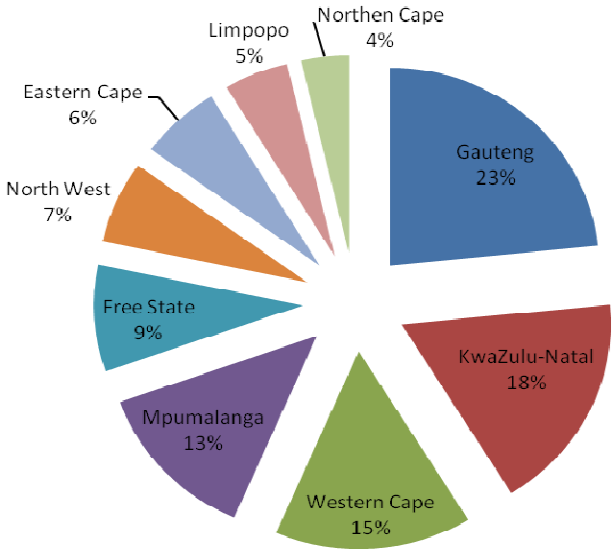

Figure 3.3: Diesel usage in South Africa by region (SAPIA, 2010)

The world fleet is expected to increase by a factor of 1.7 by the year 2050 (Kruger, 2005:1515), therefore the South African vehicle fleet can also be expected to increase by the same magnitude. The consumption of hydrogen by the vehicle fleet will also be expected to increase by the same factor. Table 3.2 shows the expected annual hydrogen consumption by province in the year 2050.

Table 3.2: South Africa's annual petroleum energy consumption for years 2010 (SAPIA, 2010) and 2050

REGION	**PETROLEUM CONSUMPTION**	**HYDROGEN CONSUMPTION**	
		2010	**2050**
Gauteng	6 323 336 240	1 818 612 406	3 091 641 091
KwaZulu-Natal	3 443 088 238	990 243 559	1 683 414 051
Western Cape	3 232 724 331	929 742 204	1 580 561 747
Mpumalanga	2 139 880 887	615 436 817	1 046 242 589
Eastern Cape	1 472 861 735	423 599 904	720 119 836
Free State	1 275 665 474	366 885 607	623 705 532
North West	1 257 894 124	361 774 508	615 016 664
Limpopo	981 036 758	282 149 415	479 654 005
Northern Cape	557 238 261	160 263 566	272 448 062
TOTAL	**20 683 726 048**	**5 948 707 987**	**10 112 803 579**

Annual petroleum consumption by province data was provided by SAPIA (2010), whereas the hydrogen consumption for 2010 was calculated via the standard enthalpies of combustion of hydrogen, diesel and petrol (ΔH_c) given by Perry's Chemical Engineers' Handbook, (Green & Maloney, 1997:186). Petroleum consumption shown in Table 3.2 represents total amounts of petrol and diesel consumed. The heats of combustion of petrol and diesel are 48 and 44.8 MJ/kg respectively. Since the total consumption of petrol and diesel in South Africa is almost shared equally, an average heat of combustion of 46.4 MJ/kg will be used in the following calculation.

From (Green & Maloney, 1997:186) the following data is obtained;

ΔH_c diesel = 44.8 MJ/kg

ΔH_c petrol = 48 MJ/kg

ΔH_c hydrogen = 121 MJ/kg

ρ (petroleum) = 0.75 (specific gravity)

Annual energy consumption = 20 683 726 048*0.75*46.4

= **719 793 666 470 MJ**

Annual hydrogen consumption **=** 719 793 666 470/121

= 5 948 707 987 kg

Hydrogen consumption figures shown in Table 3.2 were determined using the same calculation method; Kruger (2005:1515) estimated that the world vehicle fleet will increase from 900 million in 2010 to 1.5 US billion in 2050, a multiplication factor of 1.7, therefore, figures for the year 2050 were arrived at by using a multiplication factor of 1.7. The total expected hydrogen consumption for the year 2050 is given in Table 3.2, as 10 112 803 579 kg, which can be achieved by a plant or a number of plants producing a total of 163 kmol/s hydrogen.

Conclusions drawn from the market survey were as follows:

- the petroleum demand for the year 2050 can be replaced by approximately 10 US billion kilograms of hydrogen
- 10 US billion kilograms of hydrogen can be produced by a plant or a number of plants with a total output of 163 kmol/s.
- the regional hydrogen consumption for the year 2050 is summarised in Figure 3.4

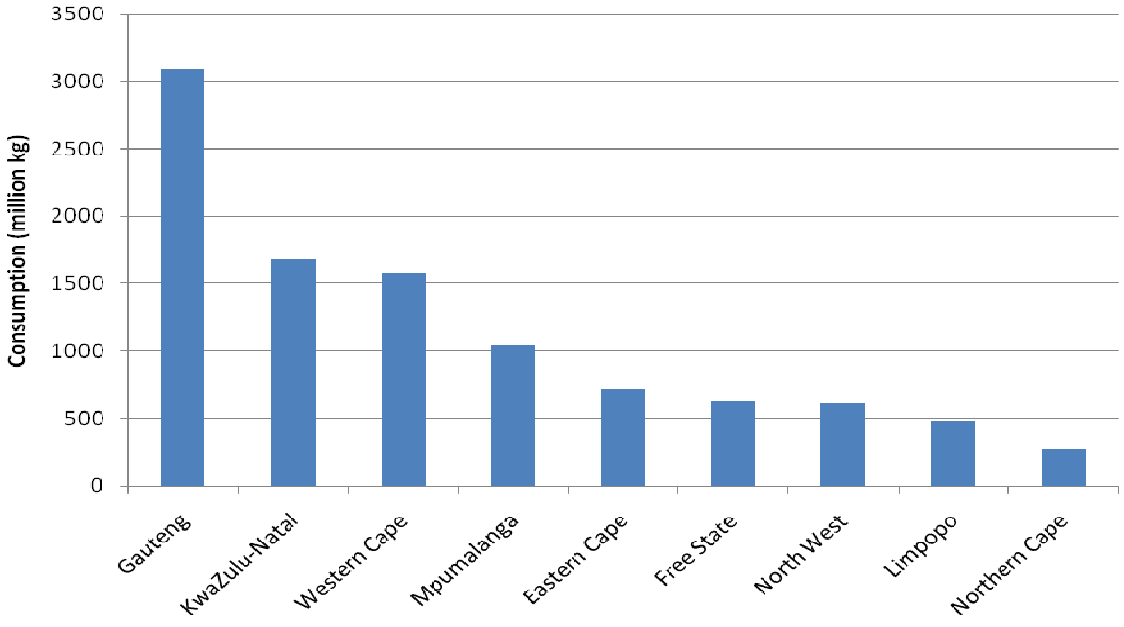

Figure 3.4: Expected regional hydrogen consumption for year 2050.

For this study, a flowsheet with a production capacity of 1 kmol/s hydrogen will be presented. A design basis of 1 kmol/s is appropriate considering the following factors:

- This study seeks to investigate the feasibility of the SI cycle for the production of hydrogen with the view of replacing petroleum energy in the South African transport sector
- Most authors (Leybros *et al.* 2010:1008; Gorensek & Summers, 2009:4098) have presented flowsheets for 1 kmol/s hydrogen output, therefore for comparison purposes, a common base of 1 kmol/s is used for this study.

3.3.3 Process block diagram

The SI cycle schematic is shown in Figure 3.5. The overall reaction involves the consumption of water to produce oxygen and hydrogen. The process is divided into three sections, i) Section I – Bunsen section; ii) Section II – acid decomposition section and iii) Section III – hydro iodide decomposition.

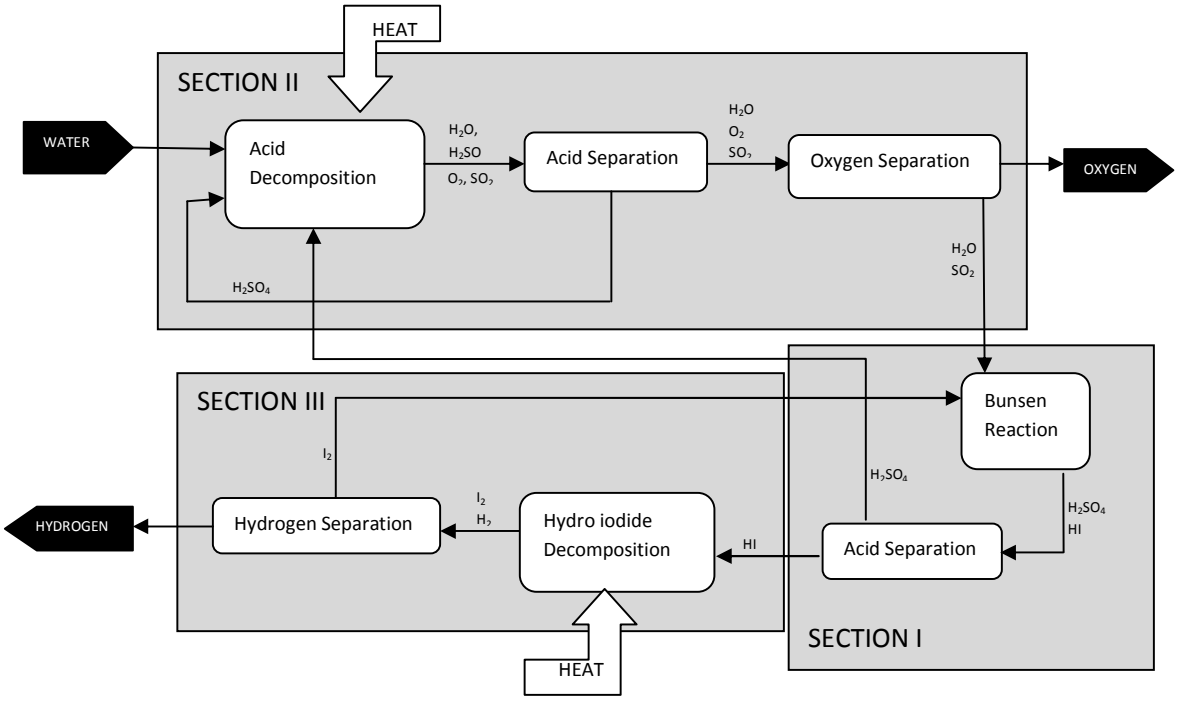

Figure 3.5: SI cycle schematic.

Section I is mainly the Bunsen reaction, Equation 3.1 shows the production of hydro-iodic acid and sulphuric acid from water, sulphur dioxide and iodine at a temperature of 120^{o}C.

$$2H_2O_{(l)} + SO_{2(g)} + I_{2(aq)} \leftrightarrow H_2SO_{4(aq)} + 2HI_{(aq)} \quad (3.1)$$

Iodine and water should be in excess, at least 9 moles of iodine and 16 moles of water as to 1 mole of sulphur dioxide (Larousse *et al.* 2009:3259). The products distribute into two immiscible aqueous acid phases. The phase rich in sulphuric acid is sent to Section II, sulphuric acid

decomposition step, Equation 3.2, where the main energy source of high temperature (800–900 ◦C) heat is put in to decompose the sulphuric acid in the gas phase into sulphur dioxide, water and oxygen. The decomposition rarely goes to completion; therefore sulphuric acid will still appear in the products. The acid is separated from the products and oxygen is separated as a product with sulphur dioxide and water returned to Section I.

$$H_2SO_{4(g)} \leftrightarrow ½\ O_{2(g)} + SO_{2(g)} + H_2O_{(g)} \quad (3.2)$$

The phase rich with hydro-iodic acid from Section I is sent to Section III where hydrogen iodide is decomposed in the vapour phase via Equation 3.3 at 300 to 600^{o}C, returning iodine to Section I and producing the final hydrogen product.

$$2HI_{(aq)} \leftrightarrow I_{2(aq)} + H_{2(g)} \quad (3.3)$$

The overall result of the reactions yields the decomposition of water into its constituent elements, hydrogen and oxygen as illustrated in Figure 3.5.

3.4 References

ERIKSSON, L., ARNHOLD, T., BECK, B., FOX, T., JOHANSSON, E. & KRIEGL, J.M. 2004. Onion design and its application to a pharmaceutical QSAR problem. *Journal of Chemometrics*, **18:**188-202, Apr.

FOO, D.C.Y., MANA, Z.A., SELVAN, M., MCGUIRE, M.L. 2005. Integrate Process Simulation and Process synthesis. http://www.cepmagazine.org. Date of access: 13 Jan. 2011.

GORENSEK, M.B. & SUMMERS, W.A. 2009. Hybrid sulfur flowsheets using PEM electrolysis and a bayonet decomposition reactor. *International Journal of Hydrogen Energy*, **34**:4097-4114, Jun.

GREEN, D.W. & MALONEY, J.O. 1997. Perry's Chemical Engineers' Handbook. McGraw-Hill.

KANE, C., REVANKAR, S.T. 2008. Sulfur–iodine thermochemical cycle: HI decomposition flow sheet analysis. *International Journal of Hydrogen Energy*, **33**:5996-6005, Sep.

KUSIAK, A., FINKE, G. 1987. Hierarchical approach to the process planning problem. Descrete Applied Mathematics, **18**:175- 184

KREITH, F., WEST, R. 2004. Fallacies of a Hydrogen Economy: A Critical Analysis of Hydrogen Production and Utilization. *Journal of Energy Resources*, **126:** 249-257, Dec.

KRUGER, P. 2005. Electric power required in the world by 2050 with Hydrogen fuel production – Revised. *International Journal of Hydrogen Energy*, **30**:1515-1522, Jun.

LAROUSSE B., LOVERA, P., BORGARD, J.M., ROEHRICH, G., MOKRANI, N., MAILLAULT, C., DOIZI, D., DAUVOIS, V.,ROUJOU, J.L., LORIN, V., FAUVET, P., CARLES, P. & HARTMAN, J.N. 2009. Experimental study of the vapour–liquid equilibria of HI–I_2 –H_2O ternary mixtures, Part 2: Experimental results at high temperature and pressure. *International Journal of Hydrogen Energy*, **34**:3258-3266, Mar.

LEYBROS, J., GILARDI, T., SATURNIN, A., MANSILLA C. & CARLES, P. 2010. Plant sizing and Evaluation of hydrogen production costs from advanced processes coupled to a nuclear heat source. Part I: Sulphur-Iodine cycle. *International Journal of Hydrogen Energy*, **35**:1008-1018, Jan.

SAPIA, 2010. Corporate Profile. http://www.sapia.co.za. Date of access: 10 Aug 2011.

THE DESIGN COUNCIL. 2010. The Design process. http://www.designcouncil.org.uk. Date of access: 13 Jan 2011.

WINKLER, H. 2006. Energy policies for sustainable development in South Africa. Options for the future. *Energy Research Centre, University of Cape Town*, **1:** 1-225, Apr

CHAPTER 4: Simulation framework

"Let's take flight simulation as an example. If you're trying to train a pilot, you can simulate almost the whole course. You don't have to get in an airplane until late in the process" Roy Romer

4.1 Introduction

Simulation is the act of reproducing the action of some general state of things by means of something suitably similar (especially for the intention of study or training). It is the technique of expressing the real world by a computer program (TSED, 2009). Simulation software is a very powerful and important tool for engineers and scientists in a variety of fields including oil and gas production, refining, chemical processing, environmental studies, and power generation. The advantages of simulation are as follows:

- In some cases, simulation eliminates the need for pilot plant construction,
- Various plant configurations can be tested on paper
- Costs are reduced due to the above mentioned advantage
- Saves time as different configurations can be tested in a short space of time
- Eliminates human errors

Therefore it is important to simulate a process before work on the ground is commenced. The major disadvantage of simulation is that in some packages, thermodynamic data is still insufficient to fully describe some systems. In the development of the SI cycle, a suitable simulation package needs to be selected; a simulation package whose use will result in a successful representation of the SI cycle.

4.2 Selection of simulation packages

There are a number of commercial simulation packages available; Table 4.1 shows the various simulation packages.

Table 4.1: Simulation packages

Package	Developer	Reference
Design-II	WinSim Inc	http://www.winsim.com/ Date of access 28 Jan. 2011
Spence	KEMA	http://kema.com/ Date of access 28 Jan. 2011
Aspen Plus	AspenTech	http://www.aspentech.com/products/aspen-plus.aspx
ProsimPlus	ProSim	http://www.prosim.net/en/modeling/prosimplus.html
ChemCad	Chemstations™	http://www.chemstations.com/ Date of access 28 Jan. 2011
CadSim Plus	Aurel Systems Inc	http://www.aurelsystems.com/csplus.htm. Date of access 28 Jan. 2011
SuperPro Designer	Intelligen Inc	http://www.intelligen.com/superpro_overview.shtml
ProModel	ProModel	http://www.promodel.com/ Date of access: 25 Jan 2011
PRO/II	SimSci-Esscor®	http://simsci.com/ Date of access: 25 Jan. 2011
SolidSim	SolidSim Eng. GmbH	http://solidsim.com/ Date of access: 25 Jan. 2011

A brief description of the main simulation packages shown on Table 4.1 is given in Appendix A. Kivisaari *et al.* (2001:112) made a study on chemical flowsheeting software as applied to hydrogen fuel cell systems. The use of three simulation packages, i.e. Design-II™, Aspen Plus™ and SPENCE® was compared. It was found that there existed some minor differences in the results given by the three simulators. The study shows that the name of the simulation package used for a certain research work is of no major importance, but what is important is the selection of thermodynamic models used to describe the system within the package. Therefore the selection of a simulation package can be based on the following:

- thermodynamic models inside the package
- cost and availability,
- technical support
- knowledge, and

- user interface friendliness.

Aspen Plus™ will be used for the simulation of the SI cycle, the reasons for choosing Aspen Plus™ are as follows:

- Aspen Plus™ includes the world's largest database of pure component and phase equilibrium data for the simulation of conventional chemical, polymer, electrolyte and solids processes (Aspen Tech, 2010)
- Regularly updated data from the U.S. National Institute of Standards and Technology (NIST) ensures easy access to the best available thermodynamic data (Aspen Tech, 2010)
- Aspen Plus has been tightly integrated with AspenTech's industry-leading cost analysis software and heat exchanger design software (Aspen Tech, 2010)
- Key equipment such as heat exchangers and distillation columns can be accurately sized from within the simulation environment (Aspen Tech, 2010)

Aspen Plus™ contains a database of physical property methods that describe different physical and chemical systems that are found in the chemical, polymer, specialty chemical, metals and minerals, and coal power industries.

4.2.1 Aspen Plus™ property models

The physical property models in the Aspen Plus™ package are categorised into i) equations of state and ii) activity coefficient models and iii) special models.

i) Equations of state

Equations of state describe a relationship between pressure (P), volume (V), and temperature (T) of pure components and/or mixtures. Equations of state are; i) good for vapour phase modelling and liquids of low polarity, ii) limited in ability to represent non-ideal liquids and iii) consistent in the critical region.

The **Peng Robinson** and **Redlich-Kwong** equations contain a combination of fitted and generated interaction parameters for all library hydrocarbon to hydrocarbon pairs, also including hydrocarbon to non-hydrocarbon binaries. The Peng Robinson equation of state is capable of predicting some specific component to component interaction parameters. The Redlich-Kwong (RK) equation of state can calculate vapour phase thermodynamic properties (Soave, 1993:345). It is reliable for systems which are at low to moderate pressures (maximum pressure 10 atm) where there is very low vapour-phase non ideality. For a more non ideal vapour phase, the Hayden-O'Connell model is recommended. Systems containing organic acids exhibit more non ideal vapour phases. The Hayden-O'Connell model is not recommended for calculating liquid phase properties. Written for pure species *i* the SRK and PR equations are special cases of the following expression:

$$P = RT/(V_i - b_i) - a_i(T)/(V_i + \varepsilon b_i)(V_i + \sigma b_i) \quad (4.1)$$

where $a_i(T) = \Omega_a \acute{\alpha}(T_{ri;}\, \acute{\omega}_i)R^2T^2_{ci}/P_{ci}$ (4.2)

$$b_i = \Omega_b RT_{ci}/P_{ci} \quad (4.3)$$

and ε, σ, Ω_a and Ω_b are equation-specific constants (Green & Maloney, 1997:18).

ii) Activity coefficient models

Activity coefficient models are good for liquid phase modelling only and can represent highly non-ideal liquids but unfortunately they are inconsistent in the critical region.

The **Wilson** equation, proposed by Grant M. Wilson in 1964 (Wilson, 1964:127) is a thermodynamically consistent equation for predicting multi-component behaviour from regressed binary equilibrium data. It can represent almost all non-ideal liquid solutions accurately except for electrolytes and solutions exhibiting little or limited miscibility, however the Wilson equation is more complex and requires more processing time than other equations. It can satisfactorily predict ternary equilibrium systems using parameters regressed from binary data. The Wilson equation gives results for weak non-ideal systems that are comparable to the ones given by the Margules and van Laar equations, but it is more accurate than the others for increasingly non-ideal systems.

The **NRTL** (Non-Random-Two-Liquid) equation, (Renon & Prausnitz, 1968:135), is a modification of the Wilson equation. It employs the statistical mechanics and the liquid cell theory to model the liquid complex. In using the statistical mechanics, the liquid cell theory, combined with Wilson's local composition model, produces an equation that can accurately represent vapour-liquid equilibrium (VLE), liquid-liquid equilibrium (LLE), and vapour-liquid-liquid equilibrium (VLLE) phase behaviour. The NRTL is reliable for ternary and higher order systems given that there are parameters obtained from binary equilibrium data. The NRTL has an accuracy comparable to the Wilson equation for VLE systems. The NRTL can use some of the equation of state methods for vapour phase thermodynamic calculations e.g. Redlich Kwong and hence the combination of the two becomes the NRTL-RK.

The **ELECNRTL** model is a variation of the NRTL model to cater for electrolytes. It involves the description of the ionic interactions along with pure component and pair-wise parameters for the ionic and non-ionic components; it is the most flexible electrolyte property method. It can handle a wide range of concentrations of aqueous and mixed solvent systems with a single pair of binary systems (Aspen Plus, 1997:19).

iii) Special models

Special methods include the **Amines Property Package**, the amines package contains the thermodynamic models developed by D.B. Robinson & Associates. The models were developed for their patented amine process plant simulator, called AMSIM (Aspen Plus™ Reference Manual, 1997).

4.3 Selection of property method for the SI cycle system

It is important to select a proper property method for a system because each property method is suitable for a certain group of components and a range of conditions, and a poor choice of a property method can lead to unreliable simulation results (Seader *et al.* 2006).

The SI process chemical species include strong acids (H_2SO_4 and HI) that dissociate hence an electrolytic model is essential for accurate and reliable modelling. Bob Seader (Seader *et al.* 2006) suggested a method for the selection of a property method; henceforth this method will be called the "Bob Seader" method. The method is an algorithm which leads to one choice of property method, because of the conditions specified in the algorithm that eliminate other property methods. The application of the algorithm to the selection of the property method for the SI cycle system is shown in Figure 4.1.

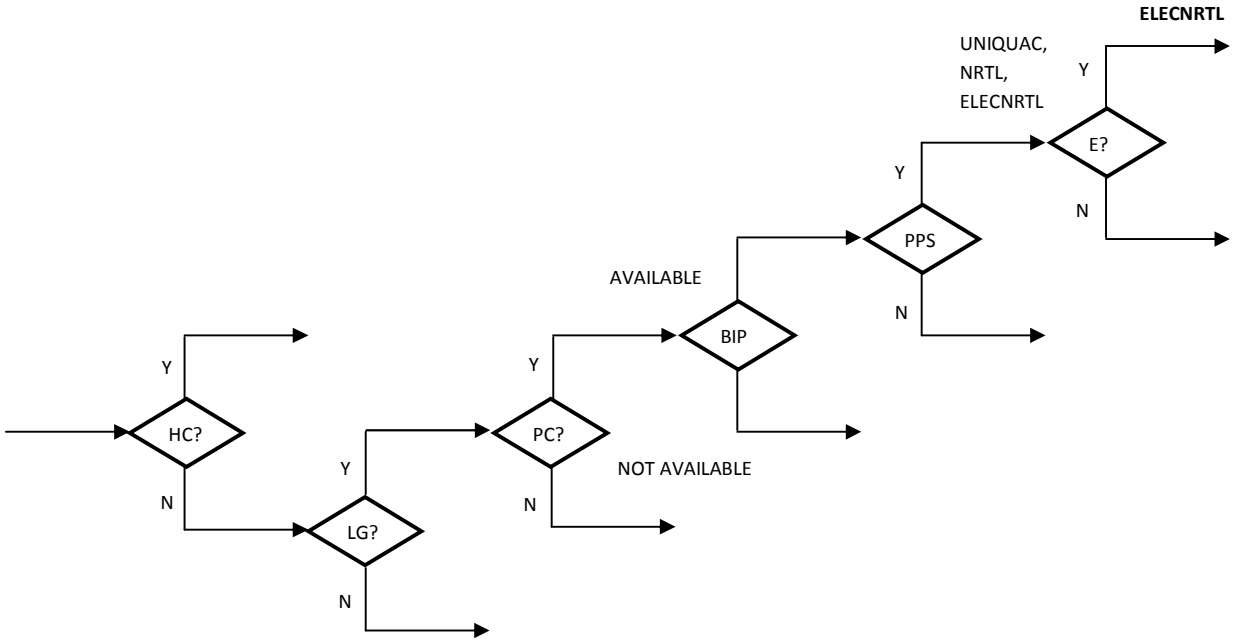

Figure 4.1: Bob Seader property selection method [HC – hydrocarbons; LG – light gas; PC – polar compound; BIP – binary interaction parameters; PPS – possible phase splitting; E – electrolytes]

In the development of the algorithm in Figure 4.1 the following factors for the SI cycle system were considered:

- The system has polar compounds, for example water and acid
- The system has light gases, for example hydrogen and oxygen
- There is a possibility of liquid-liquid phase splitting on the HI_x system
- Electrolytic compounds, for example acid dissociates into ions.

Such a system can be approximately be represented by an Aspen Plus™ simulation using the ELECNRTL physical property method.

4.4 The ELECNTRL

In Aspen Plus™, an electrolyte system is defined as a system in which there is a partial or complete dissociation of molecular species into ions in a liquid solvent, and some of the molecular species form a salt precipitation. The dissociation and precipitation reactions occur fast enough that the reactions can be said to be at equilibrium. The liquid phase equilibrium reactions that describe this action are referred to as the solution chemistry. All unit operation models provided in Aspen Plus™ can handle electrolytic reactions. The presence of ions in the aqueous and liquid phase causes highly non-ideal behaviour. Aspen Plus™ provides thermodynamic models with a databank of binary interaction parameters between water and over 600 electrolyte ion pairs. The models have been developed specifically to represent the non-ideal behaviour of liquid phase components (Aspen Plus, 1997:19).

The ELECNRTL model is based on the NRTL theory that incorporates the Wilson local composition expression. The local composition models in NRTL have proved to be very successful in representing thermodynamic properties of various electrolyte solutions and have extensively been used for the correlation of thermodynamic properties of electrolyte solutions.

The ELECNRTL is fully in agreement with the NRTL for liquid phase property calculation and uses the Redlich Kwong property method for vapour phase calculations. An ELECNRTL model can handle everything from concentrated electrolytes through dilute electrolytes to non-polar species, such as iodine, so it should be able to handle the chemistry of the SI cycle (Aspen Plus, 1997:19).

4.5 Validation of the ELECNRTL for the SI cycle system

The ELECNRTL model must be validated so as to ascertain whether it satisfactorily represents the system over the composition range and temperature under investigation. The validation will be done from the following perspective:

- The HI-H_2O binary system
- The H_2O-I_2 binary system
- The SO_2-H_2O binary system
- Constant pressure specific heat capacity

The HI-H_2O-I_2-SO_2-H_2SO_4 system involved in the process is a complex system because of the various ionisation and complexation phenomena that occur. The system can be split into different binary systems. The HI–H_2O binary system is electrolytic and exhibits a homogenous mixture. The system exhibits liquid–liquid equilibrium because of iodine's low solubility in water and the presence of a miscibility gap in the HI-H_2O binary system. Concerning the H_2O-I_2 binary system, the system is highly non ideal with liquid-liquid equilibrium shown above iodine's melting point. SO_2-H_2O binary exhibits complex phase behavior because it hydrates and shows immiscibility (Lanchi *et al.* 2009:2123). The model can be considered sufficient if it can give results of the systems discussed that are comparable with experimental data presented by different authors.

Figures 4.2 to 4.6 show the curves of the bubble pressures of the HI-H_2O-I_2-SO_2-H_2SO_4 system's binary mixtures at different temperatures and pressures presented by different authors (Kane & Revankar, 2009:5999; Lanchi *et al.* 2009:2128; Gorensek & Summers, 2007:16; Mathias & Brown, 2003:16) and data obtained from Aspen Plus™.

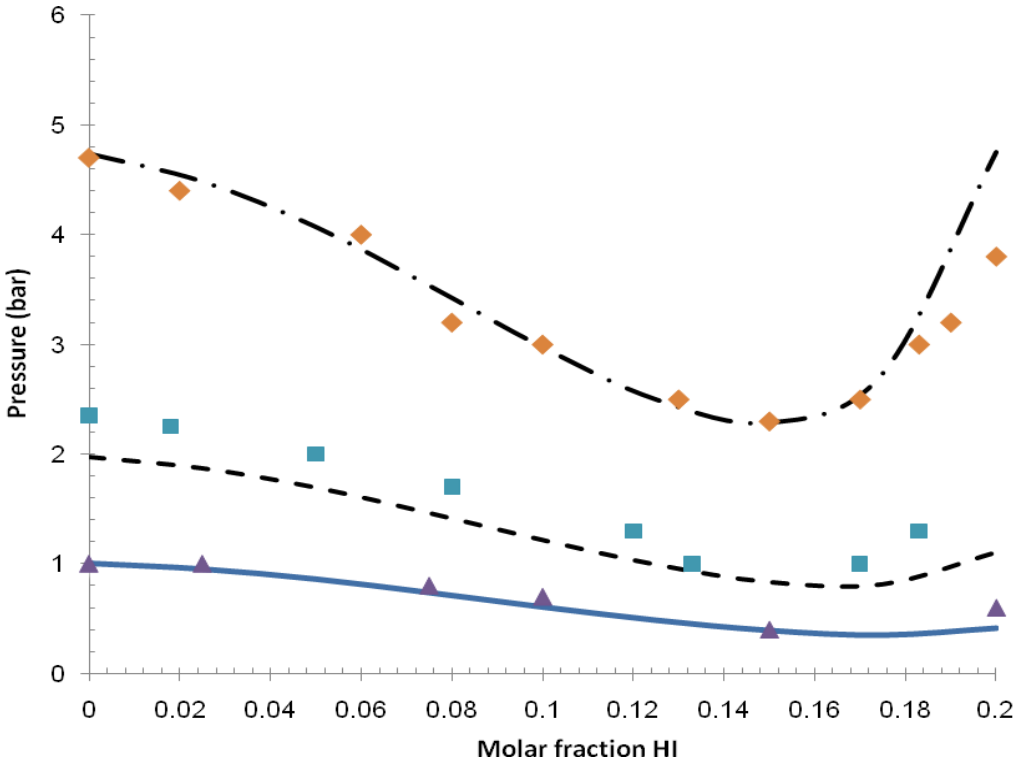

Figure 4.2: Bubble pressures of HI–H_2O mixture compared to the theoretical General Atomics (GA) analysis results [—— Aspen Plus™, 373K; - - - - Aspen Plus™, 398K; – · – Aspen Plus™, 423K; ▲ GA, 373K; ■ GA, 398K; ◆ GA, 423K] Kane & Revankar (2009:5999)

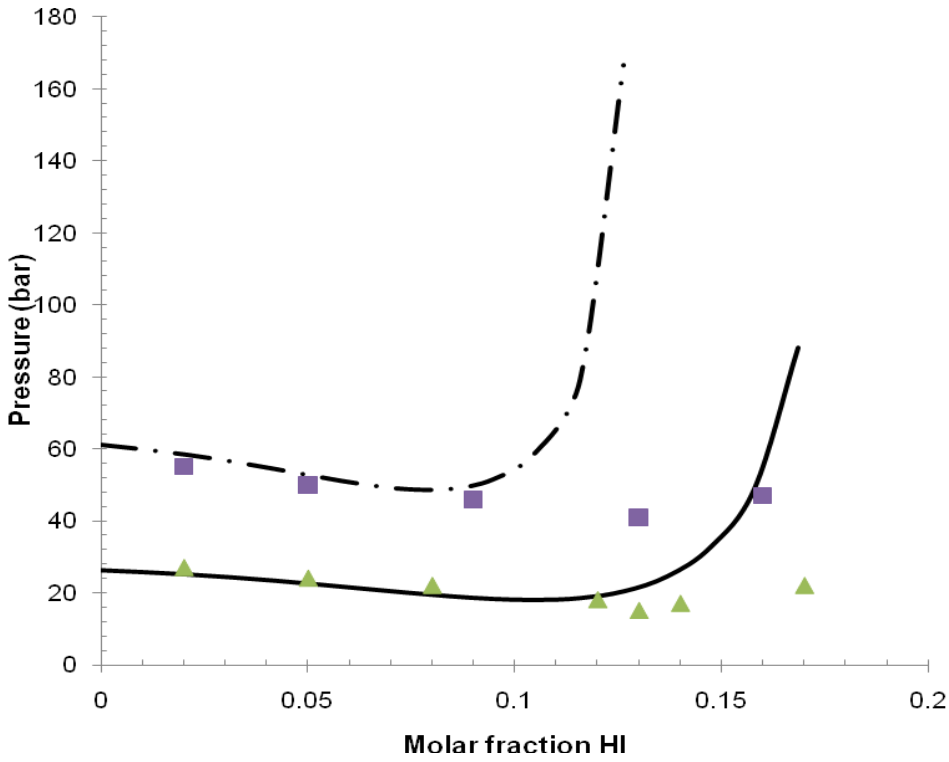

Figure 4.3: Bubble pressures of HI–H_2O mixture compared to the theoretical General Atomics (GA) analysis results [—— Aspen Plus™, 500K; –·– Aspen Plus™, 550K; ▲ Engels & Knoche, 500K; ■ Engels & Knoche, 550K] Kane & Revankar (2009:5999)

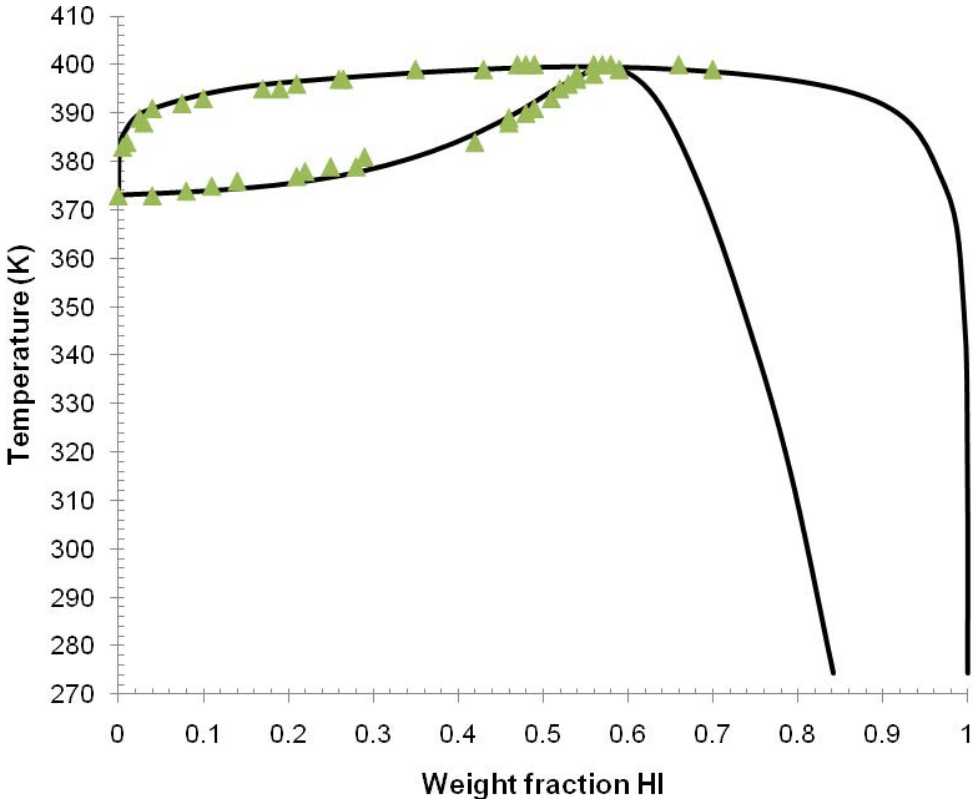

Figure 4.4: HI–H_2O binary system phase diagram at atmospheric pressure (T (K) vs HI weight fraction): comparison between Sako's experimental data and Aspen Plus™ [— Aspen Plus™; ▲ Sako] Lanchi *et al.* (2009:2128)

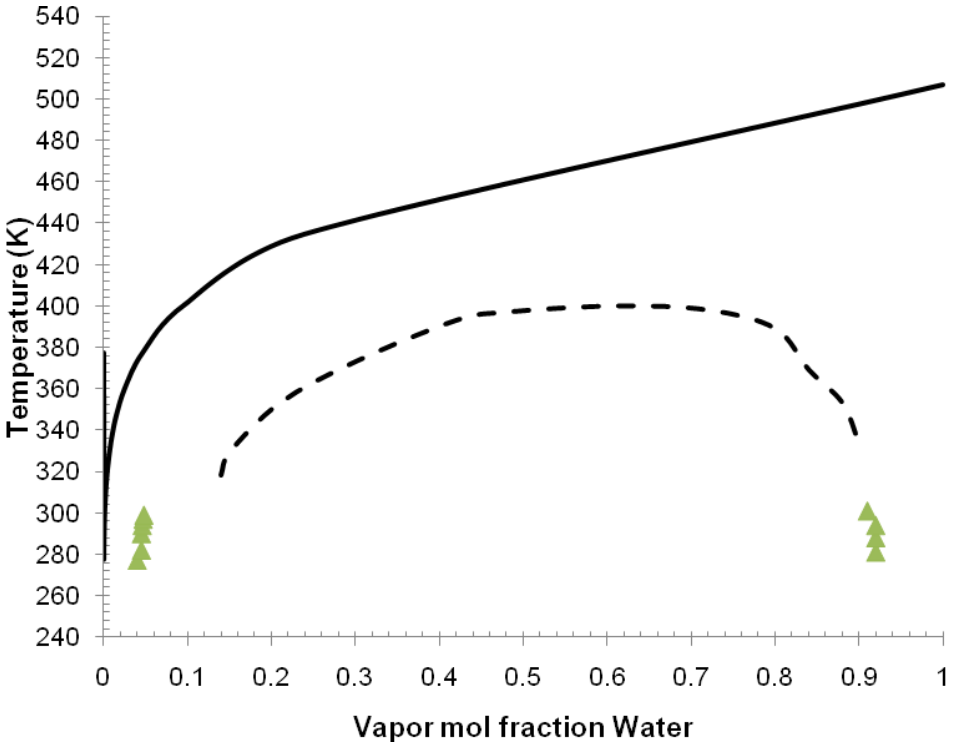

Figure 4.5: SO_2–H_2O binary system phase diagram at atmospheric pressure (T (K) vs water mol fraction): comparison between Maas & Maas and Spall's experimental data and Aspen Plus™ [── Aspen Plus™; - - Maas & Maas; ▲ Spall] Gorensek & Summers (2007:16)

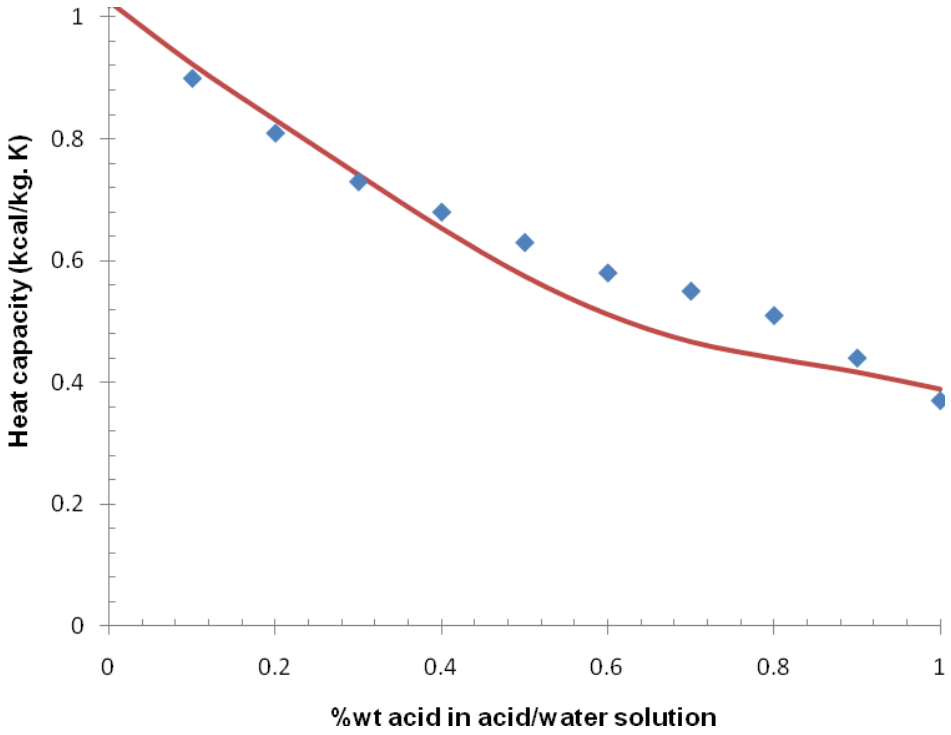

Figure 4.6: Liquid heat capacity of sulphuric acid at 10 bars (Heat capacity (kcal/kg. K) vs %wt acid): comparison between Fasullo's experimental data and Aspen Plus™
[—— Aspen Plus™; ◆ Fasullo] Mathias & Brown (2003:16)

Overall, the results show a good agreement for the HI molar range of 0 to 0.15. The electrolytic binary HI-H_2O exhibits an azeotrope at 0.157 HI molar fraction (Lanchi *et al.* 2009:2123). For HI concentrations above the azeotrope, and high pressures (> 20bar) the results given by Aspen Plus™ deviate from the experimental results. The deviation can be due to the model's failure to cater for:

- the solvation of iodides by iodine in the liquid phase,
- the non ideality of the vapour and liquid phases; the binary (HI–H_2O) or the ternary (HI–I_2–H_2O) mixtures in the HI section are strongly non-ideal solutions and partially immiscible

4.6 Summarised remarks

Although Aspen Plus™ ELECTNRTL model has been validated and will be used for the simulation, it will not predict the sulphur-iodine thermochemical cycle system with 100% confidence because of the following reasons:

- The HI–H_2–I_2–H_2O quaternary system thermodynamic behaviour is complicated. In the HI–I_2–H_2O ternary liquid phase, H_2O–I_2 and H_2O–HI show a highly immiscible and an azeotropic liquid–liquid equilibrium respectively (Cho, *et al.* 2009:501).
- SO_2 –H_2O binary exhibits complex phase behaviour of hydration and immiscibility.
- Inclusion of SO_2 further complicates the system; Henry-comp treatment of SO_2 precludes the formation of liquid phase.
- Section II has units that operate at very high temperatures that exceed the critical temperature of water (374°C). At these temperatures, ions tend to exist as pairs and this must be correctly accounted for in the model.
- Section III encounters complex behaviour of the HI-I_2-H_2O system, which includes multiple liquid phases and possible solid precipitation. While the process conditions, by design, avoid regions where multiple liquids or solid precipitation actually occur, the model must correctly account for this behaviour, if only to avoid these unfavourable regions.

Cho *et al.* (2009:501) argued that Aspen Plus™ uses the Redlich-Kwong equation of state to handle the non-ideal behaviour of HI_x gas phase. The partial pressure of hydrogen is considered via Henry constant since hydrogen exists in supercritical condition. ELECNRTL equation of state regresses VLE, LLE, SLE of HI_x systems successfully. Compared to the Neumann model, the ELECNRTL shows larger deviations in VLE of HI_x data. The ELECNRTL thermodynamic model identifies the non-ideality of the ionic liquid solutions, however, there are dissociation, complexation and precipitation reactions occurring in solution, therefore the ELECNRTL model

must be coupled with models that describe the reactions. Furthermore multiple chemistry models need to be employed because of the complexity and variety of phenomena that occur in various parts of the sulphur iodine process (Mathias & Brown, 2003).

4.7 References

ASPEN PLUS. 1997. Modeling Processes with Electrolytes: Getting started. Aspen Tech. 80p.

ASPEN TECH. 2010. Aspen Plus. http://www.aspentech.com/core/aspen-plus.aspx. Date of access: 03 Apr 2010

AUREL SYSTEMS INC. 2010. CadSim Plus. http://www.aurelsystems.com/csplus.htm. Date of access: 28 Jan. 2011

CHEMSTATIONS. 2010. ChemCAD. http://www.chemstations.com/ Date of access 28 Jan. 2011

CHO, W.C., PARK, C.S., KANG, K.S., KIM, C.H., & BAE, K.K. 2009. Conceptual design of sulfur-iodine hydrogen production cycle of Korea Institute of Energy Research. *Nuclear Engineering & Design,* **239**:501-507, Nov.

GORENSEK, M.B. 2007. Modeling sulfur dioxide solubility in sulfuric acid solutions (457c). (Paper presented at the AlChe 2007 Annual meeting on 7 November 2007. Salt Lake City)

GREEN, D.W. & MALONEY, J.O. 1997. Perry's Chemical Engineers' Handbook. McGraw-Hill. [CD]

INTELLIGEN INC. 2010. SuperPro Designer. http://www.intelligen.com/superpro_overview.shtml. Date of access: 28 Jan 2011

KANE, C., REVANKAR, S.T. 2008. Sulfur–iodine thermochemical cycle: HI decomposition flow sheet analysis. *International Journal of Hydrogen Energy*, **33**:5996-6005, Sep.

KEMA. 2010. KEMA-SPENCE for simulation of process for energy conversion and electricity production. http://www.kema.com/Images/Spence process simulation description. pdf. Date of access: 28 Jan 2011

KIVISARI, T., LAAG, P.C. & RAMSKOLD, A. 2001. Benchmarking of chemical flowsheeting software in fuel cell applications. *Journal of Power Sources* **94**:112-121, Oct.

LANCHI, M., CEROLI, A., LIBERATORE, R., MARRELLI, L., MASCHIETTI, M., SPADONI, A., & TARQUINI, P. 2009. S–I thermochemical cycle: A thermodynamic analysis of the HI–H_2O–I_2 system and design of the HI_X decomposition section. *International Journal of Hydrogen Energy*, **34**:2121-2132, Jan.

MATHIAS, P.M., & BROWN, L.C. 2003. Thermodynamics of the sulfur iodine cycle for thermochemical hydrogen production. (Paper presented at the 68TH Annual meeting of the Society of Chemical Engineers on 23 March 2003. Tokyo)

PROMODEL. 2010. ProModel. http://www.promodel.com/ Date of access: 25 Jan 2011

PROSIM. 2010. ProsimPlus. http://www.prosim.net/en/modeling/prosimplus.html. Date of access: 03 Apr 2010

RENON, H., & PRAUSNITZ, J.M. 1968. Local composition in thermodynamic excess functions for liquid mixtures. *AICHE Journal,* **14**:135-144, Jan.

SEADER, J.D., SEIDER, W.D., LEWIN, D.R. 2006. Using process simulators in Chemical Engineering. Wiley [CD].

SIMSCI-ESSCOR. 2010. PRO/II. http://simsci.com/ Date of access: 25 Jan. 2011

SOAVE, G. 1993. 20 Years of Redlich-Kwong Equation of state. *Fluid Phase Equilibria*. **82**:345-359, Feb.

SOLIDSIM ENGINEERING GMBH. 2010. SolidSim. http://solidsim.com/ Date of access: 25 Jan. 2011

TSED (The Sage English Dictionary) 2009. “Simulation”. [CD]

WILSON, G.M. 1964. Vapour-liquid equilibrium. A new expression for the excess free energy of mixing. *Journal of American Chemical Society*. **86:**127–130, Jan.

WINSIM. 2011. Design II for windows. http://www.winsim.com/design.html. Date of access: 28 Jan 2011

CHAPTER 5 – Aspen Plus™ process simulation

"Deep down, the US, with its space, its technological refinement, its bluff good conscience, even in those spaces which it opens up for simulation, is the only remaining primitive society" Jean Baudrillard

5.1 Introduction

Aspen Plus™ is a market-leading process modelling tool for conceptual design, optimisation, and performance monitoring for the chemical, polymer, specialty chemical, metals and minerals, and coal power industries (Aspen, 2010). The SI process has been simulated successfully by different authors (Leybros & Summers, 2009:9064). The conditions and some of the products specified into the simulator have been reported by different authors in the field of the SI cycle study.

5.1.1 Assumptions

The assumptions taken during the preparation of the SI cycle flowsheet were as follows:

- The ELECNRTL properties model used for the simulation accurately represent the H_2SO_4-HI-I_2-H_2O-SO_3-SO_2-O_2 system.
- High temperature sulphuric acid decomposition proceeds to thermodynamic equilibrium.
- No piping and vessel pressure drops.

5.2 Section I: The Bunsen section

5.2.1 Literature survey

The Bunsen reaction is a liquid phase exothermic reaction involving iodine, sulphur dioxide and water. The products are two immiscible aqueous acids, aqueous sulphuric acid (light phase) and a mixture of hydrogen iodide, iodine and water, referred to as HI_x (heavy phase). The reaction is summarised in Equation 5.1:

$$I_{2(l)} + SO_{2(aq)} + 2H_2O_{(l)} \longrightarrow H_2SO_{4(aq)} + 2HI_{(l)} \quad (5.1)$$

Researchers have suggested the following conditions for the Bunsen reaction. the simulation was based on a summary of what the following researchers have previously reported:

- The Bunsen reaction occurs at 127 ^oC and 2 bar, (Goldstein *et al.* 2005:621)
- The exothermic Bunsen reaction takes place mostly in a heat exchanger reactor operating at 7 bar and 105 - 120 ^oC, (Giaconia *et al.* 2007:474)
- An excess of water and iodine characterizes the feed from other sections in order to allow acceptable reaction rates and easy separation of products into two liquid phases (Giaconia *et al.* 2007:474). The allowable window ranges from 4 to 6 moles for excess iodine and 11–13 moles for excess water at 57–77 ^oC (Leybros *et al.* 2009:9064)
- The operating temperature of the iodine entering the reactor should be more than its melting temperature (Leybros *et al.* 2009:9063). The melting point of iodine is 113.5 ^oC (Green & Maloney, 1997:18).
- Experimental data indicate that the sulphuric acid phase leaves the reactor with a nearly constant molar composition close to $[H_2SO_4 + 4H_2O]$. For process design, Leybros *et al.* (2009:9063) suggested an alternative stoichiometry for Equation 5.1,

$$7I_{2(l)} + SO_{2(aq)} + 15H_2O_{(l)} \longrightarrow [H_2SO_{4(aq)} + 4H_2O_{(l)}] + [2HI_{(l)} + 9H_2O_{(l)} + 6I_2] \quad (5.2)$$

5.2.2 Conceptual development

Figure 5.1 shows a basic flow diagram for Section I, the conditions specified in the block diagram are a summary of the literature presented in Section 5.2.1.

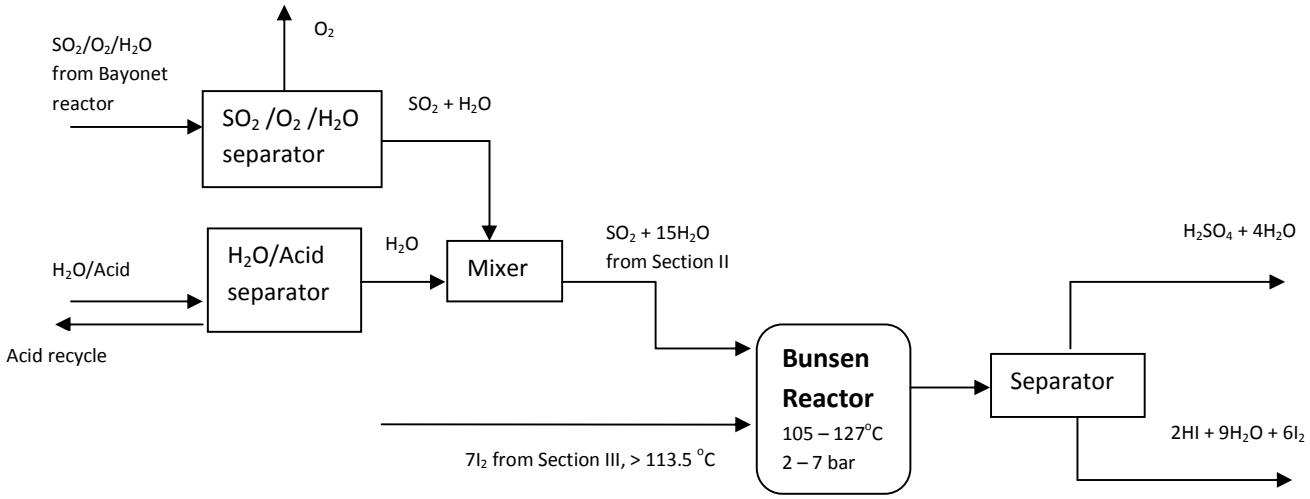

Figure 5.1: Section I process block diagram.

Since SO_2 should dissolve in the reaction medium and maintain the highest possible SO_2 partial pressure (Leybros *et al.* 2009:9064), the reactants should be in liquid phase. The operating temperature of iodine entering the reactor should be more than its melting temperature. The melting point of iodine is 113.5 ^oC (Green & Maloney, 1997:18). Therefore, the Bunsen section should include, i) SO_2-O_2 separation unit to separate O_2, preferably an SO_2 absorber unit, ii) H_2O-H_2SO_4 separation unit, preferably a distillation column and, iii) condensers to liquefy SO_2 which comes from Section II in gaseous phase, this will not be necessary since most of reactor feed is the liquid underflow from the absorption column.

The Bunsen section should consist of a reactor and some liquid separation units. Figure 5.2 shows the Aspen Plus^{TM} process simulation of Section I.

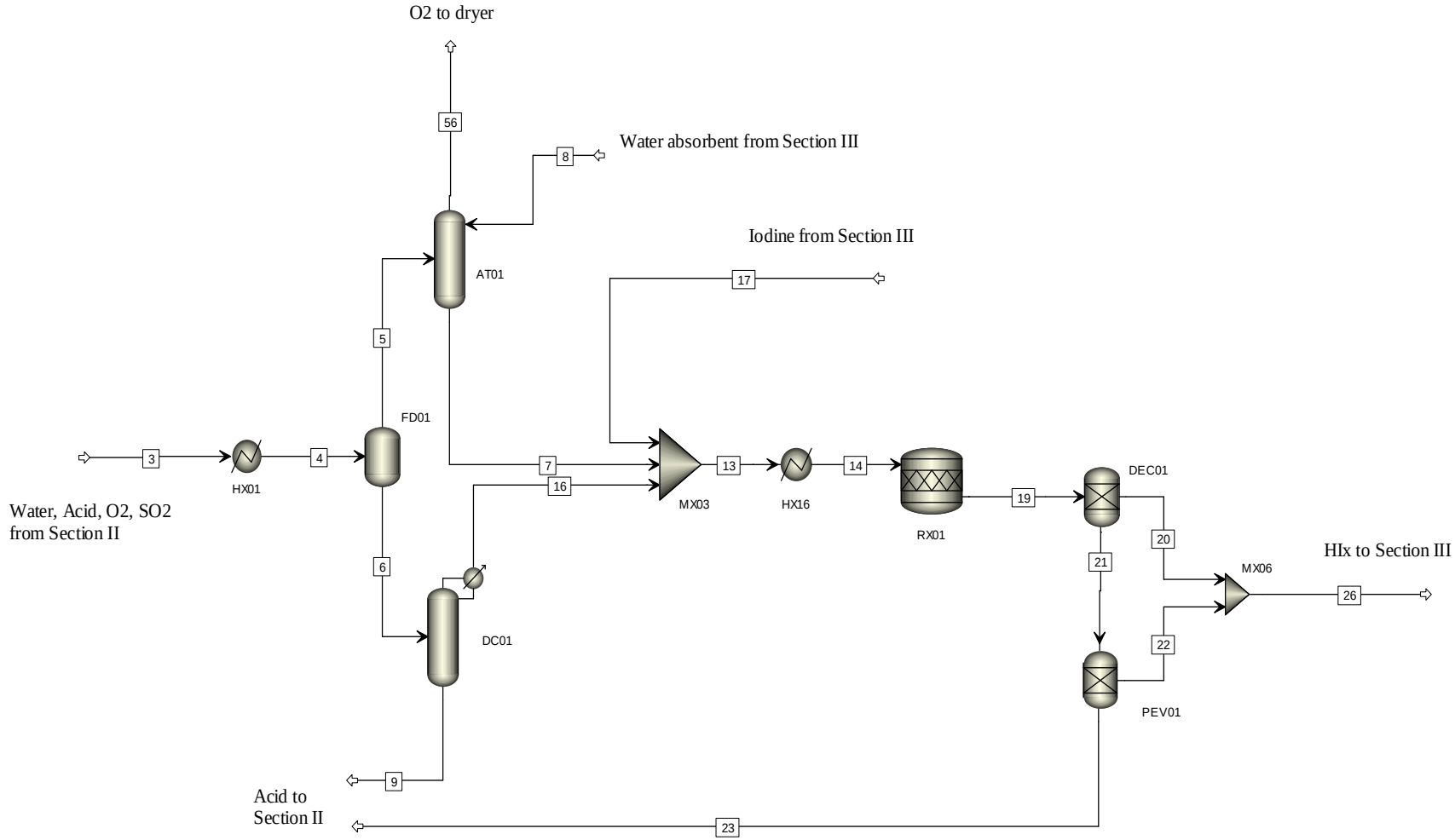

Figure 5.2: Aspen Plus^{TM} Section I flowsheet.

Table 5.1: Aspen Plus™ Section I flowsheet stream table.

Stream ID	3	4	5	6	7	8	9	13	14	16	17	19	20	21	22	23	26	56
Temperature (^{o}C)	288.6	150	150	150	57.4	49.6	315.1	76.1	106.1	42.3	120	120	120	120	120	120	121.6	49.6
Pressure (bar)	20	20	20	20	5	5	5	1	5	5	1	5	5	5	5	5	5	5
Vapour Fraction	0.246	0.160	1.000	0.000	0.000	0.000	0.000	0.020	0.020	0.000	0.000	0.000	0.000	0.000	0.000	0.000	0.000	1.000
Mole Flow (kmol/sec)	9.313	9.313	1.494	7.819	50.62	49.65	5.819	57.46	57.46	48.59	4.833	56.45	50.43	6.018	4.001	2.018	54.43	0.512
Mass Flow (kg/sec)	459.03	459.0	78.61	380.4	3363	3301	342.5	4627	4627	3281	1226	4627	4438	189.1	72.07	117.1	4510	16.29
Mole Flow (kmol/sec)																		
H_2O	2.292	1.970	0.020	1.950	39.43	39.44	0.712	41.41	41.41	38.38	0.000	36.36	32.36	4.001	4.001	0.187	36.36	0.010
H_2	0.000	0.000	0.000	0.000	0.000	0.000	0.000	0.000	0.000	0.000	0.000	0.000	0.000	0.000	0.000	0.000	0.000	0.000
O_2	0.504	0.504	0.504	0.000	0.002	0.000	0.000	0.002	0.002	0.000	0.000	0.002	0.002	0.000	0.000	0.000	0.002	0.502
H_2SO_4	0.431	0.109	0.000	0.109	0.000	0.000	0.832	0.000	0.000	0.000	0.000	0.000	0.000	0.000	0.000	0.187	0.000	0.000
SO_2	1.009	1.009	0.970	0.039	0.962	0.000	0.000	1.008	1.008	0.000	0.000	0.000	0.000	0.000	0.000	0.000	0.000	0.000
SO_3	0.000	0.000	0.000	0.000	0.000	0.000	0.000	0.000	0.000	0.000	0.000	0.000	0.000	0.000	0.000	0.000	0.000	0.000
I_2	0.000	0.000	0.000	0.000	10.20	10.20	0.000	15.03	15.03	10.20	4.833	14.03	14.03	0.000	0.000	0.000	14.030	0.000
HI	0.000	0.000	0.000	0.000	0.000	0.000	0.000	0.000	0.000	0.000	0.000	0.000	0.000	0.000	0.000	0.000	0.000	0.000
H_3O^+	2.538	2.861	0.000	2.861	0.008	0.000	2.137	0.001	0.001	0.000	0.000	3.027	2.018	1.009	0.000	0.822	2.018	0.000
HSO_3^-	0.000	0.000	0.000	0.000	0.008	0.000	0.000	0.001	0.001	0.000	0.000	0.000	0.000	0.000	0.000	0.000	0.000	0.000
I^-	0.000	0.000	0.000	0.000	0.000	0.000	0.000	0.000	0.000	0.000	0.000	2.018	2.018	0.000	0.000	0.000	2.018	0.000
HSO_4^-	2.538	2.861	0.000	2.861	0.000	0.000	2.137	0.000	0.000	0.000	0.000	1.009	0.000	1.009	0.000	0.822	0.000	0.000
OH^-	0.000	0.000	0.000	0.000	0.000	0.000	0.000	0.000	0.000	0.000	0.000	0.000	0.000	0.000	0.000	0.000	0.000	0.000
SO_3^{2-}	0.000	0.000	0.000	0.000	0.000	0.000	0.000	0.000	0.000	0.000	0.000	0.000	0.000	0.000	0.000	0.000	0.000	0.000
SO_4^{2-}	0.000	0.000	0.000	0.000	0.000	0.000	0.000	0.000	0.000	0.000	0.000	0.000	0.000	0.000	0.000	0.000	0.000	0.000

The product from Section II (Stream 3) is at a temperature of 288.6 ^{o}C and consists of 5.4 mol% O_2, 10.8 mol% SO_2 in aqueous acid. It is cooled to 150^{o}C (HX01) so as to remove most of the H_2SO_4 and remain with an SO_2-O_2-H_2O gaseous mixture (FD01). At 150^{o}C, H_2SO_4 is in liquid phase whereas SO_2, O_2 and H_2O are in gas phase, therefore at this temperature acid separation from the H_2SO_4-SO_2-O_2-H_2O mixture can be achieved by a gas liquid separator, preferably a flush drum.

The gaseous mixture of SO_2-O_2-H_2O (Stream 5) containing 64.9 mol% SO_2, 33.7 mol% O_2 and 1.4 mol% H_2O respectively, is fed to the bottom stage of the SO_2 absorber (AT01). SO_2 is a polar compound with a dipole moment of 1.6, while O_2 is non-polar (Bae & Lee, 2005:102). A solvent such as water can be effectively used to separate a mixture of SO_2 and O_2 preferably in a spray tower absorber. The SO_2 absorber will be at equilibrium stage with vapour-liquid fractionation device which operates at a pressure of 5 bars with an assumed negligible pressure drop. In this operation most of the SO_2 is liquefied and is fed to the Bunsen reactor (RX01) via Stream 7.

Stream 5 is mostly aqueous acid and is fed to a distillation column (DC01). Figure 5.3 shows the y-x diagram for H_2SO_4 – H_2O binary system, if we were to use the McCabe-Thiele method, it is clear that the acid separation could be achieved by only two stages. Since the separation is a two stage distillation process, the operating conditions of DC01 are derived by running trial and error simulations until the simulation converges. The resultant distillation column configuration is as follows: i) reflux ratio = 1.2 (by mass), ii) fixed distillate rate of 2 kmol/s, iii) pressure of 5 bars, iv) two stages and, v) the feed is at stage 2. The acid is concentrated from 2.8 wt% (Stream 5) to 23.8 wt% (stream 9) which is sent back to Section II. The water distillate (Stream 16) which contains 6.6 wt% SO_2 is sent to the Bunsen reactor.

The Bunsen reactor's (RX01) inputs are a liquid mixture of SO_2, I_2 and H_2O (Stream 6) from the SO_2 absorber, a liquid mixture of SO_2 and H_2O from the distillation column, iodine from Section III (Stream 17) and recycled HI from Section III (stream 23). Goldstein *et al.* (2005:621) and Giaconia *et al.* (2007:474) specified a temperature of 120 and 127 ^{o}C and pressures up to 7 bar for the Bunsen reaction. Also the temperature should be above the melting point of iodine (Leybros *et al.* 2009:9063). Therefore the specified temperature and pressure conditions will be

120°C and 5 bar for this simulation. The reactions specified are assumed to be 100% conversion with respect to SO_2. Since the conversion, temperature and pressure for the Bunsen reaction are known, an RStoic block is used to simulate the Bunsen reactor. The product from the Bunsen reactor (Stream 19) is 34.7 mol% H_2O, 63 mol% I_2, 0.5 mol% H_2SO_4, and 1.8 mol% HI. This product forms a two phase liquid mixture composed of the light acid phase and the heavy HI_x phase.

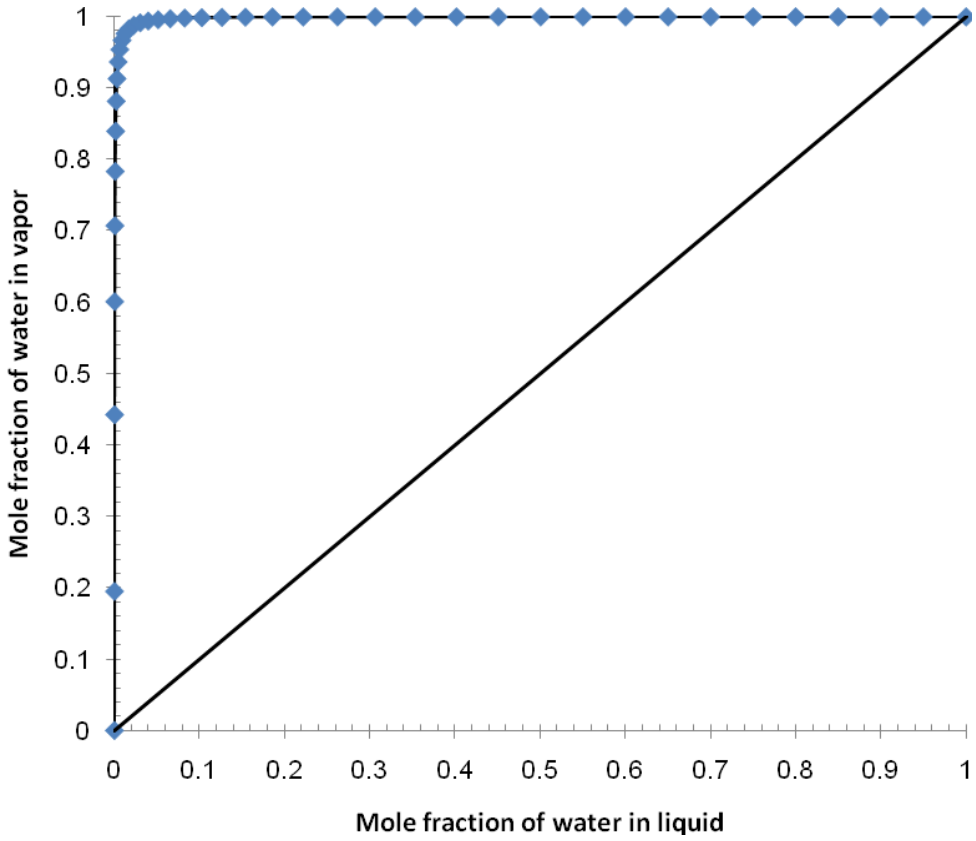

Figure 5.3: y-x diagram for H_2SO_4 – H_2O

The performance of the Bunsen section depends much on its interaction with other sections. In this section, the effect of the amount of excess iodine and water on the energy requirements of the Bunsen reactor is investigated. The allowable window ranges from 4 to 6 moles for excess iodine and 11–13 moles for excess water at 57–77 ^{o}C (Leybros *et al.* 2009:9064)

To investigate the effect of excess iodine or water on the Bunsen reaction, a separate simulation is run with the feed entering the reactor at 76^{o}C and 5 bar. The iodine or water mole flow is varied. Figures 5.4 and 5.5 show that as the amount of excess iodine is increased, the net heat duty to the reactor increases whilst the effect of excess water is opposite.

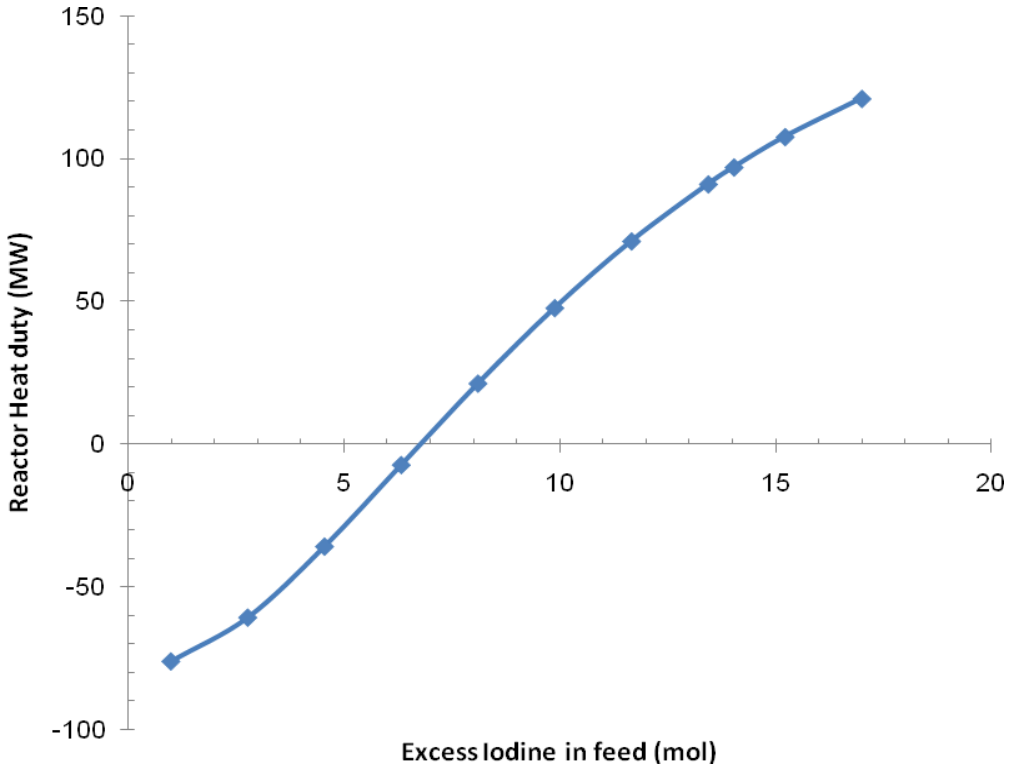

Figure 5.4: Effect of excess iodine on Bunsen reactor net heat duty

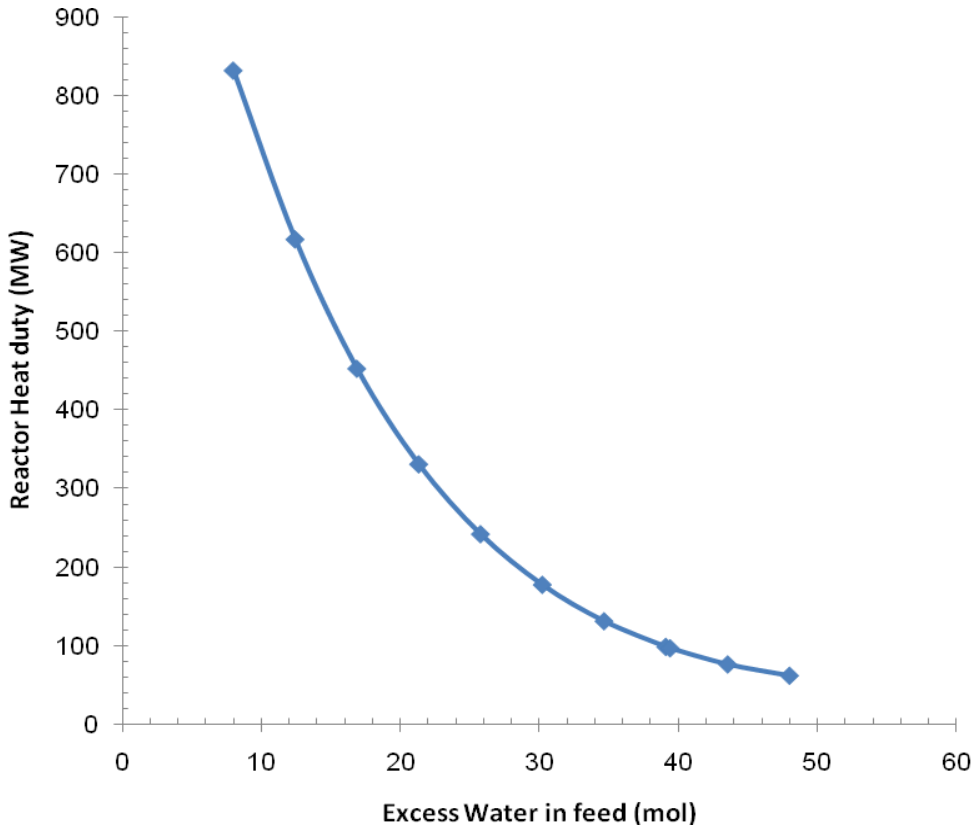

Figure 5.5: Effect of excess water on Bunsen reactor net heat duty

The trend which is shown on Figures 5.4 and 5.5 can be explained by Leybros *et al.* (2009:9062) argument that the Bunsen reaction cannot proceed in the liquid phase, without an excess of water. Solvation due to excess water is highly exothermic and allows the Bunsen reaction to proceed spontaneously. Therefore, the increase in the amount of water in the reactor feed increases the heat energy evolved due to the solvation process.

It can be deducted that, for the operation of the Bunsen reactor, the amount of excess water should be on the upper side of the optimal range of 9 to 13 moles, whilst the amount of iodine should be on lower side of 4 to 6 moles.

5.3 Section II: Sulphuric acid decomposition

5.3.1 Literature survey

Acid formed in the Bunsen reactor in Section I, must be decomposed in Section II. Sulphuric acid decomposition into water, oxygen and sulphur dioxide occurs in two successive reactions. Firstly is the formation of sulphur trioxide at temperatures below 800^{o}C as the sulphuric acid rapidly vaporizes, at above 800^{o}C, sulphur trioxide totally decomposes to sulphur dioxide and oxygen as shown in Equations 5.3 and 5.4 (Leybros *et al.* 2009:9062; Gorensek & Summers, 2009:4098; Jeong, 2005:3; Goldstein, *et al.* 2005:619);

$$H_2SO_{4(aq)} \longrightarrow SO_{3(g)} + H_2O_{(g)} \qquad (397^{o}C) \qquad (5.3)$$

$$SO_{3(g)} \longrightarrow SO_{2(g)} + {}^{1}/_{2}O_{2(g)} \qquad (867^{o}C) \qquad (5.4)$$

Extensive research has been conducted to determine the equipment and reaction conditions for the sulphuric acid decomposition step. The following research findings were used to develop the simulation:

- H_2SO_4 decomposition is the most endothermic reaction in the cycle and requires a temperature exceeding 800 ^{o}C and pressures up to 90 bar (Barbarossa *et al.* 2006:885, Gorensek & Summers, 2009:4100).
- A Bayonet type reactor being developed at Sandia National Laboratory (SNL) is suitable for the decomposition reactor (Gorensek & Summers, 2009:4100). The reactor consists of one closed ended SiC tube co-axially aligned with an open ended SiC tube to form two concentric flow paths. High-temperature heat is applied externally, except near the open end. Concentrated liquid acid is fed at the open end to the annulus, where it is vaporised before passing through an annular catalyst bed. The decomposition reaction takes place in the catalyst bed, using heat provided by the external heat source. SO_2, O_2, and H_2O vapour product returns through the centre and loses its heat to the feed through recuperation. Cooled and partially condensed product exits out the open end into a metal base or manifold at a temperature low enough (< 250^{o}C) to allow the use of poly-tetra-fluoro-ethylene (PTFE) seals.

- The Bayonet reactor inlet is maintained at temperatures below 200^{o}C. The water vapour and the sulphuric acid enter the boiler which heats the sulphuric acid solution to 450^{o}C to produce a sulphuric acid vapour. The super-heater would heat the sulphuric acid vapour to 700^{o}C and the decomposer would heat the vapours to the maximum operating temperature to provide the heat necessary to dissociate the sulphur trioxide to sulphur dioxide and oxygen. The decomposed vapours coming from the decomposer are to be recuperated in the super-heater. Further heating superheats the acid and the vaporised acid decomposes almost completely to SO_3 and H_2O prior to reaching the catalyst. Further heating in the catalyst region decomposes the SO_3 to SO_2 and O_2 (Gorensek & Summers, 2009:4100).
- The optimum Bayonet reactor feed acid concentration is 80% at 870^{o}C peak temperature (Gorensek & Summers, 2009:4104)

- 40% of the acid is decomposed to sulphur dioxide by the decomposition reactor (Norman *et al.* 1982:1)

5.3.2 Conceptual development

Decomposing the sulphuric acid at high temperature is a major challenge in all sulphur based thermochemical cycles. Careful selection of materials of construction is of major importance in the design of equipment especially for Section II. The conditions in this section will be acidic and temperatures will be above 800^{o}C and pressures up to 22 bars. In material selection, silicon carbide is the material of choice in such conditions (Gorensek & Summers, 2009:4100). Silicon carbide is ceramic and can contain the process at the required conditions without significant corrosion or deterioration, while providing adequate heat transfer characteristics. One major disadvantage is that ceramics are difficult to fabricate into desired shapes. For this dissertation an alternative material, Incoloy 800 is selected. Incoloy has been stated by researchers as a possible material for the equipment in the SI cycle (Leybros *et al.* 2010:1010). Incoloy 800 is a widely used material for the construction of equipment having high strength and resistance to oxidation, carburisation, and other harmful effects of exposure to high- temperatures.

Figure 5.6 and 5.7 show a block diagram and an Aspen Plus™ simulation for Section II, respectively. The products of the Bayonet reactor are at a high pressure and there is need to reduce the pressure because the downstream sections (Section I) operate at a much lower pressure. Also the products are a vapour-liquid mixture with un-decomposed acid occupying most of the liquid part. A flash drum can be used to separate the acid from SO_2 and O_2.

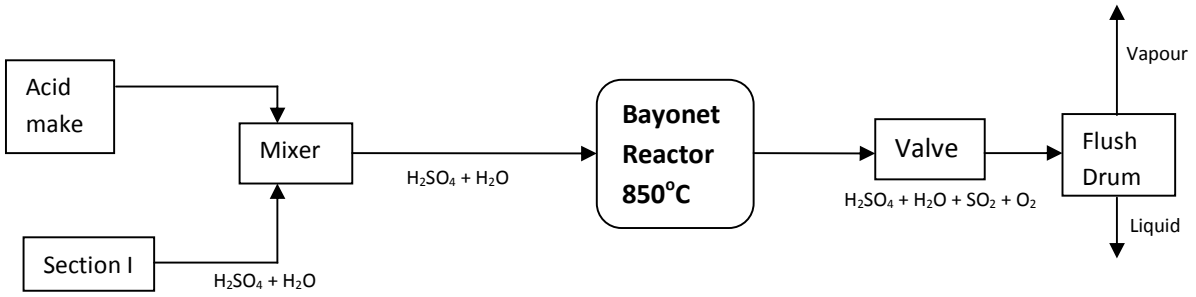

Figure 5.6: Section II process block diagram

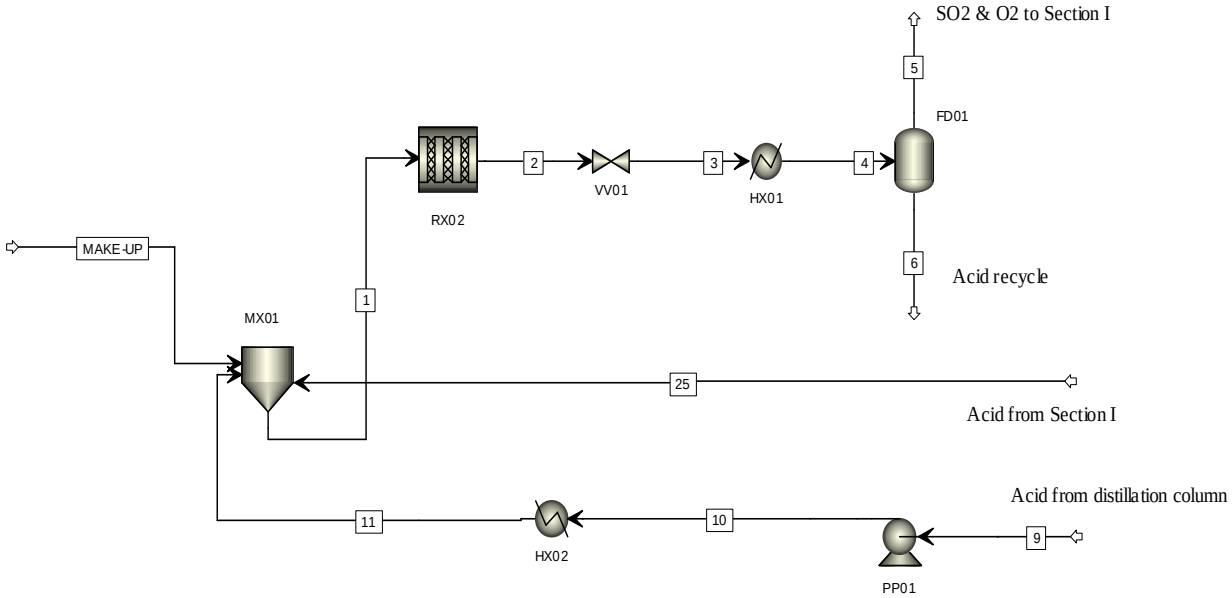

Figure 5.7: Aspen Plus™ Section II flowsheet.

In Figure 5.7, the acid make-up is introduced into the cycle by stream 'MAKE-UP'; streams 9 and 25 bring sulphuric acid from Section I. Acid and water are mixed in mixer MX01, and optimum acid concentration must be achieved inside the mixer. The mixer (MX01) is set to achieve 85% weight sulphuric acid (Stream 1), which is sent into the Bayonet reactor. This specification in industry can be achieved by introducing a PID controller for example, which reads off the concentration of stream 1 and then sends a signal to a flow control valve that is mounted on stream 'WATER'. The products of the acid decomposition (Stream 2) are sent to Section I for separation processes before being fed into the Bunsen reactor. The major advantage of the Bayonet reactor is the internal heat recuperation. A detailed design for the Bayonet reactor is shown on Figure 5.8.

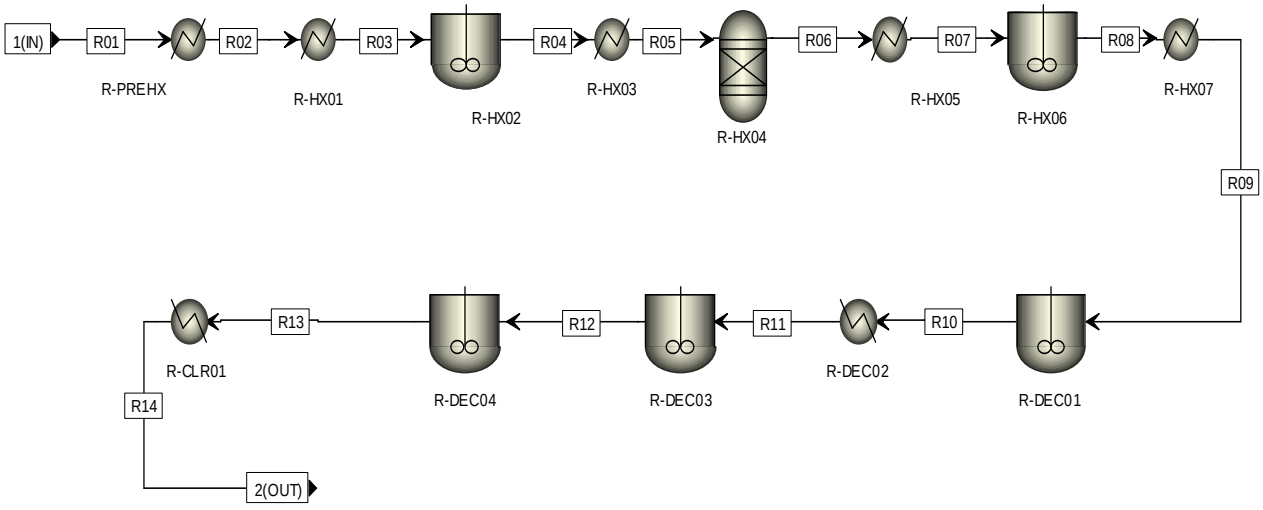

Figure 5.8: Aspen Plus^{TM} Bayonet reactor flowsheet.

The feed Stream R01 contains 84% wt acid and is pre-heated by block R-PREHX which is a heater block that calculates the heat required to raise the temperature of the reactants to 270^{o}C. This temperature is chosen because it was found that the transition from low temperature electrolyte to high temperature, complex forming model occurs at 270^{o}C (Gorensek & Summers, 2009:4102).

In Figure 5.8, heater and reactor blocks, R-HX01 and R-HX02 respectively, simulate the liquid phase decomposition of acid below 450^{o}C. The ELECNRTL property method predicts that

vaporisation starts at a temperature above 450^{o}C. R-HX03 is a heater block that vaporizes the products from R-HX02 (Stream R04) which are then transmitted to the RGibbs block, R-HX04. In these blocks Aspen Plus^{TM} ELECNRTL model predicts the formation of gaseous SO_3. The Catalyst is loaded from R-HX07, through R-DEC01 up to R-DEC04. The catalyst inlet bed temperature on R-HX07 is 675^{o}C. The SO_3 decomposition reaction is assumed to take place in R-DEC01, R-DEC03 and R-DEC04. Further cooling with recuperative heat interchange with oncoming feed stream is done in block R-CLR01. The resultant product stream is at a temperature of 290^{o}C and contains 5.4 mol% O_2, 10.8 mol% SO_2 in aqueous acid, which is sent to Section I, (Stream 2 in Figure 5.7).

Table 5.2: Aspen Plus™ Section II flowsheet stream table.

	1	R01	R02	R03	R04	R05	R06	R07	R08	R09	R10	R11	R12	R13	2	3	4	5	6	MAKE-UP	9	11	25
Temperature (ºC)	226.6	230.0	276.9	270.1	349.7	359.3	553.1	555.1	625.1	889.9	879.9	472.2	355.1	308.8	289.7	288.6	150.0	150.0	150.0	28	315.1	315.1	120
Pressure (bar)	1	1	22	22	22	22	22	22	22	22	22	22	22	22	22	20	20	20	20	1	5	22	5
Vapour Fraction	0	0	0	0	0	0	0.119	1	1	1	1	0.171	0.299	0.267	0.239	0.244	0.16	1	0	0	0	0	0
Mole Flow (kmol/sec)	7.800	7.800	7.800	7.800	7.800	7.800	9.062	9.188	9.345	9.723	9.712	9.441	9.313	9.313	9.313	9.313	9.313	1.494	7.819	0.002	5.819	5.819	2.004
Stream ID	459.0	459.0	459.0	459.0	459.0	459.0	459.0	459.0	459.0	459.0	459.0	459.0	459.0	459.0	459.0	459.0	459.0	78.62	380.4	0.158	342.6	342.6	116.3
Mole Flow (kmol/sec)																							
H_2O	0.912	0.912	0.988	0.981	2.125	0.440	0.008	0.134	0.148	0.154	0.154	0.011	2.123	2.330	2.280	2.288	1.970	0.020	1.950	0.000	0.711	0.711	0.186
H_2	0.000	0.000	0.000	0.000	0.000	0.000	0.000	0.000	0.000	0.000	0.000	0.000	0.000	0.000	0.000	0.000	0.000	0.000	0.000	0.000	0.000	0.000	0.000
O_2	0.000	0.000	0.000	0.000	0.000	0.000	0.000	0.000	0.143	0.515	0.504	0.504	0.504	0.504	0.504	0.504	0.504	0.000	0.000	0.000	0.000	0.000	0.000
H_2SO_4	1.068	1.068	1.144	1.137	2.664	0.597	0.146	0.020	0.006	0.000	0.000	0.173	0.262	0.468	0.419	0.431	0.109	0.000	0.109	0.002	0.831	0.831	0.186
SO_2	0.000	0.000	0.000	0.000	0.000	0.000	0.000	0.000	0.286	1.030	1.009	1.009	1.009	1.009	1.009	1.009	1.009	0.970	0.039	0.000	0.000	0.000	0.000
SO_3	0.000	0.000	0.000	0.000	0.000	0.000	1.262	1.388	1.116	0.377	0.399	0.128	0.000	0.000	0.000	0.000	0.000	0.000	0.000	0.000	0.001	0.001	0.000
I_2	0.000	0.000	0.000	0.000	0.000	0.000	0.000	0.000	0.000	0.000	0.000	0.000	0.000	0.000	0.000	0.000	0.000	0.000	0.000	0.000	0.000	0.000	0.000
HI	0.000	0.000	0.000	0.000	0.000	0.000	0.000	0.000	0.000	0.000	0.000	0.000	0.000	0.000	0.000	0.000	0.000	0.000	0.000	0.000	0.000	0.000	0.000
H_3O^+	2.910	2.910	2.834	2.841	1.697	3.382	5.076	5.076	5.076	5.076	5.076	4.947	2.708	2.501	2.550	2.538	2.861	0.000	2.861	0.000	2.137	2.137	0.816
HSO_3^-	0.000	0.000	0.000	0.000	0.000	0.000	0.000	0.000	0.000	0.000	0.000	0.000	0.000	0.000	0.000	0.000	0.000	0.000	0.000	0.000	0.000	0.000	0.000
I^-	0.000	0.000	0.000	0.000	0.000	0.000	0.000	0.000	0.000	0.000	0.000	0.000	0.000	0.000	0.000	0.000	0.000	0.000	0.000	0.000	0.000	0.000	0.000
HSO_4^-	2.910	2.910	2.834	2.841	0.931	3.381	0.065	0.065	0.065	0.065	0.065	0.389	2.707	2.501	2.550	2.538	2.861	0.000	2.861	0.000	2.137	2.137	0.816
OH^-	0.000	0.000	0.000	0.000	0.000	0.000	0.000	0.000	0.000	0.000	0.000	0.000	0.000	0.000	0.000	0.000	0.000	0.000	0.000	0.000	0.000	0.000	0.000
SO_3^{2-}	0.000	0.000	0.000	0.000	0.000	0.000	0.000	0.000	0.000	0.000	0.000	0.000	0.000	0.000	0.000	0.000	0.000	0.000	0.000	0.000	0.000	0.000	0.000
SO_4^{2-}	0.000	0.000	0.000	0.000	0.383	0.001	2.505	2.505	2.505	2.505	2.505	2.279	0.000	0.000	0.000	0.000	0.000	0.000	0.000	0.000	0.000	0.000	0.000

The Bayonet reactor is the most energy intensive unit in the SI process because the high temperature decomposition of sulphuric acid occurs within the reactor itself. The decomposition of sulphuric acid is strongly affected by temperature, pressure and the acid strength (Barbarossa *et al.* 2006: 889). In this study, the temperature and pressure are fixed at 890^{o}C and 22 bars respectively; therefore the acid strength becomes the variable. Since the decomposition reaction is reversible and has acid as the only reactant, the acid strength has a considerable effect on the kinetics of the reaction. Therefore there is need to investigate the effect of the Bayonet reactor feed acid strength. Figure 5.8 and 5.9 shows the effect of acid concentration on the Bayonet reactor. It is clear that the operating conditions favour high acid strength.

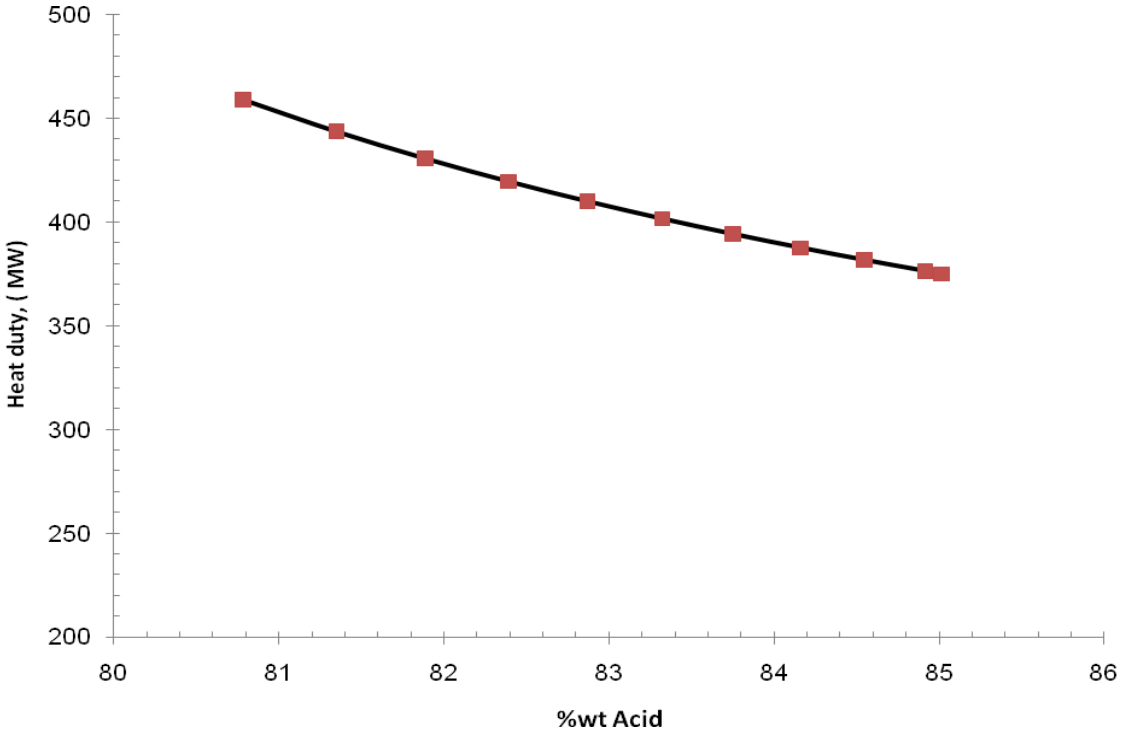

Figure 5.9: Effect of feed acid concentration on reactor heat duty, peak process temperature and pressure is 890^{o}C and 22 bar respectively

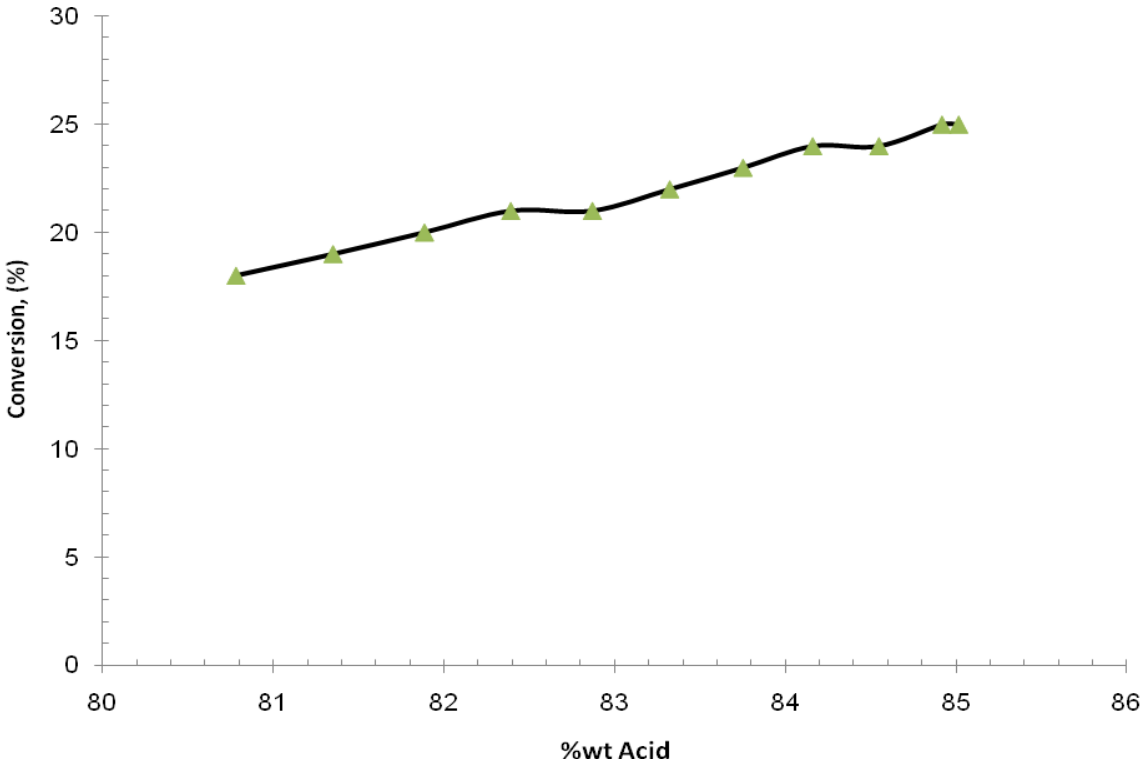

Figure 5.10: Effect of feed acid concentration on acid conversion, peak process temperature and pressure is 890^{o}C and 22 bar respectively

Gorensek & Summers (2009:4097) presented a flowchart where the acid is concentrated from 30 to 55%. The lowest heating targets of 330 MW were obtained for feed concentrations of 80% at all pressures. Heating targets were below 450 kJ/mol SO_2 provided the feed concentration was above 60 wt%. The findings of this study do not compare well with the findings reported by Gorensek & Summers (2009:4097). In this case, the heating target was less than 450 MW for acid feed concentrations of more than 80 wt%. These differences might be attributed to the molar feed flowrate. Gorensek & Summers (2009:4097) used a feed flowrate of 5.848 kmol/s whilst the one used for this study was above 6.7 kmol/s. Also the peak temperature used for this study was 890^{o}C instead of 870^{o}C presented by Gorensek & Summers (2009:4097). The results obtained from this analysis indicate that the amount of feed flow has an effect on the energy requirements of the reactor. Pumping huge amounts of feed to the reactor means an increase in the pumping

and separation costs on other Sections of the cycle. It can be deducted from Figure 5.11 that the optimal acid concentration is within the 82.5 to 83.5% range.

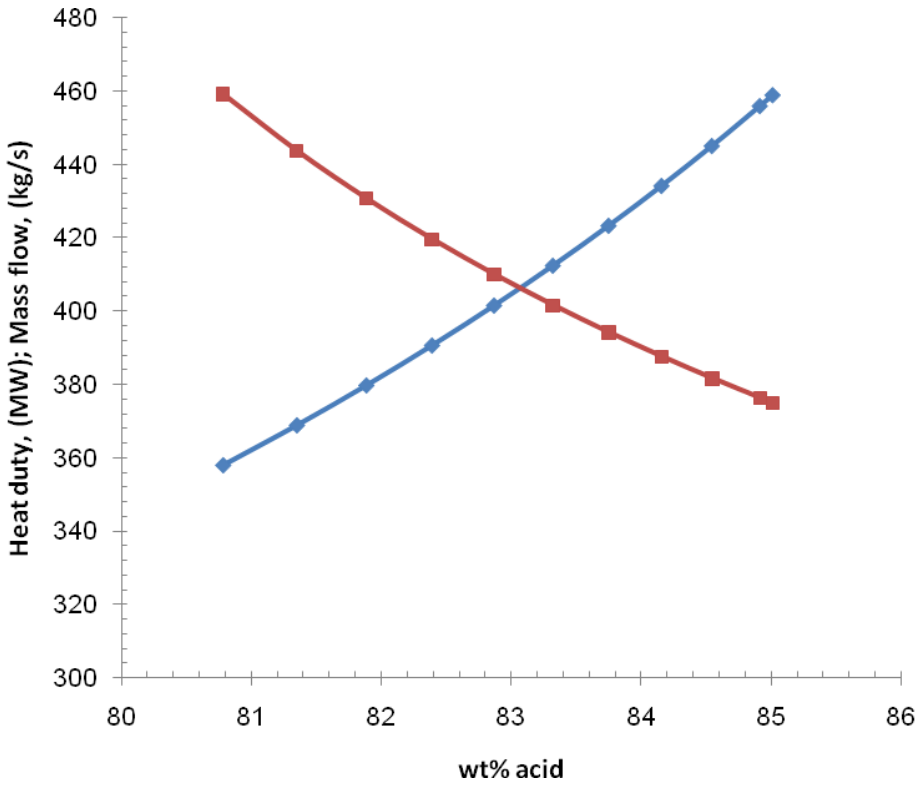

Figure 5.11: Bayonet reactor heat duty vs flow analysis [■ Reactor heat duty; ◆ Reactor feed mass flow]

5.4 Section III: Hydrogen Iodide decomposition

5.4.1 Literature survey

The hydrogen iodide decomposition reaction occurs at 450^{o}C (Leybros *et al.* 2009:9062). The process is composed of a reactive distillation column and downstream separators such as dryers and flash drums. As reported by Leybros *et al*. (2009:9062), the thermal decomposition of hydrogen iodide has a low endothermic heat of reaction.

$$2HI_{(l)} \longrightarrow I_{2(l)} + H_{2(g)} \qquad (450^{o}C) \qquad (5.5)$$

A vapour reactive column was adopted in this thesis and it has been studied by Belaissaoui *et al*. (2008:396) in the presentation of a vapour reactive distillation process simulation for hydrogen production by HI decomposition from HI–I_2–H_2O solutions. The system exhibits strong non ideality and partial immiscibility of the binary HI-H_2O and the ternary HI-I_2-H_2O (HI_x solution). Therefore it is difficult to predict the thermodynamic behaviour of the system. Much research is being conducted on this section (Kane & Revankar, 2008:5999). The main characteristics of this system are as follows (Kane & Revankar, 2008:5999):

- Azeotropes H_2O-HI binary with a liquid-liquid equilibrium
- Highly immiscible H_2O-I_2 with liquid-liquid equilibrium
- HI-I_2-H_2O mixture exhibiting two separate liquid-liquid regions
- High-temperature triple point of I_2 (114 ^{o}C) which increases the bubble temperature of the HI-I_2-H_2O ternary mixture
- existence of azeotropes in the system (Kane & Revankar, 2008:5999; Belaissaoui *et al*. 2008:405)

An operating pressure of 22 bars has been proposed because remarkable hydrogen partial pressures are only found for solutions with HI content higher than the azeotropic molar fraction and it corresponds to the minimum pressure of the boiling feed stream.

5.4.2 Conceptual development

Most researchers have reported the existence of azeotropes in the system (Kane & Revankar, 2008:5999; Belaissaoui *et al*. 2008:405). Figure 5.12 shows the vapour reactive profile for the HI-I_2-H_2O ternary system. At this stage the property set ELECNRTL is predicting the vapour-liquid-liquid immiscibility envelope as shown in Figure 5.12. The property method fails to predict any azeotropes within the system. This makes it difficult to accurately simulate the system. For this reason, a modified vapour reactive distillation process presented by Belaissaoui *et al.* (2008:396) was adopted for this study.

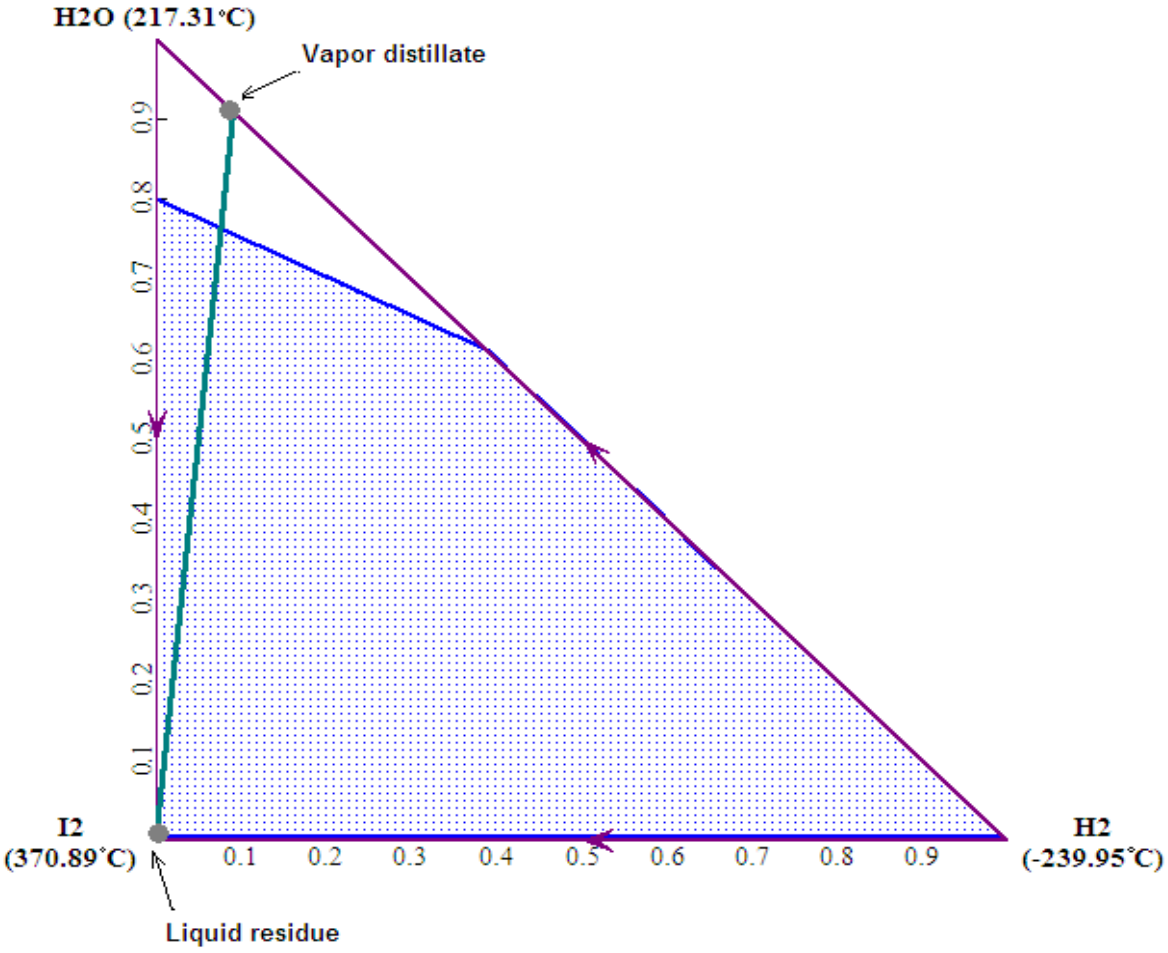

Figure 5.12: Vapour reactive profile of an HI-I_2-H_2O mixture

The design configuration consists of a single feed and entirely reactive distillation column. The column operates under a pressure of 22 bars. The feed of the reactive distillation column, coming from the Bunsen reaction section, with molar composition (HI = 0.10; I_2 = 0.39; H_2O = 0.51), is at its boiling temperature. The residue consists of 99% mol iodine. Water and produced hydrogen are recovered at the distillate with a composition of 91 and 9%mol water and hydrogen as shown by the component balance line in Figure 5.12. The column operates at a reflux ratio of 5 and is composed of 11 theoretical plates including the reboiler and the partial condenser with the feed at Stage 10 (counted downwards). The obtained HI dissociation yield is 99.6%. The reactive distillation feed composition for this simulation is shown in Table 5.3:

Table 5.3: Reactive distillation feed composition

Temperature:	260 ^oC
Pressure:	22 bar
H_2O:	50.1% mol
I_2:	38.9% mol
HI:	11.0% mol

Equation 5.5 is specified in the distillation column with a conversion of 0.996 on HI (Belaissaoui *et al*. 2008:405) Therefore no reaction kinetics i.e. reaction rates and equilibrium constants were supplied to the simulator. Figure 5.13 shows the resultant Aspen Plus^{TM} simulation.

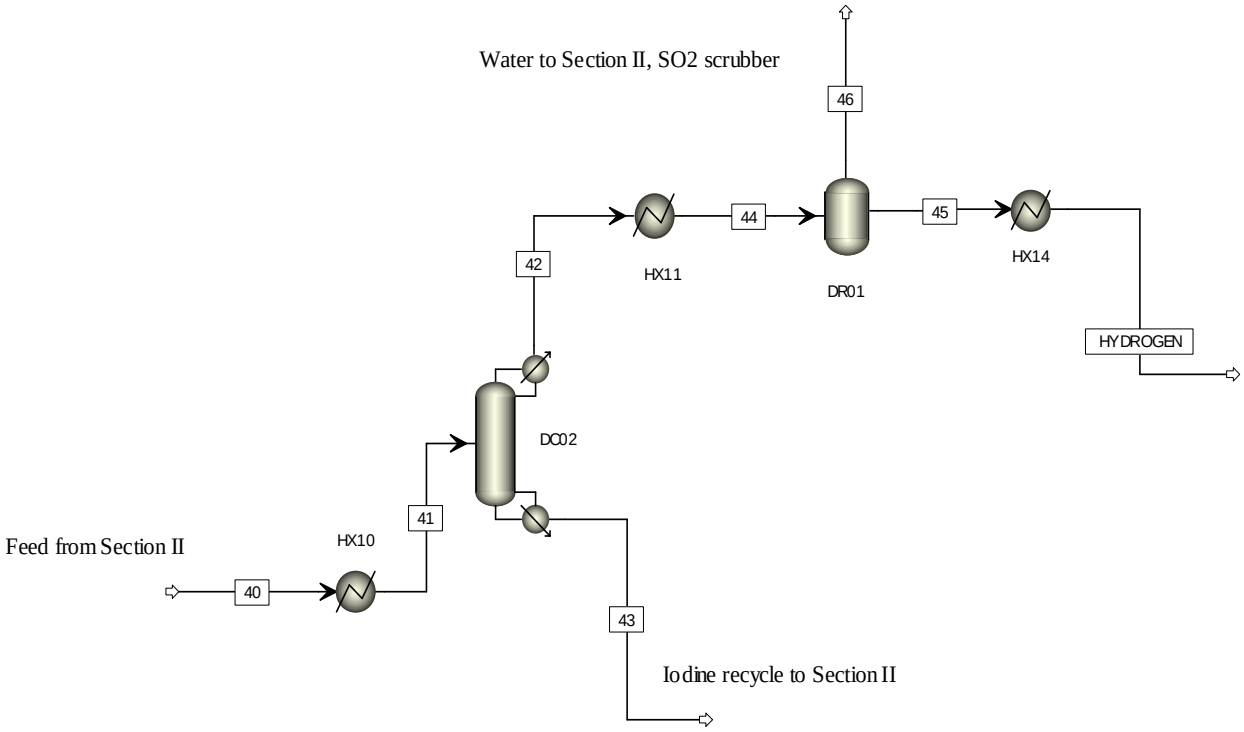

Figure 5.13: Aspen Plus^{TM} Section III flowsheet.

The reactive distillation column configuration given in Table 5.4 gave a converging simulation for DC02:

Table 5.4: Reactive distillation column configuration

Number of stages	11 (stage 1, condenser; stage 2, reboiler)
Number of reactive stages	9 (stage 2 to 9)
Feed location	Above stage 10
Liquid side stream	None
Reflux ratio	0.4
Bottoms rate (kmol/s)	7.96

The bottoms (Stream 43), contains 99.7% iodine and is recycled to Section I as a reactant in the Bunsen reactor. The overhead product of the column (Stream 42) contains 9.8% hydrogen in a hydrogen and water mixture. Chiller HX11 condenses the overhead vapour to 9.8% vapour at a temperature of 16^{o}C thereby making it possible for the separation of hydrogen from liquid water using a dryer (DR01). HX14 cools the stream to the desired product temperature of 28^{o}C. The hydrogen product purity is 99.6%mol. Stream compositions are shown in Table 5.5.

Table 5.5: Aspen Plus^{TM} Section III flowsheet stream table.

Stream ID	**40**	**41**	**42**	**43**	**44**	**45**	**46**	**HYDROGEN**
Temperature (K)	140.9	259.7	216.2	369.6	15.9	15.9	15.9	28.050
Pressure (bar)	3.5	22	22	22	5	5	5	1.013
Vapour Frac	0.016	0.562	1	0	0.098	1	0	1.000
Mole Flow (kmol/sec)	18.31	18.31	10.254	8.056	10.254	1.01	9.244	1.010
Mass Flow (kg/sec)	2232.765	2232.765	193.444	2039.321	193.4	2.095	191.349	2.095
Mole Flow (kmol/sec)								
H_2O	7.150	9.164	9.141	0.023	9.141	0.004	9.138	0.004
H_2	0.000	0.000	1.007	0.000	1.007	1.006	0.001	1.006
O2	0.000	0.000	0.000	0.000	0.000	0.000	0.000	0.000
H_2SO_4	0.000	0.000	0.000	0.000	0.000	0.000	0.000	0.000
SO_2	0.000	0.000	0.000	0.000	0.000	0.000	0.000	0.000
SO_3	0.000	0.000	0.000	0.000	0.000	0.000	0.000	0.000
I_2	7.132	7.132	0.105	8.033	0.105	0.000	0.105	0.000
HI	0.000	2.014	0.000	0.000	0.000	0.000	0.000	0.000
H_3O^+	2.014	0.000	0.000	0.000	0.000	0.000	0.000	0.000
HSO_3^-	0.000	0.000	0.000	0.000	0.000	0.000	0.000	0.000
I-	2.014	0.000	0.000	0.000	0.000	0.000	0.000	0.000
HSO_4^-	0.000	0.000	0.000	0.000	0.000	0.000	0.000	0.000
OH^-	0.000	0.000	0.000	0.000	0.000	0.000	0.000	0.000
SO_3^{2-}	0.000	0.000	0.000	0.000	0.000	0.000	0.000	0.000
SO_4^{2-}	0.000	0.000	0.000	0.000	0.000	0.000	0.000	0.000

A vapour composition profile of the HI, I_2, H_2, and H_2O system in the column is analysed. The vapour profiles are presented in Figure 5.14.

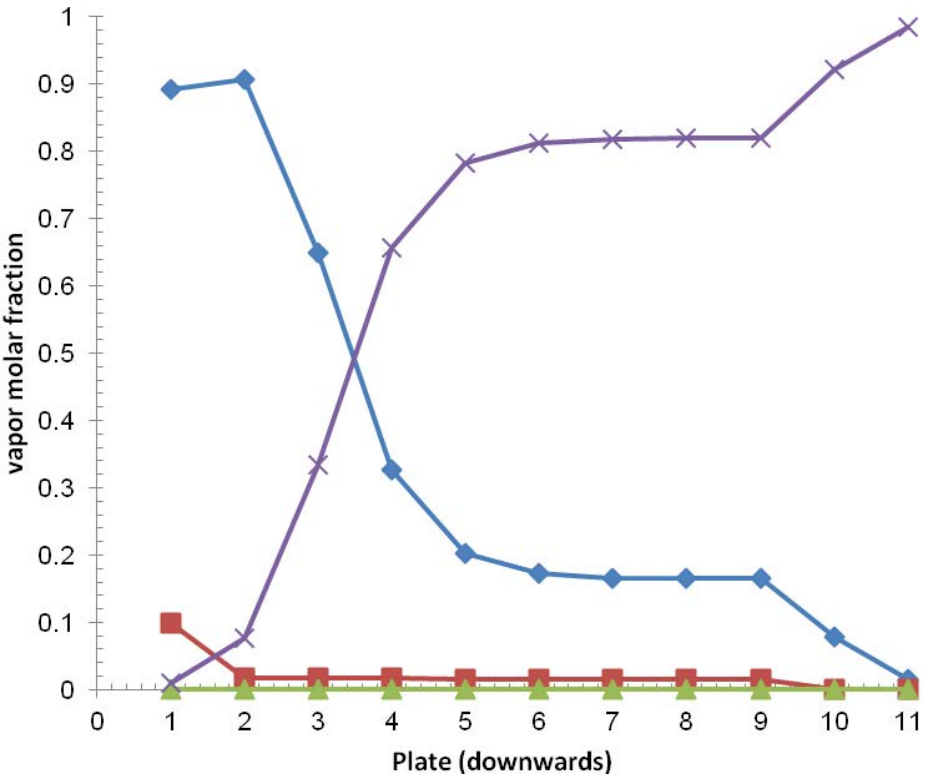

Figure 5.14: Vapour composition profiles [■ H_2; X I_2; ◆ H_2O; ▲ HI]

It is clear from Figure 5.14 that the H_2 content remains very low throughout the column and is attributed to the HI content on the incoming feed (10% mol). The high volatility of water compared to iodine means that most of the water will vaporize to vapour distillate rather than flowing into the liquid residue. As a result, most water will dilute the hydrogen product on the distillate. Belaissaoui *et al*. (2008:405) argues that hydrogen production is obtained only for very low iodine content in the rectifying section because, in this condition, the reaction equilibrium is shifted towards the production of hydrogen, according to Le Chatelier's principle. The effect is evident in Figure 5.14 where the vapour molar fraction of hydrogen is 0.1 whereas the vapour molar fraction for iodine is close to zero.

Figure 5.15 shows the temperature profile along the distillation column. The temperature increase in the lower part of the column is due to the increase in the heavy boiling compound iodine content.

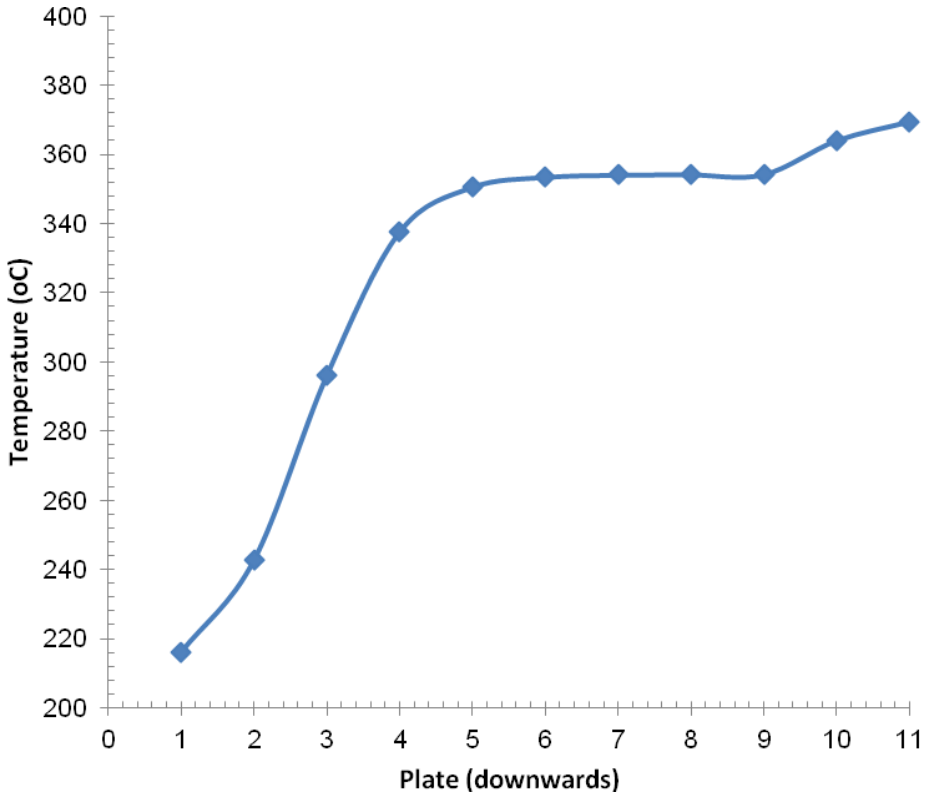

Figure 5.15: Temperature profile in the reactive distillation column.

5.5 Overall SI cycle process flowsheet

The flowsheets for each section are presented in Sections 5.2, 5.3 and 5.4. The majority of the unit operations are proven chemical process technologies. The acid decomposition reactor, Bunsen reactor and the reactive distillation column are processes which are still under research. Figure 5.16 shows the combined flowsheet for the SI cycle, stream compositions are detailed in Tables 5.1, 5.2 and 5.5. The basis is a 1 kmol/s hydrogen production rate.

There are three input streams WATER, I_2 MAKE and MAKE-UP, which represent the process water feed, iodine make-up and aqueous acid make-up respectively. Also there are three output streams, hydrogen product stream (HYDROGEN), oxygen by-product stream (OXYGEN) and the purge stream (PURGE). Purge streams and make-up streams are introduced in closed chemical processes for stability of the system and plant safety measures.

The overall mass balance of the system is summarised in Table 5.6.

Table 5.6: Overall SI cycle mass balance

Streams In	**Flow (kg/s)**
WATER	19.002
I_2 MAKE	0.145
MAKE-UP	0.158
Total	**19.305**
Streams Out	**Flow (kg/s)**
HYDROGEN	2.095
OXYGEN	16.086
PURGE	1.350
Total	**19.531**
Error (%)	**1.2**

The software package allowed for an error of 1.2% with respect to the inlet streams. This can be explained by the convergence error tolerance which has been specified into the simulator.

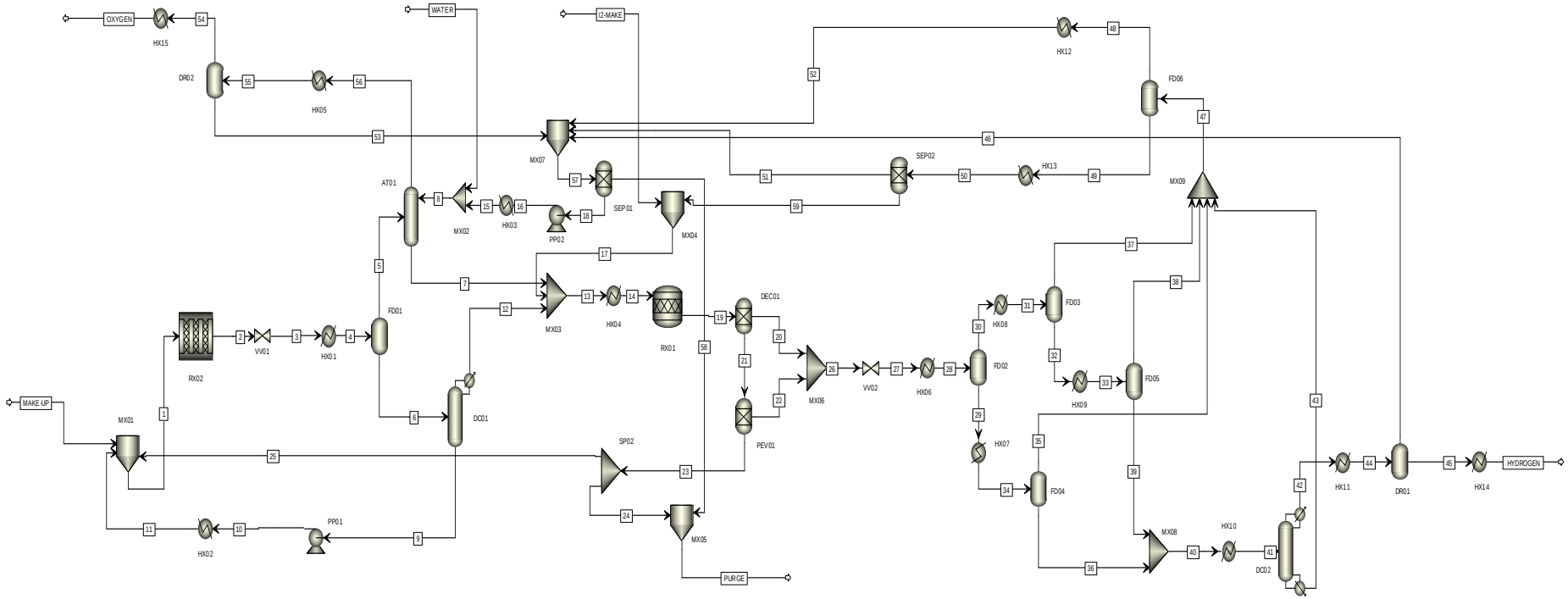

Figure 5.16: Aspen Plus^{TM} SI cycle flowsheet

5.6 References

ASPEN TECH. 2010. Aspen Plus. http://www.aspentech.com/core/aspen-plus.aspx. Date of access: 03 Apr 2010.

BAE, Y.S., LEE, C.H. 2004. Sorption kinetics of eight gases on a carbon molecular sieve at elevated pressure. *Carbon,* **43**: 95-107, Oct.

BARBAROSSA, V., BRUTTI, S., DIAMANTI, M., SAU, S. & MARIA, G.E. 2006. Catalytic thermal decomposition of sulphuric acid in sulphur–iodine cycle for hydrogen production. *International Journal of Hydrogen Energy,* **31**:883-890, Sep.

BELAISSAOUI, B., THERY, R., MEYER, X.M., MEYER, M., GERBAUD, V. & JOULIA, X. 2008. Vapour reactive distillation process for hydrogen production by HI decomposition from HI–I_2–H_2O solutions. *Chemical Engineering and Processing,* **47**:396-407, Jan.

CHO, W.C., PARK, C.S., KANG, K.S., KIM, C.H., & BAE, K.K. 2009. Conceptual design of sulfur-iodine hydrogen production cycle of Korea Institute of Energy Research. *Nuclear Engineering & Design,* **239**:501-507, Nov.

FOO, D.C.Y., MANA, Z.A., SELVAN, M., MCGUIRE, M.L. 2005. Integrate Process Simulation and Process synthesis. http://www.cepmagazine.org. Date of access: 13 Jan. 2011.

GIACONIA, A., GRENA, R., LANCHI, M., LIBERATORE, R. & TARQUINI, P. 2006. Hydrogen/methanol production by sulfur–iodine thermochemical cycle powered by combined solar/fossil energy. *International Journal of Hydrogen Energy,* **32**:469-481, Jul.

GOLDSTEIN, S., BORGARD, J.M. & VITART, X. 2005. Upper bound and best estimate of the efficiency of the iodine sulfur cycle. *International Journal of Hydrogen Energy,* **30**:619-626, Aug.

GORENSEK, M.B. 2007. Modeling sulfur dioxide solubility in sulfuric acid solutions (457c). (Paper presented at the AlChe 2007 Annual meeting on 7 November 2007. Salt Lake City)

GORENSEK, M.B. & SUMMERS, W.A. 2009. Hybrid sulfur flowsheets using PEM electrolysis and a bayonet decomposition reactor. *International Journal of Hydrogen Energy,* **34**:4097-4114, Jun.

GREEN, D.W. & MALONEY, J.O. 1997. Perry's Chemical Engineers' Handbook. McGraw-Hill.

JEONG, Y.H., KAZIMI, M.S., HOHNHOLT, K.J. & YILDIZ, B. 2005. Optimisation of the hybrid sulfur cycle for Hydrogen production. Korea: KOSEF. (Dissertation – Post-Doc Fellowship.) 60p.

KANE, C., REVANKAR, S.T. 2008. Sulfur–iodine thermochemical cycle: HI decomposition flow sheet analysis. *International Journal of Hydrogen Energy,* **33**:5996-6005, Sep.

KIVISARI, T., LAAG, P.C. & RAMSKOLD, A. 2001. Benchmarking of chemical flowsheeting software in fuel cell applications. *Journal of Power Sources* **94**:112-121, Oct.

KUSIAK, A., FINKE, G. 1987. Hierarchical approach to the process planning problem. Descrete Applied Mathematics, **18**:175- 184

LANCHI, M., CEROLI, A., LIBERATORE, R., MARRELLI, L., MASCHIETTI, M., SPADONI, A., & TARQUINI, P. 2009. S–I thermochemical cycle: A thermodynamic analysis of the HI–H_2O–I_2 system and design of the HI_X decomposition section. *International Journal of Hydrogen Energy*, **34**:2121-2132, Jan.

LAROUSSE B., LOVERA, P., BORGARD, J.M., ROEHRICH, G., MOKRANI, N., MAILLAULT, C., DOIZI, D., DAUVOIS, V.,ROUJOU, J.L., LORIN, V., FAUVET, P., CARLES, P. & HARTMAN, J.N. 2009. Experimental study of the vapour–liquid equilibria of HI–I_2 –H_2O ternary mixtures, Part 2: Experimental results at high temperature and pressure. *International Journal of Hydrogen Energy*, **34**:3258-3266, Mar.

LEYBROS, J., PHILIPPE, C., & BORGARD, J.M. 2009. Countercurrent reactor design and flowsheet for iodine-sulfur thermochemical water splitting process. *International Journal of Hydrogen Energy*, **34**:9060-9075, Sep.

MATHIAS, P.M., & BROWN, L.C. 2003. Thermodynamics of the sulfur iodine cycle for thermochemical hydrogen production. (Paper presented at the 68TH Annual meeting of the Society of Chemical Engineers on 23 March 2003. Tokyo)

NORMAN, J.H., RUSSELL, J.L., PORTER, J.T., McCORKLE, K.H., ROEMER T.S. & SHARP, R. 1978. Process for the thermochemical production of hydrogen. Patent: US 4,089,940. 6p.

SEADER, J.D., SEIDER, W.D., LEWIN, D.R. 2006. Using process simulators in Chemical Engineering. Wiley [CD].

SOAVE, G. 1993. 20 Years of Redlich-Kwong Equation of state. *Fluid Phase Equilibria.* **82**:345-359.

THE DESIGN COUNCIL. 2010. The Design process. http://www.designcouncil.org.uk Date of access: 13 Jan 2011.

TSED (The Sage English Dictionary) 2009. “Simulation”. [CD]

WILSON, G.M. 1964. Vapour-liquid equilibrium. A new expression for the excess free energy of mixing. *J. Am. Chem. Soc.* **86:**127–130, Jan.

CHAPTER 6: Process energy evaluation

"Should you find yourself in a chronically leaking boat, energy devoted to changing vessels is likely to be more productive than energy devoted to patching leaks" Warren Buffett

6.1 Introduction

Process energy optimisation through process integration can lead to substantial reduction in energy requirements, hence the cost of a process. One of the most successful and generally useful techniques is pinch technology. The term is derived from the fact that in a plot of the system temperatures versus the heat transferred, a pinch point usually occurs between the hot stream and cold stream curves (Sinnott, 2005:111). In this chapter heat integration and Pinch Technology are going to be carried out by means of AspenTech's Aspen Energy Analyzer^{TM}. A separate pinch analysis will be done for the Bayonet reactor and downstream processes.

6.1.1 Assumptions

- Heat exchange is in a single phase
- Only counter current and multi-pass shell and tube heat exchangers are considered
- Heat transfer can be achieved as needed in the high temperature decomposition reactor in order to achieve the specified approach temperatures
- No piping and vessel pressure drops
- Process water is available year round at 28^{o}C
- The minimum temperature approach between helium fluid and decomposition reactor heat exchangers is 10^{o}C and 2^{o}C for downstream heat exchangers

6.2 Heat integration

Heat integration will be divided into two parts, 1) the Bayonet decomposition reactor which is composed of a series of heat exchangers and reactors and, 2) processes which are downstream with respect to the reactor. The bayonet reactor had a separate heat integration because high temperature heat was supplied to the reactor. No heat exchange from other streams within the whole process was expected because the streams were at a lower temperature than the streams inside the reactor. Helium is assumed to be entering the bayonet reactor at 950^{o}C and exiting at 850^{o}C. The helium stream leaving the reactor may be used as a low temperature heat source for the downstream processes.

6.2.1 Decomposition reactor heat exchanger network

Pinch analysis was used to predict the high temperature heat requirement for the acid decomposition reactor. Figure 6.1 shows the Bayonet reactor detailed design.

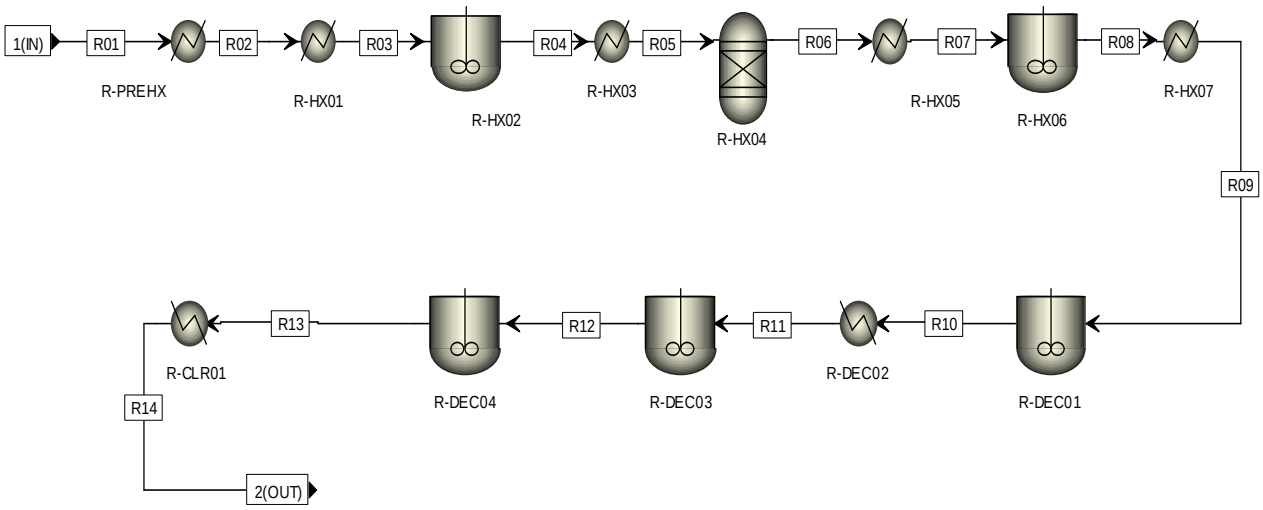

Figure 6.1: Aspen Plus^{TM} Bayonet reactor flowsheet.

The reactor model shown in Figure 6.1 contains blocks, R-PREHX, R-HX01, R-HX02, R-HX03, R-HX04 R-HX05, R-HX06, R-HX07, R-DEC01, R-DEC02, R-DEC03, R-DEC04 and R-CLR01. The feed to the reactor is pre-heated, vaporised, superheated and decomposed. The

products are then cooled and condensed. This process can be achieved by means of a Bayonet type reactor (Gorensek & Summers, 2009:4100). The feed stream R01 contains 85% wt acid; block R-PREHX is a heater block that calculates the heat required to raise the temperature of the reactants to 270^{o}C. This temperature is chosen because it was found that the transition from low temperature electrolyte to high temperature complex forming model occurs at 270^{o}C (Gorensek & Summers, 2009:4102). Reactor blocks, R-HX01 and R-HX02 simulate the liquid phase decomposition of acid below 450^{o}C. The ELECNRTL property method predicts that vaporisation starts at a temperature above 450^{o}C. R-HX03 is a heater block that vaporizes the products from R-HX02 (stream R04), and sent to an RGibbs block, R-HX04, in these blocks Aspen Plus^{TM} ELECNRTL model predicts the formation of gaseous SO_3. Catalyst is loaded from R-HX07, through R-DEC01 up to R-DEC04. The catalyst inlet bed temperature on R-HX07 is 675^{o}C. The SO_3 decomposition reaction is assumed to take place in R-DEC01, R-DEC03 and R-DEC04. R-DEC01 and R-DEC03 have zero energy input. Further cooling with recuperative heat interchange with oncoming feed stream is done in block R-CLR01. The resultant product stream is at a temperature of 290^{o}C and contains 5.4 mol% O_2, 10.8 mol% SO_2 in aqueous acid, which is sent to Section I. Table 6.1 is the problem table for the Bayonet reactor.

Table 6.1: Bayonet reactor stream heat requirements.

Stream Name	**Initial Temperature (^{o}C)**	**Target Temperature (^{o}C)**	**MC_p (kJ/^{o}C-s)**	**Enthalpy (MW)**
R01	211.7	270.1	1506.8	88.3
R02	270.1	348.8	8202.0	645.5
R03	348.8	348.8	-	0
R04	348.8	472.3	4846.9	598.6
R05	472.3	472.3	-	0
R06	472.3	552.9	26426.8	2130
R07	552.9	553.2	827333	248.2
R08	553.2	675.1	110.7	13.5
R09	675.1	550.4	-	0
R10	550.4	890.1	99.5	33.8
R11	890.1	655.1	-	0
R12	655.1	880.1	372.4	83.8
R13	880.1	289.7	5863.8	-3462

From Table 6.1, there is 1 hot stream (R13) and 7 cold streams, R09 and R11 appear to be hot streams but they involve an endothermic acid decomposition reaction which consumes some of

the energy brought by the streams. If all the energy is assumed to be exchanged ideally, the total net heat energy is positive, 379.7 MW.

However a minimum temperature of approach between the streams means that more heat should be supplied. Figure 6.2 shows the cooling and heating curves when a 10°C minimum temperature approach is specified.

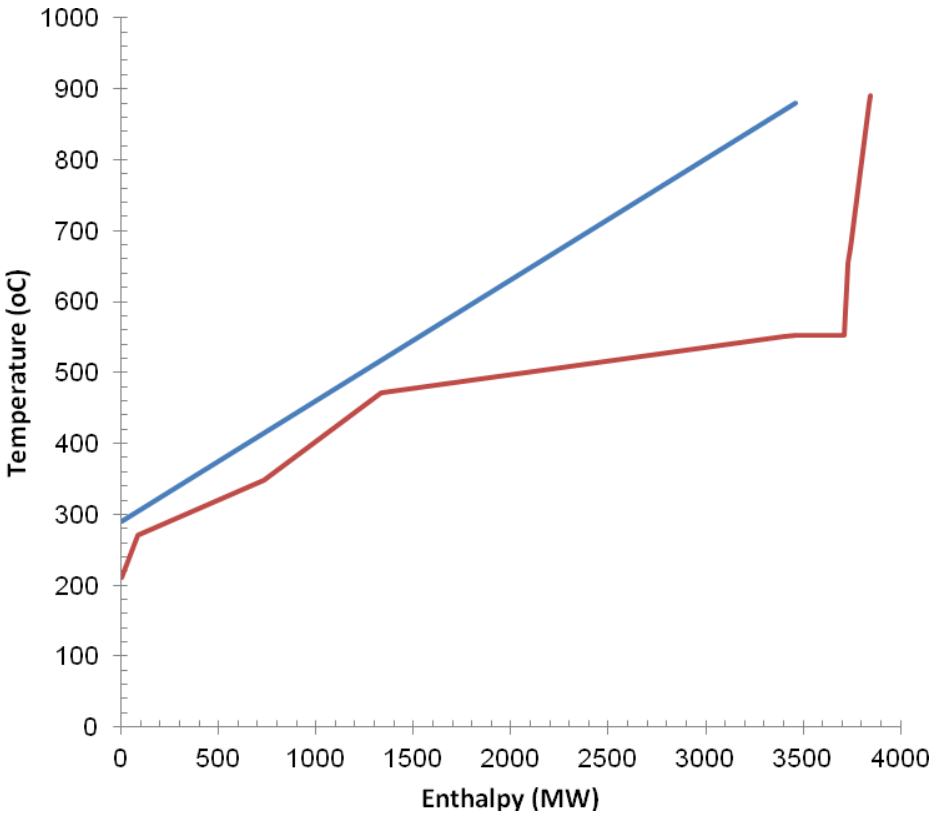

Figure 6.2: Bayonet reactor heating and cooling curves, 10°C minimum temperature approach, peak process temperature, 890°C, catalyst bed inlet temperature, 675°C.

The lower curve in Figure 6.2 represents the temperature as a function of heat input for the fluid flowing through the annulus, while the upper curve tracks the temperature of the fluid flowing

through the central tube of the bayonet as a function of heat removal. For a minimum temperature approach of 10^{o}C, the difference between the enthalpies of the two curves at the highest temperature (890^{o}C) is 380.7 MW. This is the heating target, which is the minimum high-temperature heat requirement for the reactor operating at the specified conditions. The cooling target is 0 MW, which is the difference between the enthalpies of the two curves at the lowest temperature (211^{o}C). The hot and cold pinch temperatures are 270 and 280^{o}C respectively.

Aspen Energy Analyzer^{TM} can generate "Recommended Designs" for the heat exchanger network. Appendix B shows the heat exchanger network for the Bayonet reactor. Tables 6.2 and 6.3 show a summary of the Bayonet reactor heat exchanger network design.

Table 6.2: Bayonet reactor heat exchanger network

Block ID	**Duty (MW)**	**T_{in} (^{o}C)**	**T_{out} (^{o}C)**	**Heat exchanged with**	**Names of Heat Exchanger units**
R-PREHX	88.3	211.5	270.1	R-CLR01, 87.4 MW; High temperature source, 0.9 MW	E-109, E-113
R-HX01	645.5	270.1	348.8	R-CLR01, 639 MW; High temperature source, 6.5 MW	E-108, E-115
R-HX02	0.0	348.8	348.8		
R-HX03	598.6	348.8	472.3	R-CLR01, 592.6 MW; High temperature source, 6.0 MW	E-112, E-114
R-HX04	0	472.3	472.3		
R-HX05	2130	472.3	552.9	R-CLR01, 2107.9 MW; High temperature source, 22.1 MW	E-107, E-110
R-HX06	248.2	552.9	553.2	High temperature source, 248.2 MW	E-119
R-HX07	13.5	553.2	675.1	High temperature source, 13.5 MW	E-117
R-DEC01	0	675.1	550.4		
R-DEC02	33.8	550.4	890.1	High temperature source, 33.8 MW	E-118
R-DEC03	0	890.1	655.1		
R-DEC04	83.4	655.1	880.1	High temperature source, 83.4 MW	E-116
R-CLR01	-3462	880.1	289.7	(R-PREHX, R-HX01, R-HX03, R-HX05), 3427MW; Cooling water, 34.6 MW	E-107, E-108, E-109, E-111, E-112

From Table 6.2, the pre-heater, (R-PREHX) receives heat from the cooler (R-CLR01) and the high temperature source by means of two heat exchangers (E-109 and E-113). The cooler (R-CLR01) has a total energy of 3462 MW, of which only 3427.4 MW can be transferred across the pinch by recuperation within the reactor. The transfer is achieved by five heat exchanger units, (E-107, E-108, E-109, E-111, E-112) the sizing of the heat exchangers is given in Appendix B, the rest 34.6 MW is lost to cooling water. The high temperature heat source supplies a total of 415.3 MW by means of helium entering the reactor at 950^{o}C and leaving at 850^{o}C at a flowrate

of 735 kg/s. The total number of heat exchanger units is 13 with 305 shells giving a total area of 147 300 square metres (Table 6.3)

Table 6.3: Recommended Bayonet reactor heat exchanger design

	Heat Exchanger Network	**Target**	**% of Target**
Heating (MW)	415.3	380.1	109.1
Cooling (MW)	34.61	0.0	-
Number of units	13	9	144.4
Number of shells	305	11	2773
Total area (m^2)	147 300	139 508	105.7

6.2.2 Process heat exchanger network

The problem table for the downstream processes is given in Table 6.4. There are 8 hot streams and 10 cold streams. Streams 6a and 6b are the reboiler and condenser streams respectively for the distillation column DC01. Streams 41a and 41b are for DC02 reboiler and condenser streams respectively. The stream numbers given in Table 6.4 correspond to the ones given in Chapter 5.

Table 6.4: Downstream heat requirements.

Stream Name	**Initial Temperature (^oC)**	**Target Temperature (^oC)**	**MC_p ($kJ/^oC$-s)**	**Enthalpy (MW)**
3	288.6	150	1551.9	-215.1
10	315.1	235	2078.7	-166.5
16	42.3	50	3584.4	27.6
13	75.9	105.9	3256.7	97.7
56	28.02	28.03	8200.0	0.082
27	121.6	176.9	37417.7	2069.2
29	176.9	204.9	5175.0	144.9
30	176.9	154.9	50318.2	-1107
32	154.9	157.9	162733.3	488.2
40	140.9	259.7	4391.4	521.7
42	234.5	15.9	2197.2	-480.3
48	187.6	45.9	12910.4	-1829.4
49	187.6	120	473.4	-32
45	15.9	28	28.5	0.345
6a	153.1	315.1	2637.7	427.3
41a	302.4	337.8	6590.4	233.3
6b	315.1	153.1	504.9	-81.8
41b	270.3	243.8	6467.9	-171.4

The heating and cooling curves for a 2°C temperature difference is shown in Figure 6.3.

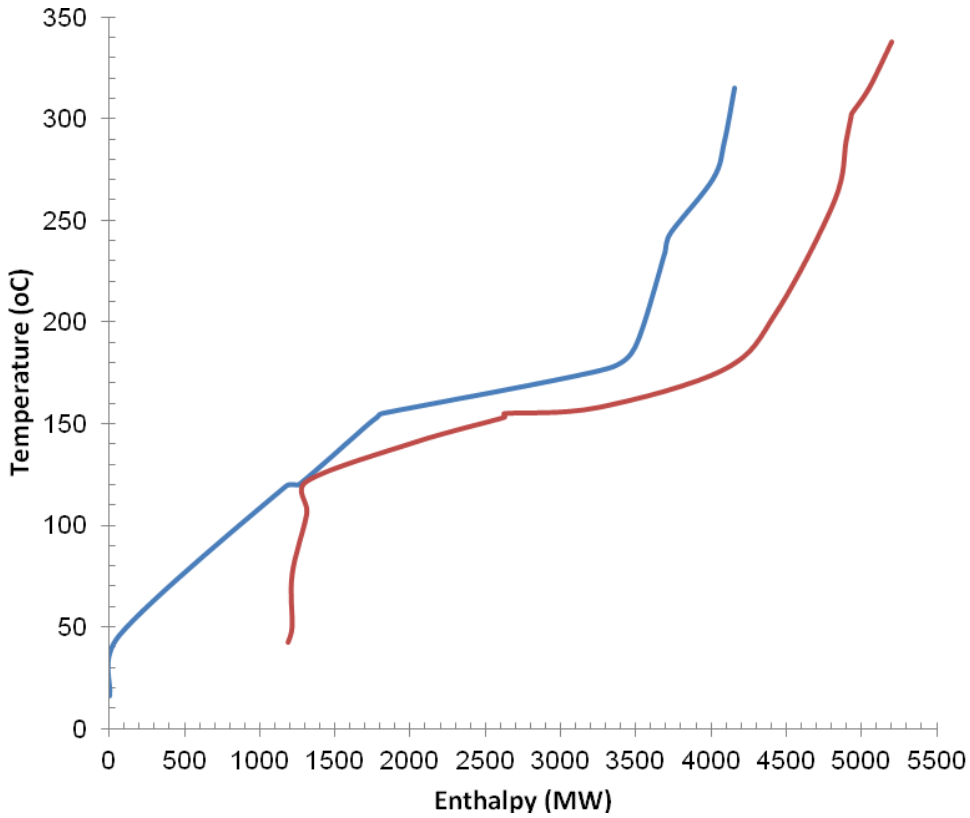

Figure 6.3: Downstream processes heating and cooling curves, 2°C minimum temperature approach.

For a minimum temperature approach of 2°C, the difference between the enthalpies of the two curves at the highest temperature is 1043 MW. This is the heating target, which is the minimum high-temperature heat requirement for the downstream processes. The cooling target is 1190 MW, which is the difference between the enthalpies of the two curves at the lowest temperature. The hot and cold pinch temperatures are 121.6 and 123.6 °C respectively. Table 6.5 shows the recommended Aspen Energy Analyzer™ design. The design is 131.5% above target. The detailed description is given in Table 6.6.

Table 6.5: Recommended downstream heat exchanger design

	Heat Exchanger Network	Target	% of Target
Heating (MW)	1372	1043	131.5
Cooling (MW)	1519	1190	127.6
Number of units	40	15	266.7
Number of shells	3395	11	8488
Total area (m^2)	1 681 000	2 577 430	65.22

Table 6.6 shows the process streams heat exchanger network. CD01 and CD02 denotes the condensers for distillation columns DC01 and DC02 respectively, the same applies for RB01 and RB02 for re-boilers. A detailed heat exchanger network is given in Appendix B.

Table 6.6: Downstream process heat exchanger network

Block ID	Duty (MW)	Tin (^oC)	Tout (^oC)	Heat exchanged with	Names of Heat Exchanger units
HX01	-215.1	288.6	150	HX06, 172.7MW; HX10, 17.9MW; HX09, 22.4MW; Refrigerant, 2.2MW	E-127, E-145, E-155, E-159
HX02	-166.5	315.1	235	HX09, 164.8MW; Refrigerant, 1.7MW	E-129, E-137
HX03	27.6	42.3	50	HX08, 27.3MW; Low temperature source, 0.3MW	E-128, E-136,
HX04	97.7	75.9	105.9	HX08, 96.7MW; Low temperature source,1.0MW	E-138, E-148
HX06	2069.2	121.6	176.9	HX01, 172.7MW; HX08, 971.9MW; HX11, (129.9 + 48.6)MW; HX12, (199.4 + 476.4)MW, HX13, 6.6MW, CD01, 42.9MW; Low temperature source, 20.7MW	E-127, E-130, E-132, E-133, E-140, E-149, E-150, E-157, E-160
HX07	144.9	176.9	204.9	Low temperature source, 144.9MW	E-144
HX08	-1107	176.9	154.9	HX03, 27.3MW; HX06, 971.9MW; HX16, 96.7MW, Cooling water, 11.1MW	E-128, E-138, E-140, E-154
HX09	488.2	154.9	157.9	HX01, 22.4MW; CD02, 126.8MW; CD01, 46.4MW, HX02, 164.8MW, Low temp source, 158.7MW	E-129, E-131, E-153, E-155, E-161
HX10	521.7	140.9	259.7	HX01, 17.9MW; HX11, 39.5MW; HX13, 13.6MW; CD01, 34.6MW, Low temperature source, 416MW	E-135, E-141, E-142, E-143, E-159,
HX11	-480.3	234.5	15.9	HX06, (129.9 + 48.6)MW; HX10, 39.5MW; Cooling water, 227MW; Refrigerant, 35.3MW	E-132, E-143, E-150, E-158, E-165
HX12	-1829.4	187.6	45.9	HX06, (476.4 + 199.4)MW; HX10, 19.1MW; Cooling water, 1153,5MW	E-130, E-149, E-151, E-156,
HX13	-32	187.6	120	HX06, 6.6MW; HX10, 13.6MW; Cooling water, 11.5, Refrigerant, 0.3MW	E-141, E-147, E-157, E-164
HX14	0.345	15.9	28	High temperature source, 0.3MW	E-163
RB01	427.3	153.1	315.1	Low temperature source, 427.3MW	E-162
RB02	233.3	302.4	337.8	Low temperature source, 233.3MW	E-134
CD01	-81.8	315.1	153.1	HX09, 46.4MW; HX10, 34.6MW; Cooling water, 0.8MW	E-131, E-142, E-166
CD02	-171.4	270.3	243.8	HX06, 42.9MW; HX09, 126.8MW; Cooling water, 1.7MW	E-146, E-160, E-161

From Table 6.6, it can be deduced that the total energy supplied by the low temperature heat source is 1273 MW. It is achieved by means of hot helium entering at 850^{o}C and leaving the plant at 575^{o}C at a flowrate of 735 kg/s. The two re-boilers for DC01 and DC02 need a total of 660.5 MW, of which 596.5 MW of energy comes from the low temperature heat source and the remaining 64 MW is achieved by heat exchange with HX02. Cooling water cools process stream to temperatures down to 30 ^{o}C, a suitable refrigerant (ammonia, R-717) is used to further cool streams to temperatures below 30^{o}C. HX11 is a chiller which cools the vapour distillate from the reactive distillation column from 234.5 to 15.9^{o}C for separation of hydrogen as product. The stream through the chiller (HX11) loses some of its heat to the reactive distillation column feed via heat exchangers HX06 and HX10 up to a temperature of 32^{o}C, the rest of the heat is lost to the refrigerant to reach the target temperature of 15.9^{o}C. The amount of refrigerant pumped is 772 kg/s with an inlet temperature of 0^{o}C and exiting at 10^{o}C.

The total work for the pumps is 0.73 MW. If a thermal to electric conversion efficiency of 50% is assumed, the total electric power requirement corresponds to a heat input of 1.46 MW.

6.2.3 Utilities schedule

For the SI cycle, it is proposed that there are three types of utilities. Heat is transferred from a high temperature source to the Bayonet reactor by means of helium entering the system at 950^{o}C and leaving at 850^{o}C. Heating requirements of other unit operations is achieved by transfer from helium entering at 850^{o}C and leaving at 575^{o}C. Overall, the helium enters the whole process at 950^{o}C and leaves at 575^{o}C. Cooling water entering at 28^{o}C is used to cool streams up to 30^{o}C, an industrial refrigerant (Ammonia, R-717) is used to cool streams which require cooling down to temperatures less than 32^{o}C. Table 6.6 shows a summary of the utilities schedule.

Table 6.7: Utilities schedule

Utility	**Inlet Temperature (^{o}C)**	**Outlet Temperature (^{o}C)**	**Flow (kg/s)**	**Target load (MW)**
Helium	950	575	735	1424
Water	28	33	55410	1159
Ammonia, R-717	0	10	772	30.87

6.3 Energy and Exergy analyses

Total energy consists of available energy plus unavailable energy. Considering flows of energy in a process, total energy is simply called energy and available energy is called exergy and are defined mathematically as:

$$\text{Energy} = \text{enthalpy} \times \text{flow (MW)} \quad (6.1)$$

$$\text{Exergy} = \text{availability} \times \text{flow (MW)} \quad (6.2)$$

Exergy analysis combines the principle of conservation of energy with the second law for the design and analysis of energy systems. Exergy is a measure of a numerical quantity of a flow and is defined as the maximum work that can be produced by a flow of energy as it comes to equilibrium with a reference point. Exergy analysis can point out whether or not, by how much; it is possible to design more efficient energy processes by reducing the inefficiencies in existing ones (Rosen, 2008:6922). It is assumed in this analysis that the heat is generated by a high temperature gas cooled reactor (HTGR) and electricity is generated from a hydro electric power plant. Helium is used as the heat transport fluid in the HTGR and transports thermal energy from the nuclear reactor at 950^{o}C, and returns at 575^{o}C.

6.3.1 Analysis methodology

Energy efficiency (E_η) and exergy efficiency (E_ε) are defined as follows:

$$E_\eta = (\text{energy in products})/(\text{total energy input}) \quad (6.3)$$

$$E_\varepsilon = (\text{exergy in products})/(\text{total exergy input}) \quad (6.4)$$

The reference point has a temperature of 298K, a pressure of 1 atm. The reference point emulates the natural environment and has been extensively used in analyses of energy systems in the past (Rosen, 2008:6922).

Figure 6.4 shows the Energy and Exergy flow diagram for the SI cycle presented in this study.

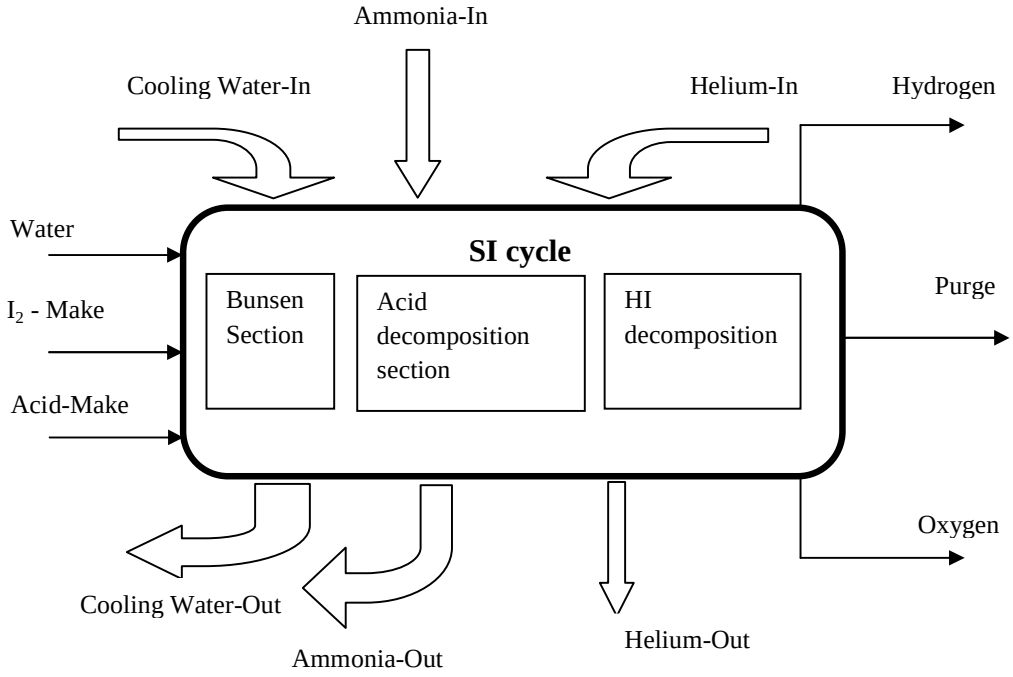

Figure 6.4: Energy flow diagram for the SI cycle [⟶ process streams; ⟹ utility streams]

The decomposition reactor is heated by a high temperature source in the form of hot helium coming from an HTGR at 950^{o}C. The helium exits the decomposition reactor at 850^{o}C and is used as a low temperature source for the Bunsen reaction and HI decomposition sections. Overall, the helium enters the system at 950^{o}C and leaves at 575^{o}C at a flow of 735 kg/s. The separation units include heat exchangers where the streams need to be cooled to a temperature below that of the incoming cooling water. Ammonia (R-717) is used as a refrigerant in this case, it enters the system at 0^{o}C and leaves at 10^{o}C at a flow of 772 kg/s. The electricity supplied to the system is assumed to be converted from a heat source at a heat to electric conversion efficiency of 50%. The total electric energy for the process is 0.73 MW and corresponds to a low temperature heat source supplying 1.46 MW of energy. Aspen Plus^{TM} is used to simulate the flow-rates, enthalpy and availability of process streams, and Aspen Energy Analyzer^{TM} is used to simulate the recommended heat exchanger network together with the flow-rates of utility streams.

6.3.2. Results and discussion

The results of the energy and exergy analysis are shown in Table 6.8.

Table 6.8: Process data extracted from the Aspen Plus™ and Aspen Energy Analyzer™ SI cycle heat exchanger network model.

Stream	Temperature (^oC)	Flow (kg/s)	Availability (MJ/kg)	Enthalpy (MJ/kg)	Exergy (MW)	Energy (MW)
Water	28	19.002	-13.175	-15.842	-250.35	-301.03
I_2-Make	28	0.145	0.016	0.063	0.00	0.01
Acid-Make	28	0.158	-7.088	-8.358	-1.12	-1.32
Helium-In	950	735	4.533	4.813	3331.76	3537.56
Cooling Water-In	28	55410	-13.175	-15.863	-730026.75	-878968.83
Ammonia-In	0	772	-0.948	-2.740	-731.86	-2115.28
Hydrogen	28	2.095	-0.390	-0.343	-0.82	-0.72
Oxygen	28	16.086	-0.015	-0.013	-0.24	-0.21
Purge	99	1.350	-5.570	-6.475	-7.52	-8.74
Helium-Out	575	735	3.159	2.876	2321.87	2113.86
Cooling Water-Out	33	55410	-13.175	-15.842	-730026.75	-877805.22
Ammonia-Out	10	772	-0.950	-2.700	-733.40	-2084.40

The lower heating value of hydrogen is 242 kJ/mol (Gorensek & Summers, 2009:4098), therefore for a hydrogen production rate of 1 kmol/s the power output from the system is 242 MW. The total exergy input is the difference between the exergies of the helium incoming and outgoing streams (3331.76 – 2321.87 = 1010 MW). The total exergy of the streams entering and leaving the system in Figure 6.4 is -727 768 and -728 446 MW respectively. The difference in the incoming and outgoing exergy is 768 MW; the value corresponds to the total exergy consumed by the whole process. The sum of the exergy consumed by the system and the power

output is equivalent to the total exergy input. The results of the exergy analysis are shown in Figure 6.5.

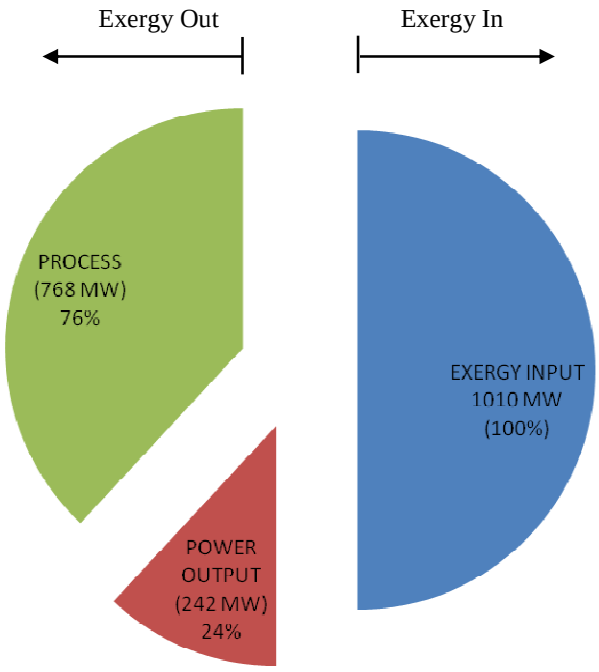

Figure 6.5: Exergy pie diagram.

The total energy input is also (3537.36 – 2113.86 = 1423.5 MW). The process streams leaving the system i.e. (purge, oxygen and hydrogen streams), carry energy out of the system which is the heat lost by the system. The heat carried out of the system by the utility streams is the difference between the energy of the outgoing and incoming utility streams. The heat rejected by the system is the total of the heat contained in the process streams leaving the system and the heat carried out by the utility streams. Therefore:

Heat rejected = heat loss + cold utility load

From Table 6.7, cold utility load = 1159 + 30.87 = 1189.87 MW

Therefore:

Heat rejected = (-7.52 - 0.24 - 0.82) + 1189.87

= 1181.29 MW

The results of the energy analysis are shown in Figure 6.6.

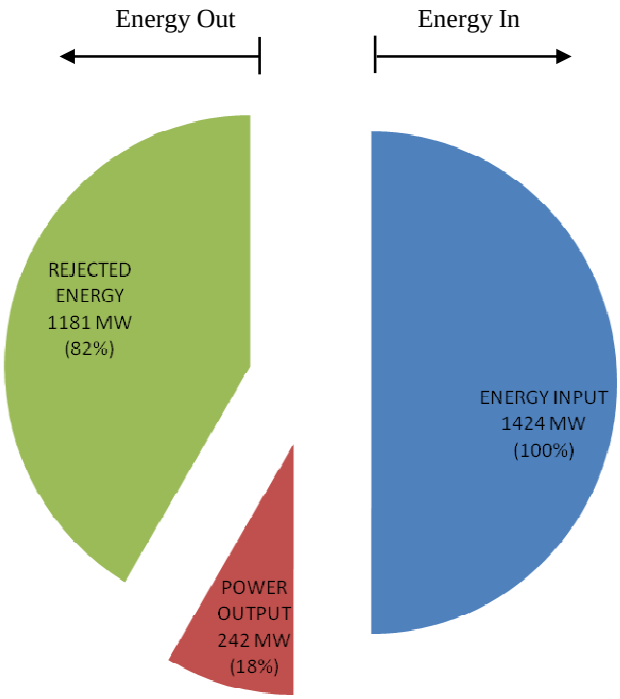

Figure 6.6: Energy pie diagram

From Figures 6.5 and 6.6 that the energy and exergy efficiencies of the SI cycle proposed in this study are 18 and 24% respectively. The energy and exergy efficiencies of an Ispra Mark-10 cycle were determined to be 20.5 and 24.7%, respectively (Rosen, 2008:6922). Currently there are few studies on the SI cycle that have included exergy analyses to complement the energy and other information presented. For example, in an assessment of solar hydrogen production via a two-step water-splitting thermochemical cycle based on Zn/ZnO redox reactions, a maximum exergy conversion efficiency of 29% is reported for the closed cycle when using a solar cavity-receiver operating at 2030 ^{o}C and subjected to a solar flux concentration ratio of 5000 (Steinfield, 2002:611). Energy and exergy analyses of the four-step adiabatic UT-3 thermochemical process for hydrogen production were undertaken and the efficiencies of the process were determined to

be 49% and 53% based on energy and exergy respectively (Sakurai *et al.* 1996:858). The values for the energy and exergy analyses obtained in this study compare well with an analysis of the Ispra Mark-10 cycle done Rosen (2008:6922). The Ispra Mark-10 is also a sulphur based cycle.

6.4 References

GORENSEK, M.B. & SUMMERS, W.A. 2009. Hybrid sulfur flowsheets using PEM electrolysis and a bayonet decomposition reactor. *International Journal of Hydrogen Energy*, **34**:4097-4114, Jun.

LEYBROS, J., GILARDI, T., SATURNIN, A., MANSILLA C. & CARLES, P. 2010. Plant sizing and Evaluation of hydrogen production costs from advanced processes coupled to a nuclear heat source. Part I: Sulphur-Iodine cycle. *International Journal of Hydrogen Energy*, **35**:1008-1018, Jan.

LEYBROS, J., GILARDI, T., SATURNIN, A., MANSILLA C. & CARLES, P. 2010. Plant sizing and Evaluation of hydrogen production costs from advanced processes coupled to a nuclear heat source. Part II: Hybrid-Sulphur cycle. *International Journal of Hydrogen Energy*, **35**:1019-1028, Jan.

ROSEN, M.A. 2008. Exergy analysis of hydrogen production by thermochemical water decomposition using the Ispra Mark-10 Cycle. *International Journal of Hydrogen Energy*, **33**:6921-6933, Oct.

SAKURAI, M., BILGEN E., TSUTSUMI, A. & YOSHIDA, K. 1996. Adiabatic UT-3 thermochemical process for hydrogen production. *International Journal of Hydrogen Energy* **21**:865–70, Feb.

SINNOTT, R.K. 2005. Chemical Engineering Design. Oxford: Elsevier Butterworth-Heinemann. 1038p **(Coulson & Richardson's Chemical Engineering series, vol. 6.)**

STEINFELD, A. 2002. Solar hydrogen production via a two-step water splitting thermochemical cycle based on Zn/ZnO redox reactions. *International Journal of Hydrogen Energy*, **27**:611-619, Jan.

CHAPTER 7: Economic evaluation

"There can be economy only where there is efficiency". Benjamin Disraeli (1804-1881)

7.1 Introduction

A suitable plant design is one that presents a process that is capable of operating under profit yielding conditions (Peters & Timmerhaus, 1991:150). Hence, there is need to identify all costs associated with the running of the SI cycle. The aim of this chapter is to present a preliminary economic evaluation of the process presented in this study. The economic evaluation presents an opportunity to evaluate the economic viability of the SI cycle compared to other hydrogen producing technologies. The different economic evaluation methods for industrial processes are:

- Order-of-magnitude estimate (ratio estimate) based on similar previous cost data.
- Study estimate (factored estimate) based on knowledge of major items of equipment.
- Preliminary estimate (budget authorisation estimate; scope estimate) based on sufficient data to permit the estimate to be budgeted (Peters & Timmerhaus, 1991:160)

In this study, the economic evaluation was done using the Order-of-magnitude estimate in conjunction with a study estimate based on the knowledge of the equipment of the SI cycle process.

7.1.1 Assumptions

- The cost of high temperature heat and refrigeration is equivalent to the cost of the same amount of energy delivered by the local electricity grid
- SI plant is coupled to an already existing high temperature heat source
- SI plant construction and commissioning is similar to a typical nuclear plant; 5 years (World Nuclear Association, 2011)
- The products are not stored, but are pipelined
- Cost of labour is $28/hr (Bridegam, 2010:41)
- The expected plant operating life is above 25 years

7.2 Capital investment

The investment cost of an industrial plant can be estimated using the total cost of equipment. The SI cycle presented in this study is composed of the following major processing equipment:

- Heat exchangers
- Reactors
- Absorber
- Distillation columns
- Centrifugal Pumps
- Electric Motors
- Agitators (Mixers)

Seider *et al.* (2004:505) presented the equations for calculating the purchase costs of a variety of chemical processing equipment. The detailed equipment cost calculation is presented in Appendix C.

7.2.1 Equipment cost

The SI equipment cost is categorised into the following:

- The Bayonet reactor, which constitutes of internal reactors and heat exchangers
- The process heat exchanger network, and
- Other equipment such as columns, flush drums and mixers.

A summary of the equipment costing done in Appendix C is shown in Table 7.1. It is clear that the heat exchanger network constitutes most of the total cost of equipment for the SI process.

Table 7.1: Share of equipment cost for the proposed SI cycle.

Equipment	**Cost ($)**	**Percentage (%)**
Bayonet Reactor	233 427 699	15.8
Heat Exchanger Network	1 233 856 474	83.7
Other	6 401 530	0.5
Total	**1 473 685 703**	**100**

The SI process is a process that converts water into hydrogen with the input of water, the energy supplied to the process should be comparable with the power output of the process, therefore a lot of heat integration is needed in order to utilize all the energy supplied as much as possible. The total SI cycle equipment cost is comprised of 15.8% Bayonet reactor and 83.7% heat exchanger network (Table 7.1). There is need to optimize the heat exchanger network in terms of cost and energy efficiency because the results of the optimisation will greatly affect the performance of the whole process.

7.2.2 Estimation of capital investment

The aim of this section is to estimate the amount of fixed-capital investment for the SI cycle process plant if the purchased-equipment cost is $1.4 US trillion (Table 7.1). The ranges of process-plant component cost outlined in Appendix C, Table C.6, given by Peters *et al.* (1991:167) will be used in the estimation. The cost of purchased equipment is the foundation step for the estimation of capital investment in this study. The ratio with respect to the cost of equipment in the ranges given in Appendix C, Table C.6 is used in Table 7.2. The flowsheets for each of the sections are presented in this study. Besides the main components i.e. the Bunsen reactor, Bayonet reactor and the reactive distillation column the equipment combine a set of proven chemical process technologies (Leybros *et al.* 2010: 1010). The whole set of heat exchangers are sized using Aspen Plus^{TM} Heater block and Aspen Energy Analyzer^{TM}, the results of sizing are given in Appendix B. All fluid properties used in the sizing calculations were determined using Aspen Plus^{TM} software.

The results of the estimation are shown in Table 7.2.

Table 7.2: Estimation of fixed capital cost for the SI cycle

Components	**% of purchased equipment**	**Cost ($)**
Purchased equipment	100	1 473 685 703
Purchased equipment installation	35	515 789 996
Instrumentation and controls (installed)	20	294 737 141
Piping (installed)	50	736 842 851
Electrical (installed)	25	368 421 425
Buildings (including services)	45	663 158 566
Yard improvements	12.5	184 210 713
Service facilities (installed)	50	736 842 851
Land	5	73 684 285
Engineering and supervision	52.5	773 684 994
Construction expense	40	589 474 281
Contractor's fee	15	221 052 855
Contingency	37.5	552 632 139
Total		**7 184 217 800**

The fixed capital cost of the proposed SI cycle process is $7.2 US trillion (Table 7.2). The estimated capital cost per unit power output is $ 29 862/kW, however, the value does not compare with other processes presented by the US Energy Information Administration (EIA). The estimated capital cost per kilowatt for a solar thermal power generating plant is $3 149/kW (EIA, 2007). The huge difference between the SI cycle and the solar thermal power plants may be due to the difference in technologies used for each system. Also there are many uncertainties linked with the evaluation of the SI thermochemical cycle because most of the technologies have not yet been applied on large scale.

7.3 Profitability measures

A chemical plant must demonstrate the capability of making profit so as to attract investors. The profitability analysis was carried out by estimating the production cost, working capital and calculating the rate of return on investment, (ROI) and payback period (PBP).

7.3.1. Production cost and profit

The total annual production cost is equal to the sum of the cost of manufacture and the total cost of the general expenses (Seider *et al.* 2004:577). Busche, (1995:1) presented a typical cost sheet outline for an industrial plant, where general expenses are estimated as a percentage of the total sales revenue. The cost sheet outline presented by Busche, (1995:1) was used as the foundation for the estimation of production cost for the SI cycle process. The cost outline is shown in Appendix C.

The aim of this sub-section is to estimate the annual production cost for a 7920 hr/yr continuous SI cycle process operation with the following conditions:

Feedstock	18 kg/s @ \$0.19/tonne (Conradie *et al.* 2001:21)
Hydrogen product	2 kg/s @ \$21/kg (Nicholas & Orgden, 2009)
Oxygen by-product	16 kg/s @ \$0.25/kg (NASA, 2001)
Total bare module costs	\$ 67 862 399 (Appendix C)
Site preparation and service facilities	\$ 921 053 564 (Table 7.2)
Cost of contingencies at 5% of direct permanent investment	
High temperature heat	1424 MW @ \$0.04/kWh (NERSA, 2010)
Cooling water	55 410 kg/s @ \$0.013/tonne, (Busche, 1995)
Refrigerant	32.9 MW @ \$0.04/kWh (NERSA, 2010)
Total cost of 1 year utilities	\$ 482 083 969
Allocated costs for utilities	\$ 500 000 000
Operators	6 per shift (2 per section per shift)
Labour cost	\$28/hr (Bridegam, 2010:41)

Outdated unit costs of materials have been updated by factoring inflation indices.

Total depreciable capital (C_{TDC}) is computed as follows:

C_{TDC} = direct permanent investment + contingency (7.1)

The direct permanent investment (C_{DPI}) is the sum of the total bare module, site preparation and allocated utilities costs.

C_{DPI} = \$67 862 399+ \$921 053 564 + \$500 000 000

= \$1 488 915 963

C_{TDC} = \$1 563 361 761

Table 7.3 shows the cost sheet for the estimation of the hydrogen production cost of the SI cycle.

Table 7.3: Estimation of production cost.

Cost Factor	Annual cost ($)
Feedstock (water)	**98 842**
Utilities	
Cooling water (CW)	20 854 019
High Temperature Heat	451 123 200
Refrigerant	10 422 720
Total Utilities	**482 399 939**
Operations (O)	
Direct wages and benefits (DW&B)	1 747 200
Direct salaries and benefits	262 080
Operating supplies and services	104 832
Technical assistance to manufacturing	312 000
Control laboratory	342 000
Total labour -related operations	**2 768 112**
Maintenance (M)	
Wages and benefits (MW&B)	54 717 662
Salaries and benefits	13 679 415
Materials and services	54 717 662
Maintenance overhead	2 735 883
Total maintenance	**125 850 622**
Total of M&O-SW&B	70 406 357
Operating overhead	
General plant overhead	4 998 851
Mechanical department services	1 689 753
Employee relations department	4 153 975
Business services	5 210 070
Total operating overhead	**16 052 649**
Property taxes and insurance	**31 267 235**
Depreciation (D)	
Direct plant	77 868 941
Allocated plant	35 400 000
Total depreciation	**113 268 941**
COST OF MANUFACTURE (COM)	**771 706 340**
General Expenses	
Transfer expense	13 124 644
Direct research	62 998 290
Allocated research	6 562 322
Administrative expense	26 249 288
Management incentive compensation	16 405 805
TOTAL GENERAL EXPENSES (GE)	**125 340 349**
TOTAL PRODUCTION COST (C)	**897 046 689**
Sales	
Hydrogen product	1 197 504 000
Oxygen co-product	114 960 384
TOTAL SALES	**1 312 464 384**
GROSS EARNINGS	**415 417 695**
NET EARNINGS (PROFIT) at Income tax of 40%	**249 250 617**
PRODUCTION COST ($/kg)	**16**

The estimated production cost for the proposed SI cycle is $16/kg provided that the plant will run continuously for 7920 hours per year. Leybros *et al.* (2010:1008) evaluated the cost of producing hydrogen from the SI cycle to be $15/kg for a hydrogen production capacity of 2 kg/s (57024 t/yr). Also Wang *et al.* (2009:9) estimated a production cost of $1.60 – 1.93/kg for a production capacity of 200 million t/yr. The production cost value obtained in this study compares well with Leybros *et al.* (2010:1008) because the production capacities are the same, Wang *et al.* (2009:9) value is way less because production capacity factors affect the cost of production.

7.3.2 Working capital

Working capital is funds needed by a firm to meet its obligations until payments are received from others for goods they have received from the firm. In general, the working capital is current assets minus current liabilities, where current assets are cash reserves, inventories and accounts receivable (Seider *et al.* 2004:580). Seider *et al.* (2004:580) state that the working capital for a chemical plant is the sum of cash reserves, inventory and account receivable minus accounts payable, the basis of calculation which follows general accounting principles is as follows:

- 30 days of cash reserves amounts to 8.33% of the annual cost of manufacture, COM, (assuming 30 days is 1/12 of a year)
- 7 days of inventories of liquid and solid products (excluding gas) at their sales price, which assumes that the products are shipped out once each week, whilst gas products are not stored, but are pipelined. Amounting to 1.92% of the annual sales of liquid and solid products
- 30 days of accounts receivable for product at the sales price, amounting to 8.33% of the annual sales of all products, meaning a customer is given 30 days to make payments.
- 30 days of accounts payable by the company for feedstock at the purchase price, amounting to 8.33% of the annual feedstock costs.

For the proposed SI cycle process:

C_{TDC}	= $ 1 563 361 761
COM	= $ 771 706 340
Hydrogen sales	= $ 1 197 504 000
Oxygen sales	= $ 114 960 384
Cost of feedstock	= $ 98 842

Therefore:

Cash reserves	= 0.0833(771 706 340) = $ 64 283 138
Inventories	= zero (products are not stored)
Accounts receivable	= 0.0833(1 197 504 000 + 114 960 384) = $ 109 328 283
Accounts payable	= 0.0833(98 842) = $ 8 233

Therefore:

Working capital	= **$ 173 603 188**

7.3.3 Rate of Return on Investment (ROI)

ROI is the yearly interest rate made by profits on the initial investment (Seider et al. 2004:582). A high ROI means that investment profits compare favourably to investment costs. ROI analysis compare investment cash inflows and cash outflows by constructing a ratio, or percentage. In most ROI analysis, a ROI percentage greater than zero means the investment returns more than its cost. For the analysis, the plant is assumed to operate each year at full capacity for 7920 hours per year for its expected operating life of more than 25 years. The year-end ROI for the plant operating life is calculated by use of spreadsheets using Equation 7.2 as the Simple ROI formula.

Simple ROI = [(Total cash inflows) – (Total cash outflows)]/(Total cash outflows) (7.2)

Table 7.4 shows the Simple ROI for the investment, in each period. For the years of plant operation, the cash inflows are the product sales revenue given Table 7.3 and the cash outflow is

the total production cost also given in Table 7.3. The values are assumed to be consistent for the 25 years of the plant operating life.

Table 7.4: Simple ROI for the project's first 25 years

	NOW	**Year1**	**Year2**	**Year3**	**Year4**	**.....**	**Year18**	**Year19**	**....**	**Year24**	**Year25**
CASH INFLOW ($mil)	0	1312	1312	1312	1312	.....	1312	1312	....	1312	1312
CASH OUTFLOW ($mil)	7184	897	897	897	897	.....	897	897	....	897	897
NET CASH FLOW ($mil)	-7184	415	415	415	415	.....	415	415	....	415	415
CUMULATIVE INFLOW	-7184	-6769	-6354	-5939	-5524	.....	286	701	....	2776	3191
SIMPLE ROI	-100%	-84%	-71%	-60%	-51%	.....	1%	3%	....	10%	11%

From Table 7.4, it is clear that the ROI is positive at year-end 18 and further on the assumption that the cash inflows and outflows are going to be consistent for the plant operating life. It takes 18 years for the investment ROI to be positive because the initial capital investment is large, magnitude of above 5 times, compared to the cash inflow for the first year of production. This is expected for a project of this magnitude.

7.3.4 Payback analysis

The time required for the annual earnings to equal the original investment is called the payback period (Seider *et al.* 2004:583). Payback period (PBP) should not be used for final decisions regarding large projects because it gives no consideration to the period of plant operation after the payback period. The cumulative cash flow graph in Figure 7.1 shows roughly the point in time when the cumulative cash flow breaks even, that is, when cumulative incoming returns exactly balance cumulative outflows.

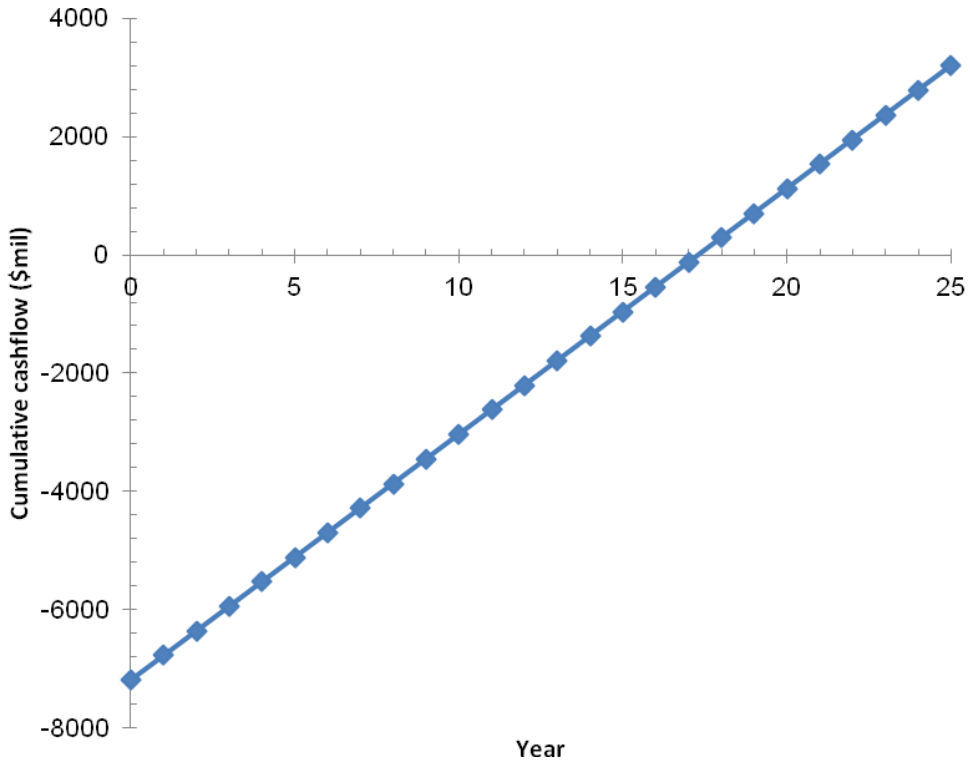

Figure 7.1: Cumulative cash flow graph

Using Conradie *et al.* (2001:21) argument about urban water supply, it can be argued for the energy supply industry that private operators want a scenario where there can be little competition, need a fair return on capital. Similarly, for public sector operators a sensible return on capital is important. For any given hydrogen unit price, a very low return on capital implies overuse of capital which means capital is being wasted relative to other uses of that capital. Similarly, high returns on capital indicate opportunities to increase production and reduce hydrogen prices. Conversely, the return on capital will vary directly with the hydrogen selling price. The SI cycle project is a low risk project because the product, hydrogen, will be the driving force of the perceived hydrogen economy (Gregory, 1973:13). Although the project requires large amounts of capital investment and operating costs a ROI of 11% on year 25 and a PBP of 17.3 years respectively reflects that the SI cycle is capable of operating profitably.

7.3.5 Discounted cash-flow rate of return (DCFRR)

The DCFRR is the annual rate of return that makes the net present value of all cash flows (both positive and negative) from a particular investment to be equal to zero. By calculating the net present worth for various interest rates, it is possible to find an interest rate at which the cumulative net present worth at the end of the project is zero (Sinnott, 2005:273). The DCFRR rule states that an investment is acceptable if the DCFRR exceeds the required rate of return (or the interest rate for discounting purposes) and it should be rejected otherwise (Discuss-Economics, 2011).

The DCFRR is determined by trial and error method with the help of a spreadsheet to establish the interest rate to be applied to the cash flow each year, such that the original investment would be reduced to zero during the useful life of the project (Seider et al. 2004:608) A value of 43.1% is obtained for a hydrogen selling price of $18.6/kg, that gives an annual sales revenue of $1176 million (Appendix C, Table C.8). The DCFRR is expected to be higher if the hydrogen selling price is increased to $21/kg. The DCFRR is a measure of the maximum rate that the project could pay and still break even by the end of the project life, and is also independent of the amount of capital used. Considering an income tax of 40%, a DCFRR value of 43.1% shows that the project is profitable.

7.4 Project sensitivity analysis

The profitability of a project depends on the cash flows associated with the project, which in turn depend on many factors (Discuss-Economics, 2011):

- The capital investment required by the project.
- The revenues to be expected and their evolution in time.
- The discount interest rate, which in turn depends on the required return on the project.
- The inflation component and the uncertainty component.
- The selling price and or production rate

The selling price and or production rate can be affected by inflation; generally inflation obliges to increase the selling price and production rate. To study the effect of the increment on the profitability, the dependence of the DCFRR on production rate, operating costs, ROI and capital investment is investigated. Spider diagrams illustrate the impact on project economics when any one parameter is changed while other parameters are held constant. The steeper the curve the more sensitive project economics is to the change in the parameter.
Figure 7.2 shows the results of the sensitivity analysis.

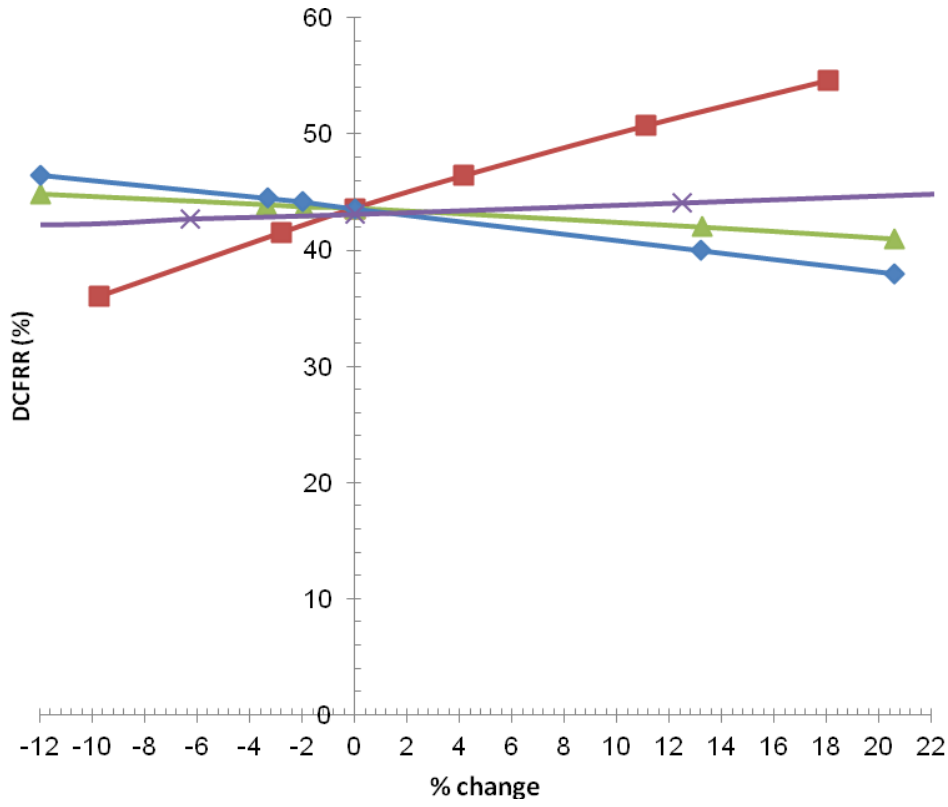

Figure 7.2: DCFRR sensitivity analysis for the SI cycle project [■ Production rate; ▲Operating and Maintenance costs; ◆ Capital Investment; x ROI]

It is clear from Figure 7.2, basing on the steepness of the lines, that the project is more sensitive to the production rate and the capital investment. The production rate is proportional to the selling price; therefore the production rate and selling price should be most closely examined for accuracy and reliability. The results of the sensitivity analysis compares with one presented by Smith (1999:4), i.e. the analysis shows the general trend for most large scale projects. Smith (1999:4) stated the following points:

- Price and revenue are usually the only positive component of the cash flow. They are largely determined by selling price, but any production factors that influence the amount of product sold will have a parallel effect.
- The cash flow is a direct function of the margin between revenue and operating costs, so operating costs exert a negative impact on the cash flow and the return.

- In terms of the total cash flow, the capital cost can be a relatively small number. However, capital is input at the very beginning of the project and has a high negative influence on the discounted cash flow, since the positive cash flows which follow are discounted increasingly the further away they are in time.

7.5 References

BRIDEGAM, M.A. 2010. Unions and labour laws. Infobase Publishing. 121p

BUSCHE, R.M. 1995. Venture Analysis: A framework for venture planning. (Course notes delivered as part of the lecture for Bio-en-gene-er Associates in Wilmington.) Delaware. (Unpublished)

CONRADIE, B., GOLDIN, J., LEIMAN, A., STANDISH, B. & VISSER, M. 2001. Competition in the Water Industry. (Paper presented for the Development Policy Research Unit in August 2001. University of Cape Town.)

DISCUSS-ECONOMICS. 2011. Project Evaluation – Sensitivity Analysis (Cash Flow). http://www.discusseconomics.com. Date of access: 02 Nov 2011

ENERGY INFORMATION ADMINISTRATION. 2007. Annual Energy Outlook. http:// www.eia.gov/forecasts. Date of access: 25 Sep 2011

GORENSEK, M.B. & SUMMERS, W.A. 2009. Hybrid sulfur flowsheets using PEM electrolysis and a bayonet decomposition reactor. *International Journal of Hydrogen Energy*, **34**:4097-4114, Jun.

GREGORY D.P. 1973. The Hydrogen Economy. *Scientific American*, **228**:13-21, Jan.

LEYBROS, J., GILARDI, T., SATURNIN, A., MANSILLA C. & CARLES, P. 2010. Plant sizing and Evaluation of hydrogen production costs from advanced processes coupled to a nuclear heat source. Part I: Sulphur-Iodine cycle. *International Journal of Hydrogen Energy*, **35**:1008-1018, Jan.

NATIONAL AERONAUTICS & SPACE ADMINISTRATION. 2001. NASA Facts: Space shuttle use of propellants and fluids. http://www-pao.ksc.nasa.gov/kscpao/nasafact. Date of access: 26 Sep 2011

NATIONAL ENERGY REGULATOR OF SOUTH AFRICA. 2010. Eskom average price. http://www.nersa.org.za/Admin. Date of access: 25 Sep 2011

NICHOLAS, M. & OGDEN, J. 2009. Analysis of a Cluster Strategy for Near term Hydrogen Infrastructure Rollout in Southern California. (Presentation for the Institute of transportation studies in November 2009. University of California.)

ORME, C.J., KLAEHN, J.R. & STEWART, F.F. 2009. Membrane separation processes for the benefit of the sulfur–iodine and hybrid sulfur thermochemical cycles. *International Journal of Hydrogen Energy*, **34**:4088-4096, Aug.

PETERS, M.S. & TIMMERHAUS, K.D. 1991. Plant design and economics for chemical engineers. McGraw-Hill. 923p

SEIDER, W. D., SEADER, J.D., & LEWIN, D.R. 2004. Product and Process Design Principles: Synthesis, Analysis, and Evaluation. Wiley. 802p

SINNOTT, R.K. 2005. Chemical Engineering Design. Oxford: Elsevier Butterworth-Heinemann. 1038p **(Coulson & Richardson's Chemical Engineering series, vol. 6.)**

SMITH, L.D. 1999. Discounted cash flow analysis Methodology and Discount rates. Unpublished. 15p

WANG, Z.F., NATERER, G.F., GABRIEL, K.S., GRAVELSINS, R. & DAGGUPATI, V.N. 2009. Comparison of sulfur–iodine and copper–chlorine thermo-chemical hydrogen production cycles. *International Journal of Hydrogen Energy*, **xxx:** 1-11, Sep.

WORLD NUCLEAR ASSOCIATION. 2011. Nuclear Power in South Korea. http://world-nuclear.org. Date of access: 27 Oct 2011

CHAPTER 8: Conclusion and Recommendations

"A conclusion is the place where you get tired of thinking". Arthur Bloch

8.1 Introduction

In this study an SI cycle flowsheet for producing hydrogen has been developed. The SI cycle splits water into hydrogen and oxygen. The combined process flowsheet is presented in Chapter 5. The energy, exergy and economic analysis are presented in Chapters 6 and 7 respectively. The results obtained are used to come up with a conclusion on different aspects of the SI cycle.

The main objective of this study was to develop an Aspen Plus^{TM} simulation of the SI cycle for the production of hydrogen. The development of the study required the production of an optimised flowsheet and an economic and energy analysis of the SI thermochemical cycle.

8.2 Findings of the study

The majority of the processes within the SI cycle can be described accurately by the ELECNRTL model. However, the system exhibits a high degree of non ideality and partial immiscibility of the binary HI-H_2O and ternary HI-I_2-H_2O systems. Leybros *et al.* (2009:9060) described the HI_x system using a modified model derived from the NRTL equation. The ELECNRTL is also a modified NRTL equation. Therefore it can be concluded that the simulation presented using the ELECNRTL proves to some greater extent that the SI cycle is feasible.

The lower heating value (LHV) energy and exergy efficiencies of the SI cycle proposed in this study are 18 and 24% respectively. The flowsheet requires 380.1 MW high temperature heat and 1043 MW low temperature heat. A total of 1423.1 MW is consumed. The energy input is 59% higher than that of HTGR powered water electrolysis which requires 895 MW (with an assumed pressure of 120 bars for the H_2 product) (Leybros *et al.* 2009:9074).

The estimated production cost for the proposed SI cycle is $16/kg provided that the plant will run continuously for 7920 hours per year. The evaluated cost compares well with the value obtained by the evaluation done by Leybros *et al.* (2010:1008), which gave the cost of producing

hydrogen from the SI cycle as $15/kg for a hydrogen production capacity of 1 kmol/s. Wang *et al.* (2009:9) estimated a production cost of $1.60 – 1.93/kg for a production capacity of 200 million t/yr which is equivalent to 3510 kmol/s. The annual CE Indices for the years 2009 and 2010 are 521.9 and 556.2 respectively (Chemical Engineering, 2011). Therefore Wang *et al.* (2009:9) cost extrapolated to 2010 would be in the range $1.7 – 2.06/kg. Wang *et al.* (2009:9) production cost is less than the value obtained for this analysis, one of the reasons may be because of production capacity factors.

The ROI of the investment becomes positive after 18 years, with a payback period of 17.3 years. This is typical of a low risk project with a huge amount of capital investment. However, such projects do not attract funding from the private sector as the period for the investors to recover the initial funds used is long. Therefore this is a project that needs to be undertaken by the governments of the individual nations.

8.3 Recommendations for further study

Studies should be extended to the production of hydrogen by thermochemical cycles coupled with a high temperature solar heat source. In a presentation to the Stanford Global Climate and Energy Project (Schultz, 2003:16), it was reported that solar furnaces at the National Renewable Energy Laboratory demonstrated 51% collection efficiency at 2000^{o}C in the process fluid for thermal cracking of methane. Sandia National Laboratory (SNL) also demonstrated the matching of solar energy to thermo-chemical cycles and hot sand temperatures of up to 1000^{o}C have been reported (Summers, 2009:16).

The experimental proof of concepts was based on literature presented by authors from different institutes, funding should be made available for researchers to perform validation experiments of results which have been presented by other authors.

In order to demonstrate fully the SI cycle, an integrated, closed-loop laboratory or pilot scale model should be constructed consisting of all the unit operation units. A pilot plant with an input of water as low as 10 kg/min is possible.

The OLI Systems, Inc.'s Mixed Solvent Electrolyte (MSE) model used by Gorensek & Summers (2009:4097) describes the H_2SO_4-H_2O-SO_3-SO_2-O_2 system better than the ELECNRTL model. Therefore the MSE model should be made available and incorporated into the Aspen Plus^{TM} database for future researchers, especially for the purposes of modelling the high temperature acid decomposition step.

.

8.4 References

ASPEN TECH. 2010. Aspen Plus. http://www.aspentech.com/core/aspen-plus.aspx. Date of access: 03 Apr 2010

CHEMICAL ENGINEERING. 2011. Economic Indicators. http://www.che.com. Date of access: 25 Sep 2011

LEYBROS, J., CARLES, P. & BORGARD, J.M. 2009. Countercurrent reactor design and flowsheet for iodine-sulfur thermo-chemical water splitting process. *International Journal of Hydrogen Energy*, **34**:9060-9075, Sep.

LEYBROS, J., GILARDI, T., SATURNIN, A., MANSILLA C. & CARLES, P. 2010. Plant sizing and Evaluation of hydrogen production costs from advanced processes coupled to a nuclear heat source. Part I: Sulphur-Iodine cycle. *International Journal of Hydrogen Energy*, **35**:1008-1018, Jan.

ROSEN, M.A. 2008. Exergy analysis of hydrogen production by thermochemical water decomposition using the Ispra Mark-10 Cycle. *International Journal of Hydrogen Energy*, **33**:6921-6933, Oct.

SCHULTZ, K. 2003. Thermochemical Production of Hydrogen from Solar and Nuclear Energy. (Presentation to the Stanford Global Climate and Energy Project on 14 April 2003. San Diego.)

SUMMERS, W.A. 2009. Hybrid Sulfur Process Overview. (Paper presented at the SDE Info Exchange and Workshop on 20 April 2009. Aiken.)

Appendix A: Simulation packages

A.1 Design-II™

Design-II™ developed and marketed by WinSim is a steady-state process simulator, It has been licensed to WinSim since 1995, when the company purchased the rights to the program from ChemShare Corporation. WinSim has over a thousand subscribed users of Design-II™ throughout the world. The company is based in Sugar Land, Texas (WinSim, 2010). Among other characteristics, Design-II™ has the capabilities of performing accurate process simulation for chemical and hydrocarbon processes including refining, refrigeration, petrochemical, gas processing and treating, pipelines, fuel cells. Design-II™ for Windows was the first process simulator developed specifically for Windows computing. Design-II™ for Windows has been leading the way in simulation technology since the early 90s.

A.2 SPENCE®

KEMA has developed a software package called SPENCE® for simulation of processes for energy conversion systems and electricity production. SPENCE® is intended to support chemical engineers employed within electricity companies or industry. SPENCE® is a static flow sheet simulator based on thermodynamics to determine the technical data and merits of energy conversion systems, including:

- efficiency
- environmental impact
- cost benefits.

Developed in 1982, the program has been continuously improved during 25 years of research activities in improving the processes of electricity production (KEMA, 2010).

A.3 Aspen Plus™

Aspen Plus™ is a market-leading trademark in process modelling tools for conceptual design, optimisation, and performance tracking and checking for the chemical, polymer, specialty chemical, metals and minerals, and coal power industries. Aspen Plus™ is an element of AspenTech's AspenONE® Process Engineering applications (AspenTech, 2010).

A.4 Prosim Plus™

Prosim Plus™ is a process/chemical engineering software that performs accurate mass and energy balance calculations for different kinds of industrial steady-state processes. It is used in design as well as in operation of existing plants for process optimisation, units troubleshooting or debottlenecking, plants revamping or carrying out front-end engineering analysis. Prosim Plus™ has many applications in industries such as chemical, pharmaceutical, petrochemical, oil, gas treatment, refining, specialty chemical, and in engineering companies. Its rich thermodynamic package and its flexible structure permit the simulation of almost all systems encountered (Prosim, 2010).

Appendix B: Process heat exchanger network (HEN)

B.1 Bayonet reactor internal heat recuperation

The streams shown in Figure B.1 (R01 to R13), are the Bayonet reactor internal streams presented in Chapter 6. For example, the feed stream R01 is pre-heated to 212 ^{o}C by the high temperature heat source through heat exchanger E-113, heat exchange with stream 13 by means of heat exchanger E-109 brings the stream to the desired temperature of 270 ^{o}C. A brief description of the Bayonet reactor HEN and the sizes of the individual heat exchangers is given is Table B.1.

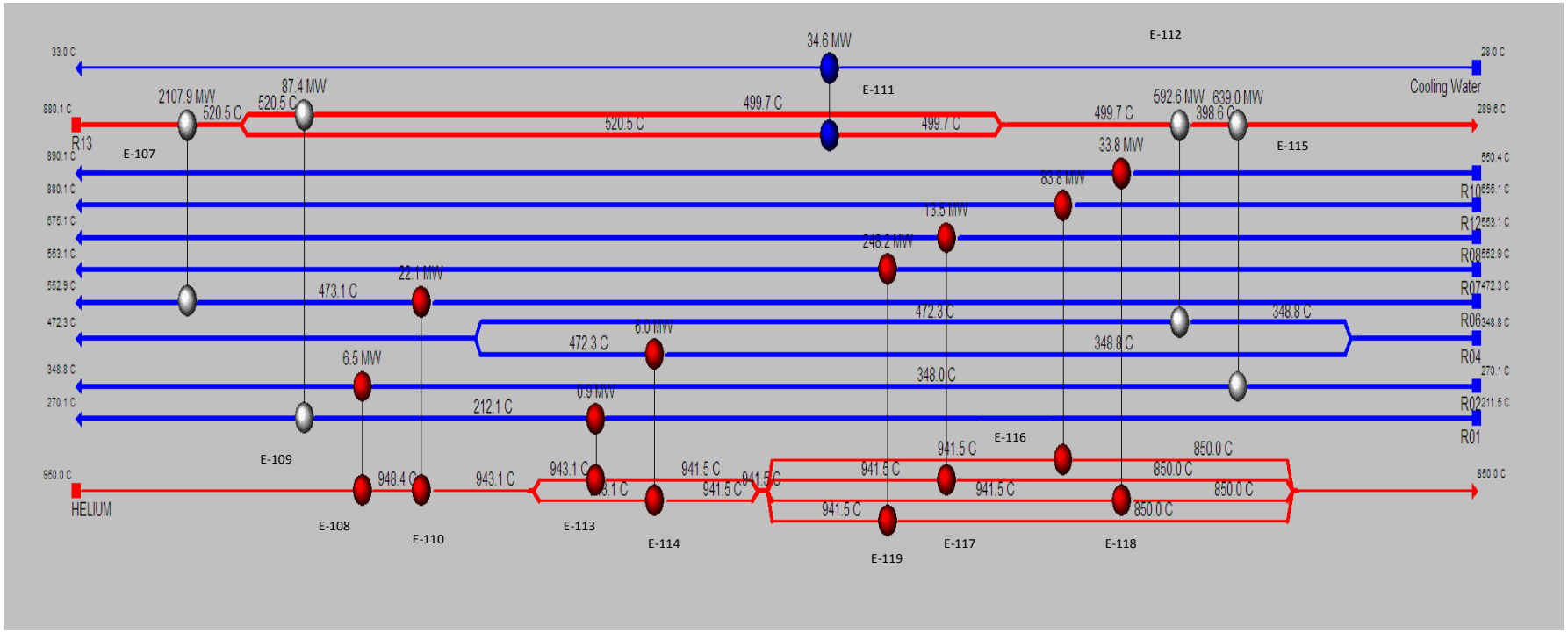

Figure B.1: Bayonet reactor HEN

B.2 Aspen Energy Analyzer™ Bayonet reactor HEN sizing results

Table B.1: Aspen Energy Analyzer™ Bayonet reactor HEN sizing results

Heat Exchanger	Load (MW)	Area (m^2)	Shells	LMTD (^oC)	Overall U ($kJ/s.m^2.C$)	Fouling Factor	Hot Stream	Hot T_{in} (C)	Hot T_{out} (C)	Cold Stream	Cold T_{in} (C)	Cold T_{out} (C)
E-107	2108	3.65E04	74	144.9	0.4250	0.9371	R13	880.1	520.5	R06	473.1	552.9
E-108	6.455	25.28	1	600.9	0.4250	1.0000	Helium	950.0	948.4	R02	348.0	348.8
E-109	87.42	2016	5	420.8	0.1619	0.9972	R13	520.5	499.7	R01	212.1	473.4
E-110	22.08	109.8	1	268.6	0.4250	1.0000	Helium	948.4	943.1	R06	472.3	553.1
E-111	34.62	104.1	1	473.1	0.6929	0.9999	R13	520.5	499.7	Cooling water	28.0	33.0
E-112	592.6	4.60E04	93	37.56	0.4250	0.8059	R13	499.7	398.6	R04	348.8	472.3
E-113	0.883	7.468	1	730.5	0.1619	1.0000	Helium	943.1	941.5	R01	211.5	212.1
E-114	5.986	26.62	1	529.5	0.4250	0.9999	Helium	943.1	941.5	R04	348.8	472.3
E-115	639.0	5.53E04	111	32.72	0.4250	0.8290	R13	398.6	289.6	R02	270.1	348.0
E-116	83.80	4816	10	115.6	0.1619	0.9309	Helium	941.5	850.0	R12	655.1	880.1
E-117	13.53	115.9	1	281.4	0.4250	0.9761	Helium	941.5	850.0	R08	553.1	675.1
E-118	33.80	609.5	2	140.8	0.4250	0.9278	Helium	941.5	850.0	R10	550.4	890.1
E-119	248.2	1714	4	340.7	0.4250	1.0000	Helium	941.5	850.0	R07	552.9	553.1

B.3 Aspen Energy Analyzer™ Downstream processes HEN sizing results

Table B.2: Aspen Energy Analyzer™ Downstream processes HEN sizing results

Heat Exchanger	Load (MW)	Area (m^2)	Shells	LMTD	Hot Stream	Hot Tin (C)	Hot Tout (C)	Cold Stream	Cold Tin (C)	Cold Tout (C)
E-148	0.997	9.66	1	624.8	He	716.6	686.4	HX16	75.9	76.2
E-150	48.62	32010	66	16.04	HX11	157.4	135.2	HX06	122.9	137.0
E-140	971.0	44710	360	14.58	HX08	174.4	155.1	HX06	137.0	162.9
E-138	96.73	11550	24	83.88	HX08	176.9	174.4	HX16	76.2	105.9
E-142	34.60	13960	28	27.14	CD01	223.2	154.7	HX10	145.0	165.0
E-135	416.1	4536	10	570.2	He	850.0	715.6	HX10	165.0	259.7
E-133	20.69	209.40	1	610.9	He	850.0	715.6	HX06	162.9	176.9
E-166	0.818	28.46	1	151.4	CD01	154.7	153.1	Refrigerant	0.0	5.0
E-151	18.29	667.80	2	144.4	HX12	172.2	133.8	Refrigerant	6.5	9.2
E-153	127.8	1527	4	517.2	He	686.4	660.7	HX09	155.8	156.6
E-157	6.628	2384	5	27.82	HX13	158.2	144.2	HX06	122.7	122.9
E-161	126.8	12550	26	101.1	CD02	270.0	243.8	HX09	154.9	155.7
E-159	17.89	15180	31	12.46	HX01	161.5	150.0	HX10	140.9	145.0
E-149	476.4	24330	100	20.74	HX12	172.2	133.8	HX06	122.9	137.0
E-139	72.86	4197	9	91.43	DEC01	120.0	119.0	Cooling water	28.0	28.2
E-147	0.320	10.34	1	163.0	HX13	187.6	158.2	Refrigerant	9.2	9.8
E-134	233.3	3138	7	460.9	He	850.0	715.6	RB02	302.4	337.8
E-136	0.276	2.32	1	734.8	He	850.0	715.6	HX03	42.3	50.0
E-128	27.32	2110	5	129.5	HX08	176.9	174.4	HX03	42.3	50.0

Table A.2 continued

E-165	3.275	9162	19	20.94	HX11	32.0	15.9	Refrigerant	0.0	5.0
E-162	427.2	7011	15	382.5	He	660.7	575.0	RB01	153.1	315.1
E-158	227.0	40160	81	30.56	HX11	135.2	32.0	Cooling water	28.2	29.0
E-160	42.89	3193	7	134.4	CD02	270.0	243.8	HX06	121.6	122.7
E-144	144.9	1756	4	510.1	He	715.6	686.4	HX07	176.9	204.9
E-146	1.714	34.63	1	260.7	CD02	270.3	270.0	Refrigerant	9.2	9.8
E-127	172.7	37540	76	47.48	HX01	288.6	177.3	HX06	162.9	176.9
E-131	46.38	4403	9	105.5	CD01	315.1	223.2	HX09	156.6	157.9
E-129	164.8	14570	30	113.3	HX02	315.1	235.0	HX09	156.6	157.9
E-164	11.47	584.0	2	103.4	HX13	144.2	120.0	Cooling water	28.2	28.2
E-163	0.345	6.64	1	321.4	He	660.7	575.0	HX14	289.0	301.1
E-155	22.35	19400	39	11.55	HX01	175.9	161.5	HX09	155.7	155.8
E-137	1.665	33.33	1	263.1	HX02	315.1	235.0	Refrigerant	9.8	10.0
E-141	13.59	8477	18	17.53	HX13	187.6	158.0	HX10	145.0	165.0
E-143	39.55	39880	80	11.38	HX11	175.4	157.4	HX10	145.0	165.0
E-145	129.9	67.77	1	167.1	HX01	177.3	175.9	Refrigerant	9.2	9.8
E-132	2.151	46020	94	29.47	HX11	234.5	175.4	HX06	162.9	176.9
E-130	199.4	122000	386	9.943	HX12	187.6	172.2	HX06	162.9	176.9
E-154	11.07	390.70	1	149.2	HX08	155.1	154.9	Refrigerant	5.0	6.5
E-152	0.736	34.88	1	111.1	DEC01	119.0	119.0	Refrigerant	6.5	9.2
E-156	1135	131400	263	46.98	HX12	133.8	45.9	Cooling water	29.0	33.0

Appendix C: Economic Evaluation

C.1 Calculation of Equipment cost

An investment cost of an industrial plant can be estimated with knowledge of the total equipment cost. The SI cycle presented in this study is composed of the following major processing equipment:

- Heat exchangers
- Reactors
- Absorber
- Distillation columns
- Centrifugal Pumps
- Electric Motors
- Agitators (Mixers)

Seider *et al.* (2004:505) presented the equations for calculating the purchase costs of a variety of chemical processing equipment. The form of the equations is as follows:

$$C_P = \exp\{A_0 + A_1[\ln(S)] + A_2[\ln(S)]^2 + \ldots..] \quad (C.1)$$

Where C_P – purchase cost ($)

A – constant

S – size factor

The costs of processing equipment change with time; a correction factor called the cost index (Seider *et al.* 2004:483) is used to obtain the current value of the equipment cost. The index commonly used is the Chemical Engineering (CE) Plant Index (Chemical Engineering, 2011). Table C.1 shows the CE Index for 2010.

Table C.1: CE Index for October 2010 (Chemical Engineering, 2010)

Equipment	**CE Index**
Heat exchanger	667.5
Process machinery	617.8
Pipe, Valves and Fittings	627.0
Process Instruments	840.2
Pumps and Compressors	426.0
Electrical equipment	902.5
Structural supports and Miscellaneous	484.7
Construction labour	330.6
Buildings	503.2
Engineering and Supervision	336.6

C.1.1 Bayonet reactor

The Bayonet reactor consists of a heat exchanger network and six internal reactors (Chapter 6). The six reactors are considered to be pressure vessels with a volume of 250 m^3 each and the liquid phase reactors (R-HX02, R-HX04 and R-HX06) are equipped with agitators driven by electric motors. The individual heat exchangers in the Bayonet reactor heat exchanger network are shown in Appendix B.

The objective is to calculate the total cost of the Bayonet reactor consisting of six cylindrical vessels, with an inside diameter of 3 m (118 in.) and a length of 10 m (393.7 in). The reactor feed is 85% aqueous sulphuric acid pumped at 7.8 kmol/s (61776 lbmol/hr), at a pressure of 22 bar (319 psia). The vessel will be oriented in horizontal position. Three reactors handle the liquid phase which is perfectly mixed by an agitator for each with a 700 Hp, 3600 rpm electric motor. The internal heat recuperation is achieved by an internal heat exchanger network with individual shell and tube heat exchanger units outlined in Appendix B, Table A.1, and each tube length is 6 m. The materials of construction are Incoloy 800 for the pressure vessels and stainless steel for the heat exchanger network. The barometric pressure at the plant site is 1 atm (14 psia). The CE indices for the pressure vessels and heat exchangers, and for the electric motor are assumed to be 667.5 and 902.5 respectively (Table C.1)

Seider *et al.* (2004:527) suggested the following equations for the calculation of the purchase cost of pressure vessels, electric motors and heat exchangers for a base CE Index of 394.

Pressure vessels

$$C_P = (F_M C_V + C_{PL})(667.5/394) \quad (C.2)$$

$$C_V = \exp\{8.717 - 0.233[\ln(W)] + 0.04333[\ln(W)]^2\} \quad (C.3)$$

$$W = \pi(D_i + t_S)(L + 0.8D_i)t_S\rho \quad (C.4)$$

$$C_{PL} = 1580(D_i)^{0.20294} \quad (C.5)$$

$$t_P = P_d D_i/(2SE - 1.2P_d) \quad (C.6)$$

$$P_d = \exp\{0.606008 + 0.91615[\ln(P_o)] + 0.0015655[\ln(P_o)]^2\} \quad (C.7)$$

Where:

C_V – cost of empty vessel

F_M – material factor = 3.7 for Incoloy 825 (Seider *et al.* 2004:531)

C_{PL} – cost for platforms and ladders

W – weight of the shell (lb)

D_i – internal diameter of vessel (inch)

P_d – internal design gauge pressure (psig)

P_o – operating pressure (psig)

t_S – shell thickness (inch)

t_P – wall thickness (inch)

S – maximum allowable stress = 14500 psi (SMC, 2004)

E – weld efficiency (1.0)

ρ = density of material (lb/in^3)

Electric motors for agitators

$$C_P = (F_{TM} C_B)(902.5/394) \quad (C.8)$$

$$C_B = \exp\{5.4866 + 0.13141[\ln(P_C)] + 0.053255[\ln(P_C)]^2 + 0.028628[\ln(P_C)]^3 - 0.0035549[\ln(P_C)]^4\} \quad (C.9)$$

Where:

F_{TM} – motor type factor = 1.0 (Seider *et al.* 2004:511)

C_B – base cost

P_C – power consumption (hp)

Heat Exchangers

$$C_P = (F_P F_M F_L C_B)(667.5/394) \quad \text{(C.10)}$$

$$C_B = \exp\{11.147 - 0.9186[\ln(A)] + 0.09790[\ln(A)]^2\} \quad \text{(C.11)}$$

$$F_M = 2.7 + (A/100)^{0.07} \quad \text{(C.12)}$$

$$F_P = 0.9803 + 0.018(P/100) + 0.0017(P/100)^2 \quad \text{(C.13)}$$

Where:

F_L – tube length correction factor

A – surface area (ft^2)

P – shell side pressure (psig)

The specifications and costs of the reactors and the heat exchanger network after applying Equations C.1 to C.13 are shown in Table C.2 and C.3. The total cost of the Bayonet reactor is $233 427 699 of which the internal heat exchanger network constitutes 98% of the total cost.

Table C.2: Bayonet reactor internal reactors cost and specifications

Reactor	**R-HX02**	**R-HX04**	**R-HX06**	**R-DEC01**	**R-DEC03**	**R-DEC04**
Diameter (m)	3	3	3	3	3	3
Length (m)	10	10	10	10	10	10
Inlet Pressure (bar)	22	22	22	22	22	22
Design Pressure (bar)	26	26	26	26	26	26
Inlet Temperature (^OC)	348.7	359	553	675	890	655
Design Temperature (^OC)	1000	1000	1000	1000	1000	1000
Internals	Agitator	Agitator	Agitator	Nil	Nil	Nil
Wall thickness (cm)	4.0	4.0	4.0	4.0	4.0	4.0
Cost ($mil)	**872 300**	**872 300**	**872 300**	**814 600**	**814 600**	**814 600**

Table C.3: Bayonet reactor internal heat exchangers cost and specification.

Heat Exchanger	**Area (m2)**	**Cost ($)**
E-107	3.6E04	51 021 028
E-108	25.28	135 878
E-109	20.16	131 695
E-110	109.8	208 539
E-111	104.1	203 923
E-112	4.6E04	73 632 458
E-113	7.468	128 111
E-114	26.62	137 029
E-115	5.5E04	96 870 857
E-116	4816	3 792 995
E-117	115.9	213 439
E-118	609.5	563 469
E-119	1714	1 327 578
		228 366 999

C.1.2 Downstream heat exchangers

Equations C.10 to C.13 are used to calculate the sizes of the individual heat exchangers. The material of construction is stainless steel, shell and tube with a tube length of 6 m.

Table C.4: Downstream heat exchanger network equipment cost and specifications

Heat Exchanger	**Area (m^2)**	**Cost ($)**
E-148	9.66	119 642
E-150	32010	40 349 492
E-140	44710	66 237 299
E-138	11550	10 123 453
E-142	13960	13 692 756
E-135	4536	3 550 215
E-133	209.40	267 556
E-166	28.46	138 633
E-151	667.80	603 066
E-153	1527	1 122 182
E-157	2384	1 707 275
E-161	12550	11 206 334
E-159	15180	15 281 503
E-149	24330	27 269 393
E-139	4197	3 261 530
E-147	10.34	126 756
E-134	3138	2 397 452
E-136	2.32	147 042
E-128	2110	1 522 919
E-165	9162	8 039 363
E-162	7011	5 497 501
E-158	40160	60 012 220
E-160	3193	2 292 523
E-144	1756	1 275 105
E-146	34.63	144 123
E-127	37540	50 980 406
E-131	4403	3 227 382
E-129	14570	13 599 475
E-164	584.0	546 130
E-163	6.64	120 533
E-155	19400	19 938 279
E-137	33.33	142 957
E-141	8477	7 312 622
E-143	39880	59 388 372
E-145	67.77	173 519
E-132	46020	69 202 149
E-130	122000	331 629 935
E-154	390.70	413 678
E-152	34.88	144 347
E-156	131400	400 651 355
E-148	9.66	119 642
TOTAL		**1 233 856 474**

C.1.2 Other equipment

The process flowsheet contains 6 flash drums which can be treated as pressure vessels containing little internals. Also there are two pumps (PP01 and PP02), a centrifugal pump should be selected if the pumping requirements are as follows: (Seider *et al.* 2004:507)

- Volumetric flow rate up to 0.32 m^3/s
- Total head up to 975 m, and
- Kinematic viscosity less than 0.0002 m^2/s

For requirements that are outside the specified range, it is assumed that two or more centrifugal pumps are placed in parallel. Therefore pump PP02 which pumps 1.3 m^3/s of liquid is considered to be four centrifugal pumps installed in parallel to achieve the required flowrate. The Bunsen reactor, absorber and distillation columns are considered as pressure vessels. The other equipment on the list is mixers (agitators). Seider *et al.* (2004:505) gives the following correlations for the purchase costs of the equipment listed in this sub-section

Pumps

$$C_P = F_{TP}F_MC_B \quad (C.14)$$

$$C_B = \exp\{9.2951 - 0.6019[\ln(S)] + 0.0519[\ln(S)]^2\} \quad (C.15)$$

$$S = F(H)^{0.5} \quad (C.16)$$

Where:

F_{TP} – pump type factor = 2.0 for single stage pump (Seider *et al.* 2004:508)

S – size factor

H – pump head (ft)

F – flowrate (gal/min)

The cost electric motor for the pump drive will be added to the cost of the pump, the correlations for determining the purchase coats are given in Equations C.8 and C.9

Agitators

$$C_P = 1810S^{0.34} \quad \text{(C.17)}$$

Where:

S – size factor (Hp)

Table C.5 is obtained when Equations C.2 to C.17 are used for equipment costing.

Table C.5: Cost of other equipment

Equipment	Quantity	Description	Unit Cost ($)	Total Cost ($)
Bunsen Reactor				
Vessel	1	Diameter, 3 m; Length, 10 m; Stainless Steel	246 673	246 673
Agitator	1	250Hp, 1800rpm	25 342	25 342
Distillation Column				
DC01	1	Diameter, 1 m; Length, 5 m; Stainless Steel	72 799	72 799
DC02	1	Diameter, 2 m; Length, 10 m; Stainless Steel	178 189	178 189
Centrifugal Pumps				
PP01	2	total flow = 0.25 m3/s; total head = 130m	40 200	80 400
Motor drive	2	max 250Hp, 1800rpm	34 264	68 528
PP02	4	total flow = 1.34 m3/s; total head = 7 m	43 469	173 877
Motor drive	4	max 250Hp, 1800rpm,	34 264	137 056
Flush Drums				
FD01	1	Diameter, 2 m; Length, 5 m; Stainless Steel	121 951	121 951
FD02	1	Diameter, 2 m; Length, 5 m; Stainless Steel	121 951	121 951
FD03	1	Diameter, 2 m; Length, 5 m; Stainless Steel	121 951	121 951
FD04	1	Diameter, 2 m; Length, 5 m; Stainless Steel	121 951	121 951
FD05	1	Diameter, 2 m; Length, 5 m; Stainless Steel	121 951	121 951
FD06	1	Diameter, 2 m; Length, 5 m; Stainless Steel	121 951	121 951
Dryers				
DR01	1	Diameter, 2 m; Length, 5 m; Stainless Steel	121 951	121 951
DR02	1	Diameter, 2 m; Length, 5 m; Stainless Steel	121 951	121 951
Absorber	1	Diameter, 2 m; Length, 10 m; Stainless Steel	178 189	178 189
Mixers	9	Diameter, 8 m; Length, 5 m; Stainless Steel	473 874	4 264 867
Total				**6401530**

C.2 Estimation of fixed capital investment

The fixed capital investment of an industrial plant can be estimated with knowledge of the total equipment cost. The typical share of equipment costs for multipurpose plants is shown in Table C.6.

Table C.6: Typical percentages of fixed capital investment values for direct and indirect cost segments for multipurpose plants or large additions to existing facilities (Peters *et al.* 1991:167).

Component	**Range, %**
	Direct costs
Purchased equipment	15-40
Purchased equipment installation	6-14
Instrumentation and controls (installed)	2-8
Piping (installed)	3-20
Electrical (installed)	2-10
Buildings (including services)	3-18
Yard improvements	2-5
Service facilities (installed)	8-20
Land	1-2
	Indirect costs
Engineering and supervision	4-21
Construction expenses	4-16
Contractor's fee	2-6
Contingency	5-15

The ranges of process-plant component cost outlined in Table C.6 are used for the estimation of the fixed capital investment.

C.3 Estimation of production cost

Table C.7: Cost sheet outline [DW&B = direct wages and benefits; MW&B = maintenance wages and benefits; M&O-SW&B = maintenance and operations salary, wages and benefits; C_{TDC} = total depreciable capital; C_{alloc} = allocated costs for utility plants] (Busche, 1995:1)

Cost Factor	**Typical Factor**
Feedstock (raw materials)	
Utilities	
High temperature heat	\$0.041/kW
Cooling water (CW)	\$0.013/tonne
Refrigeration	\$0.057/kW.hr
Operations (labour related) (O)	
Direct wages and benefits (DW&B)	\$28/operator-hr
Direct salaries and benefits	15% of DW&B
Operating supplies and services	6% of DW&B
Technical assistance to manufacturing	\$52000/(operator/shift)-yr
Control laboratory	\$57000/(operator/shift)-yr
Maintenance (M)	
Wages and benefits (MW&B)	
Fluid handling process	3.5% of C_{TDC}
Salaries and benefits	25% of MW&B
Materials and services	100% of MW&B
Maintenance overhead	5% of MW&B
Operating overhead	
General plant overhead	7.1% of M&O-SW&B
Mechanical department services	2.4% of M&O-SW&B
Employee relations department	5.9% of M&O-SW&B
Business services	7.4% of M&O-SW&B
Property taxes and insurance	2% of C_{TDC}
Depreciation	
Direct plant	8% of ($C_{TDC} - 1.18C_{alloc}$)
Allocated plant	6% of $1.18C_{alloc}$
COST OF MANUFACTURE (COM)	Sum of above
General Expenses	
Selling (or transfer) expense	3% (1%) of sales
Direct research	4.8% of sales
Allocated research	0.5% of sales
Administrative expense	2.0% of sales
Management incentive compensation	1.25% of sales
TOTAL GENERAL EXPENSES (GE)	
TOTAL PRODUCTION COST (C)	COM + GE

C.4 Estimation of the Total bare module costs

To produce the estimate, two variables are needed, the production rate and the flowsheet showing reactors, separation equipment and gas compressors. Pumps and heat exchangers are not considered (Seider *et al.* 2004:498).

The production factor, F_{PR} and module costs, C_M are computed as follows:

$$F_{PR} = [(\text{Main product flow rate, lb/yr})/10000000)]^{0.6} \quad \text{C.18}$$

$$C_M = F_{PR}F_M(\text{design pressure, psia}/100)^{0.25}(\$130000) \quad \text{C.19}$$

where F_M is the material factor, 2.0 and 2.5 for stainless steel and Incoloy 825 respectively.

The total bare module cost, C_{TBM}, is computed using the Marshall and Swift Process Industries Average Cost (MS) Index as follows (Seider *et al.* 2004:499):

$$C_{TBM} = F_{PI}(\text{MS Index}/1103)\sum C_M \quad \text{C.20}$$

where F_{PI} is the piping and instrumentation factor, 2.15, for fluids handling processes (Seider *et al.* 2004:499) and the MS Index for 2010 is 1457 (Chemical Engineering, 2011).

From Table C.8,

$$\sum C_M = \$23\ 894\ 982$$

$$C_{TBM} = 2.15(1457/1103)\ \$23\ 894\ 982$$

$$= \$67\ 862\ 399$$

Table C.8: Estimation of the total bare module costs

Equipment	**Design Pressure**	**Material**	F_M	F_{PR}	C_M
	(psi)				
Reactors					
RX01	72	Stainless steel	2	4.5	1077752
RX02	319	Incoloy 825	2.5	4.5	1954535
Distillation Column					
DC01	72	Stainless steel	2	4.5	1077752
DC02	319	Stainless steel	2	4.5	1563628
Flush Drums					
FD01	290	Stainless steel	2	4.5	1526811
FD02	50	Stainless steel	2	4.5	983849
FD03	50	Stainless steel	2	4.5	983849
FD04	50	Stainless steel	2	4.5	983849
FD05	50	Stainless steel	2	4.5	983849
FD06	50	Stainless steel	2	4.5	983849
Dryers					
DR01	72	Stainless steel	2	4.5	1077752
DR02	319	Stainless steel	2	4.5	1563628
Absorber	72	Stainless steel	2	4.5	1077752
Mixers					
MX01	15	Stainless steel	2	4.5	728130
MX02	29	Stainless steel	2	4.5	858589
MX03	15	Stainless steel	2	4.5	728130
MX04	15	Stainless steel	2	4.5	728130
MX05	50	Stainless steel	2	4.5	983849
MX06	72	Stainless steel	2	4.5	1077752
MX07	50	Stainless steel	2	4.5	983849
MX08	50	Stainless steel	2	4.5	983849
MX09	50	Stainless steel	2	4.5	983849

C.5 Estimation of the DCFRR

Table C.9: Estimation of the DCFRR (values in $million), for a hydrogen price of $18.6/kg and an income tax of 40%.

Year	Total Depreciable Capital	Working Capital	Depreciation	Production Cost Excluding Depreciation	Sales Revenue	Net Earnings	Cash Flows	Cumulative Present Value @43.1%
1	-22.65						-22.65	-22.65
2	-22.65						-22.65	-42.35
3	-22.65						-22.65	-53.48
4	-22.65						-22.65	-61.27
5	-22.65	-162.25					-184.90	-105.86
6			5.66	869.00	1176	180.91	186.57	-74.33
7			10.76	869.00	1176	177.85	188.61	-52.00
8			9.68	869.00	1176	178.50	188.18	-36.38
9			8.72	869.00	1176	179.07	187.79	-25.46
10			7.85	869.00	1176	179.60	187.45	-17.82
11			7.06	869.00	1176	180.07	187.13	-12.48
12			6.68	869.00	1176	180.30	186.98	-8.73
13			6.68	869.00	1176	180.30	186.98	-6.11
14			6.69	869.00	1176	180.29	186.98	-4.27
15			6.68	869.00	1176	180.30	186.98	-2.98
16			6.69	869.00	1176	180.29	186.98	-2.08
17			6.68	869.00	1176	180.30	186.98	-1.45
18			6.69	869.00	1176	180.29	186.98	-1.01
19			3.34	869.00	1176	182.30	185.64	-0.70
20				869.00	1176	184.31	184.31	-0.48
21				869.00	1176	184.31	184.31	-0.33
22				869.00	1176	184.31	184.31	-0.23
23				869.00	1176	184.31	184.31	-0.15
24				869.00	1176	184.31	184.31	-0.10
25		196.25		869.00	1176	184.31	346.56	-0.03

Appendix D: References

ASPEN TECH. 2010. Aspen Plus. http://www.aspentech.com/core/aspen-plus.aspx. Date of access: 03 Apr 2010

BUSCHE, R.M. 1995. Venture Analysis: A framework for venture planning. (Course notes delivered as part of the lecture for Bio-en-gene-er Associates in Wilmington.) Delaware. (Unpublished)

CHEMICAL ENGINEERING. 2011. Economic Indicators. http://www.che.com. Date of access: 25 Sep 2011

KEMA. 2010. KEMA-SPENCE for simulation of process for energy conversion and electricity production. http://www.kema.com/Images/Spence process simulation description.pdf. Date of access: 28 Jan 2011

PETERS, M.S. & TIMMERHAUS, K.D. 1991. Plant design and economics for chemical engineers. McGraw-Hill. 923p

PROSIM. 2010. ProsimPlus. http://www.prosim.net/en/modeling/prosimplus.html. Date of access: 03 Apr 2010

SEIDER, W. D., SEADER, J.D., & LEWIN, D.R. 2004. Product and Process Design Principles: Synthesis, Analysis, and Evaluation. Wiley. 802p

SPECIAL METALS CORPORATION. 2004. The story of the "INCOLOY® alloys series," from 800, through 800H, 800HT. http://www.specialmetals.com. Date of access: 15 Sep 2011

WINSIM. 2011. Design II for windows. http://www.winsim.com/design.html. Date of access: 28 Jan 2011